Catalytic advancements in carboxylic acid ketonization and its perspectives on biomass valorisation

Bert Boekaerts[a] and Bert F. Sels[a]

[a] Dept. of Microbial and Molecular Systems (M²S), Centre for Sustainable Catalysis and Engineering (CSCE), KU Leuven, Celestijnenlaan 200F, 3001 Leuven, Belgium.

E-mail: bert.sels@kuleuven.be

Abstract

Ketonization of (biomass) carboxylic acids is increasingly showing its potential as upgrading strategy to renewable fuels and chemicals. Due to the growing amount of recent studies, an updated and critical overview of the catalytic advancements are warranted. Metal oxide and zeolite catalysts are discussed, alongside their proposed mechanisms and elementary steps. Substrate-surface interactions, structure-function correlations and kinetic studies have contributed to a better understanding of the requirements for ketonization catalysis, though the mechanism and rate-determining step(s) are still under debate. As a result, targeted modifications to improve catalytic performance are being established. Furthermore, substrate properties such as chain length, branching, unsaturation and additional functionalities have been identified as crucial for their reactivity. However, additional research is necessary to better integrate ketonization into future biorefineries. This includes development of kinetic models for oleochemicals conversion, catalyst design and regeneration. Finally, techno-economic and sustainability assessments are lacking to incentivize industrial implementation.

Keywords: Ketonization, Carboxylic acid, Metal oxide, Biomass, Oleochemistry

1. Introduction

In recent years, there has been a notable increase in academic and patent literature covering the topic of catalytic ketonization. In this C-C coupling reaction, also referred to as ketonic decarboxylation, two carboxylic acids react to form one ketone molecule with cogeneration of water and carbon dioxide by-products (eq. 1):

$$RCOOH + R'COOH \rightleftharpoons RCOR' + H_2O + CO_2 \qquad (eq.\,1)$$

Given the absence of solvents, additives or other toxic/harmful compounds, ketonization shows promise as a clean (biomass) upgrading step. Although already described in the 19th century for commercial production of acetone[1, 2], current global challenges have revitalized its relevance for biomass valorisation. Efficient, renewable and sustainable bio-based processes, energy sources and chemicals are required to mitigate the harmful impact of a fossil-based economy on climate, environment and socio-economic and geopolitical stability.[3, 4] Lignocellulose (plant cell wall) and triglycerides (vegetable/algae oils and animal fats) are the two major biomass sources of carboxylic acids that show promise for conversion to bio-based fuels and chemicals via ketonization (Figure 1).[5]

Lignocellulose is the most abundant form of biomass and consists of a complex matrix of three biopolymers: cellulose, hemicellulose and lignin.[6] To convert these polymers into valuable fuels and chemicals, three main pathways exist which are pyrolysis, hydrolysis and gasification.[7] Pyrolysis is a process in which lignocellulose is decomposed under oxygen free conditions at elevated temperatures (~200-800 °C) for seconds (fast pyrolysis) or for hours up to days (slow pyrolysis). Besides gaseous

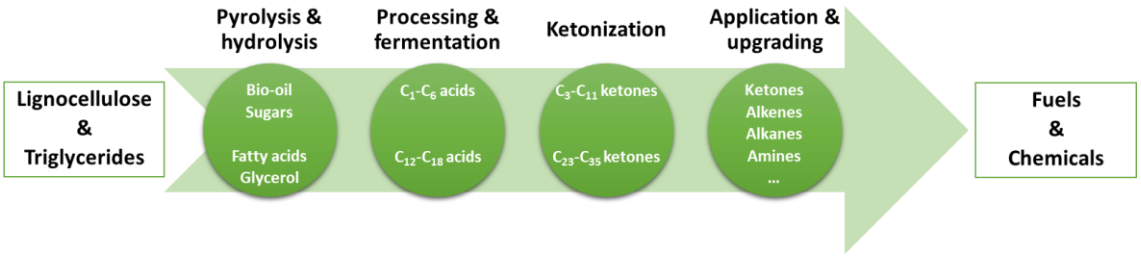

Figure 1: Lignocellulose and triglycerides as biomass carboxylic acid sources for renewable fuels and chemicals via ketonization

products (CO, CO_2 and H_2), a solid biochar fraction and liquid bio-oil are obtained.[8] This liquid bio-oil is a complicated mixture comprising hundreds of compounds including water, carbohydrates, hydrocarbons and oxygenated organics such as acids, ketones, furans and aldehydes. The acids that are present in pyrolysis bio-oil are typically short-chain carboxylic acids such as formic, acetic and propionic acid.[9, 10] Due to its modest energy content, thermal and chemical instability, high water content and corrosiveness, bio-oil is considered to be of low quality, and thus it requires further upgrading to be used as a suitable bio-fuel.[11] Ketonization of the carboxylic acids to partially deoxygenate them to short-chain ketones (typically C_3-C_9), which can serve as precursors for fuels and chemicals, is one of the prominent upgrade strategies to achieve this.[12] And so, bio-oil upgrading will be critically reviewed in this work. Hydrolysis is a second pathway to convert lignocellulose which starts with decomposition of the biopolymer matrix into sugar monomers at elevated temperatures (100-250 °C) in the presence of acid, base or enzyme. These sugars can be subsequently transformed into acid platform molecules via either thermochemical or bio-catalytic processes. The Biofine process is a nice example of the first, where lignocellulose sugars are converted into carboxylic acid ketonization substrates such as acetic, levulinic and lactic acids via acid hydrolysis (with diluted H_2SO_4) and dehydration reactions.[13] Additionally, carboxylic acids can also be obtained via fermentation pathways using (metabollicaly engineered) enzymes as bio-catalysts. These typically include lactic, levulinic, 3-hydroxypropionic, succinic and adipic acids among others.[14-16] Free fatty acids and their derivatives, which usually originate from triglyceride biomass, can also be produced via fermentation of lignocellulose sugars.[17-19] Finally, these carboxylic acids can then be utilized as ketonization substrates, demonstrating the potential of combining (enzymatic) biological and chemocatalytic processes for biomass valorisation.

Triglycerides (TG), free fatty acids (FFA) and fatty acid methyl esters (FAME) form the main components of vegetable and algae oils and animal fats, which are a second biomass resource for ketonization.[20] A triglyceride is an ester molecule of one glycerol entity attached to three long-chain carboxylic acid species, commonly called fatty acids. These are generally in the C_{12}-C_{18} range and can be identical or different in both carbon chain length and degree of unsaturation and branching. A hydrolysis step is required to convert triglycerides into their fatty acid monomers, which is performed commercially via different routes.[21, 22] One industrial example is the Colgate-Emery technology that utilizes a continuous counter current process where triglycerides and subcritical water react at elevated temperatures (250-300 °C) and pressures (50-60 bar) with very high yields (98%) of free fatty acids and glycerol by-product (10 wt%).[23] These FFA can then be used as substrates for ketonization towards long-chain ketones (typically C_{23}-C_{35}), which can be used directly as chemicals in inks[24], washing formulas[25], waxes[26], phase change materials[27], antibacterial agents[28], etc. Furthermore they can be converted into paraffinic waxes and lubricants via hydrodeoxygenation and hydro-isomerisation downstream processing.[29-31]

Few ketonization reviews have been written in the past, and each of them had a different focus such as the possible reaction mechanisms[32-34], theoretical approaches and modelling of the chemistry and catalysis[35, 36], and the use of different feedstocks (acid, aldehyde, alcohol, ester)[37]. Due to the rapid increasing number of recent studies since these reports, an exhaustive updated overview of the advancements in this field seems desirable, particularly for biomass upgrading. Furthermore, the large variety in reported catalysts, reaction conditions and reactor systems often leads to contradicting conclusions. Therefore, the purpose of this overviewing work is twofold: to firstly critically review ketonization with focus on the advancements in the area of heterogeneous catalysis, and secondly to highlight its future research opportunities, specifically with regard to biomass carboxylic acid valorisation.

2. Ketonization mechanism

For the purpose of further discussion, an overview of recent research concerning non-fatty acid ketonization is presented in Table 1. This table does not reflect a comprehensive collection of all literature discussing this topic, but rather it wants to show to the reader the wide variety in catalysts, substrates, reaction conditions and process systems studied. Many materials have been used as (heterogeneous) catalysts for carboxylic acid ketonization, including metal oxides, metals, metal salts, zeolites, bifunctional catalysts, etc. As shown in Table 1, metal oxides, whether pure, mixed or bifunctional have dominated this research field. In general, these are divided into highly basic (e.g. low lattice energy as MgO, CaO, BaO…) and amphoteric (e.g. high lattice energy such as TiO_2, CeO_2, ZrO_2…) materials, of which the latter have shown to be the most active, selective and often stable. While there is currently still an ongoing debate regarding the exact reaction mechanism, its intermediates and rate-determining step, a general terminology exists to describe the chemistry on these different metal oxide types. On low lattice energy materials, the C-C coupling proceeds through a bulk ketonization pathway, while surface ketonization occurs on high lattice energy catalysts. It is important to note that nearly all mechanistic studies have been performed on the gas-phase ketonization of C_2-C_4 acids due to their ease of use, well documented (physico-) chemical properties and known interactions with metal oxide materials. In contrast, liquid phase ketonization reactions and the use of fatty acids (therein) have been described far less.

Table 1: Selected overview of ketonization of non-fatty acid (derivatives) in academic literature.

Substrate	Catalyst	Reactor	T (°C)	P (bar)	X (%)	Y (%)	Ref.
Hexanoic acid	ZrO_2	Fixed bed	360	/	75	69	[38]
Acetic + Isobutyric acid	ZrO_2	Fixed bed	400	1	100	/	[39]
Levulinic acid (50 wt% H_2O)	Red Mud	Batch	365	55 (H_2)	100	/	[40]
Iso-Pentanoic acid	Red Mud	Batch	365	55 (H_2)	25	7	[40]
Acetic acid	Ru/TiO_2	Fixed bed	285	/	29	29	[41]
Dimethyl adipate	$Ce_xZr_{1-x}O2/Al_2O_3$	Fixed bed	400	/	100	75	[42]
Pivalic acid	CeO_2/Mn_2O_3	Fixed bed	375	1 (N_2)	0	0	[43]
3,3-Dimethylbutanoic acid	CeO_2/Mn_2O_3	Fixed bed	375	1 (N_2)	0	0	[43]
3-Methylbenzoic + Phenylacetic acid	Fe_3O_4	Flask	250	/	100	80	[44]
Acetic + Propionic acid	$Zn_xZr_yO_z$	Fixed bed	450	/	/	~25	[45]
Acetic acid	CeO_2	Batch	300	30-40 (N_2)	~90	76	[46]
Acetic acid	HZSM-5	Fixed bed	300	1 (He)	~16	~15	[47]
Acetic acid	NaX	Fixed bed	500	1 (N_2)	100	58	[48]
Ethyl acetate	SiO_2/Al_2O_3	Fixed bed	500	1 (N_2)	100	25	[48]
Decanoic acid	TiO_2	Fixed bed	350	1 (N_2)	100	70	[49]
16% Acetic acid in model solution	$Fe_{0.2}Ce_{0.2}Al_{0.6}O_x$	Fixed bed	400	/	100	~80	[50]
Pyrolysis acid solution	ZrO_2/FeO_X	Fixed bed	350	1 (N_2)	~100	30	[51]
Acetic acid (2 M in H_2O)	ZrO_2/C	Batch	340	/	39	38	[52]
Acetic acid (in H_2O)	Ru/TiO_2	Batch	200	50 (N_2)	~75	~75	[53]
Livestock manure slurry liquid (~15% acetic acid)	ZrO_2/FeO_X	Fixed bed	450	1 (N_2)	~100	/	[54]
Heptanal	CeO_2	Fixed bed	450	/	~100	88	[55]
Butanoic acid	Fe	Flask	300	/	100	70	[56]
Acetic acid	Pr_6O_{11}	Fixed bed	350	1 (N_2)	80	80	[57]
Ethyl heptanoate	MnO_2/Al_2O_3	Fixed bed	425	/	91	73	[58]
Isopropyl butyrate	Sn–Ce–Rh–O	Fixed bed	370	1 (N_2)	93	34	[59]
Acetic acid	ZrO_2 + Cu/SiO_2	Fixed bed	260	2 (H_2 in He)	11	~10	[60]
Acetic acid	Co/CeO_2	Fixed bed	500	1 (N_2)	75	45	[61]
Bio-oil aqueous phase (8.2% Acetic acid)	MnO_2	Fixed bed	335	/	83	/	[62]
Acetic acid (10% in H_2O)	La_2O_3/ZrO_2	Fixed bed	295	96 (N_2)	28	28	[63]
Acetic acid (1.7 M in H_2O)	$Ru/TiO_2/C$	Batch	180	28-56 (N_2)	18	18	[64]
Cyclopropane carboxylic acid	CeO_2/TiO_2	Fixed bed	450	8 (N_2)	87	70	[65]
Acetic acid in bio-oil model mixture	NbOx	Batch	200	13 (N_2)	15	/	[66]
Decanol	Fe_3O_4	Fixed bed	380	1 (N_2)	100	~7	[67]
Propionic acid	MnOx/CeO_2/MCM-41	Fixed bed	410	/	73	73	[68]
Acetic acid	Ti/Beta	Fixed bed	450	1 (N_2)	100	70	[69]

/: Not mentioned; ~: Approximately

2.1 Bulk ketonization

This reaction pathway mostly occurs for solid metals, metal salts and in the bulk of low lattice energy oxides (M= Ca, Mg, …) when contacted with carboxylic acids at high temperatures (typically 350-500 °C) (eq. 2). In the first step, the carboxylic acids are deprotonated on the metal oxides with formation of bulk metal carboxylate salts and lattice hydroxyls. Next, thermal decomposition of the metal salt yields the ketone product and bulk metal carbonate. Finally, the metal oxide phase may be recuperated with release of CO_2 and water.[70, 71] With regard to the exact mechanism, Hites *et al*. have investigated the product

distribution and intermediates formed during pyrolysis of deuterated calcium decanoate at 500 °C via gas chromatography-mass spectrometry (GC-MS). While 10-nonadecanone was the main product (28% yield), a series of ketones C_nCOC_9 (n= 1-9) and lower molecular weight <C_9 monoalkenes and alkanes were also obtained. It was shown that a fraction of these smaller products could be secondary products from 10-nonadecanone decomposition at high temperature, while they could also be formed during the primary conversion reaction. Based on the mass spectrometry results, a free radical mechanism including both alkyl and acyl radical initiators was proposed.[72] Both may be formed during metal salt decomposition, and (re)combination of these radical species can result in C-C coupling to higher molecular weight ketones and metal carbonates. As a side reaction, disproportionation of the radical intermediates can result in reduced selectivity to the main ketone as smaller organics are formed. At these temperatures, cracking side reactions can also produce the intermediates with lower carbon numbers.[32] It is clear that the ketonization selectivity may be compromised significantly when stochiometric or catalytic amounts of these active materials are chosen as they require conditions that promote unwanted side reactions.

$$\begin{gathered} \boldsymbol{MO_2 + 2RCOOH \rightleftharpoons M(RCOO)_2 + 2OH} \\ \boldsymbol{M(RCOO)_2 \rightleftharpoons RCOR + MCO_3} \\ \boldsymbol{MCO_3 + 2OH \rightleftharpoons MO_2 + CO_2 + H_2O} \\ \hline \boldsymbol{MO_2 + 2RCOOH \rightleftharpoons MO_2 + RCOR + CO_2 + H_2O} \end{gathered} \qquad (\boldsymbol{eq.2})$$

Examples of active materials that show this ketonization behaviour are not limited to alkali (Na) and alkali earth (Mg, Ca) metal oxides, but also include highly basic rare earth metal oxides (La_2O_3, Pr_6O_{11}, Nd_2O_3)[57], metals[73] and even amphoteric oxides (CeO_2, Ca/Zn/AlO_x)[46, 74]. Davis *et al*. used iron powder (Fe) as a catalyst in a high temperature reflux system to couple various carboxylic acids via ketonization. In this case however, the catalyst was not recovered in its original form (Fe), but rather ferrous oxide was formed, which in next reaction cycles could serve as ketonization catalyst. Hydrogen (H_2) was created as additional side product besides CO_2 and H_2O from the initial contact between the carboxylic acid and metal (eq. 3).[56] Although ketonization on amphoteric oxides is generally believed to occur via a surface mechanism, Snell *et al*. have suggested both bulk and surface mechanisms on CeO_2 catalysts, depending on the applied temperature regime.[46] Very recently, a similar hypothesis was proposed by Ling *et al*. for the ketonization of acetic acid on Ca/Zn/AlO_x metal oxides.[74] Both will be discussed in more detail in the next section of this work. Therefore, a strict distinction between bulk and surface ketonization might not always be appropriate as general terms for metal oxide materials and may generate further confusion for interested readers.

$$\begin{gathered} \boldsymbol{Fe + 2RCOOH \rightleftharpoons Fe(RCOO)_2 + H_2} \\ \boldsymbol{Fe(RCOO)_2 \rightleftharpoons FeO + RCOR + CO_2} \\ \boldsymbol{FeO + 2RCOOH \rightleftharpoons FeO + RCOR + CO_2 + H_2O} \\ \hline \boldsymbol{Fe + 4RCOOH \rightleftharpoons FeO + 2RCOR + H_2 + H_2O + 2CO_2} \end{gathered} \qquad (\boldsymbol{eq.3})$$

2.2 Surface ketonization

The surface reaction is considered to be dominant on amphoteric oxides (TiO_2, ZrO_2, …). However, it has also been proposed for basic oxides (e.g. MgO) under certain reaction conditions[75], demonstrating once more the complex nature of the coupling reaction and the ongoing discussion around reaction intermediates and pathways. Since its discovery, multiple surface mechanisms have been proposed: concerted, acid anhydride, ketene and β-ketoacid mechanisms. Based on our current understanding of ketonization, the experimental and theoretical evidence suggests that the β-ketoacid mechanism is the most plausible, while some of the others may rather likely represent accompanying side reactions. We will still critically discuss the other pathways, as it informs the readers on the different molecules associated with or observed during ketonization. Furthermore, new reports are still being published which question the β-ketoacid mechanism, for which evaluation of the proposed arguments against it is highly valuable.

2.2.1 Concerted mechanism

The concerted surface mechanism, of which the core principle is the simultaneous formation of both the C-C bond and CO_2 in the same step, was investigated on monoclinic zirconia (*m*-ZrO_2) via DFT modelling by Pulido *et al*. for gas-phase acetic acid ketonization, in which a ($\bar{1}11$) slab model was used.[76] Here, the unit cell consisted of 4 Zr atoms and 8 O atoms, of which 4 Zr atoms and 7 O atoms were assigned as inequivalent. In the first step, one acid molecule binds to the catalyst surface via deprotonation, after which interaction with a second weakly adsorbed neighbour can occur via methyl carbanion transfer. A new C-C bond is formed, and de-hydroxylation of the second acid occurs at the same time (Figure 2 top). This step, where simultaneously old bonds are broken and new ones are formed (endotherm, +45 kJ/mol), is considered to be rate-determining

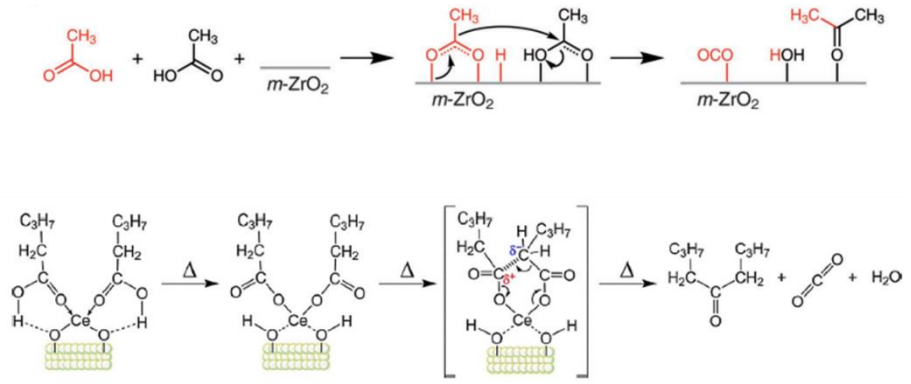

Figure 2: Concerted ketonization mechanism of acetic acid on monoclinic zirconia as studied by Pulido *et al.* (top).[76] Concerted ketonization mechanism on ceria for pivalic acid coupling as presented by Kulyk *et al.* (bottom). [78] Reprinted from [76] and [78], Copyright (2012) and (2017) with permission from Wiley.

with an activation energy of 154 kJ/mol. Water is formed by reaction (endotherm, + 120 kJ/mol) of an adsorbed proton and neighbouring hydroxyl group originating from the two substrate molecules (136 kJ/mol activation energy). Finally, desorption of all 3 ketonization products closes the catalytic cycle. Given the higher activation energy of this pathway compared to that of the β-ketoacid route (see further), a concerted mechanism is unlikely. The hypothesis is further reinforced by the isotopic labelling experiments of Dooley *et al.*, which indicate that the occurrence of the concerted mechanism is unconvincing.[77] Recently however, the concerted pathway was again proposed by Kulyk *et al*. for the ketonization of valeric acid on a ceria nanoparticle catalyst.[78] Here, the authors propose that both carboxylic acids are adsorbed and deprotonated on the same cerium atom, resulting in two monodentate valerate species and consequently a six-membered cyclic structure as concerted transition state (Figure 2 bottom). This is a different take on the concerted mechanism compared to the aforementioned DFT study on ZrO_2, as in that case it was assumed that more than one Zr atom is participating. However, several remarks must be made at this point. First, this proposed CeO_2 surface is illustrated as being terminated by Ce metal atoms (instead of the expected oxygen atoms), which would imply a reduced-like surface. It is unclear from this work whether and how two carboxylic acids can adsorb on the common Ce atom of a stochiometric surface. In a prior surface study by Kim *et al*. the ketonization of carboxylic acids on a {114}-faceted TiO_2 (001) surface was also proposed to include coordination of two carboxylic acids on the same fourfold coordinated Ti^{4+} atoms, although no direct evidence was provided.[79] Secondly, DFT studies have since shown that adsorption of two carboxylic acids on the same metal atom is highly unlikely, due to high steric repulsion.[36] Thirdly, the presence of two monodentate valerate species on the same metal atom is a hypothesis based on infrared spectroscopy measurements that show the presence of weakly bound acid (1680–1690 cm^{-1}) on the surface, while the authors state that the presence of this interaction and complex cannot be decisively confirmed in this manner. This also applies to determination of the pre-exponential factor of the proposed kinetic model of this study, of which the order of magnitude was used as argument against a β-ketoacid mechanism. In conclusion, the concerted ketonization mechanism seems unlikely based on our current understanding and available evidence, although no theory can be dismissed entirely based on the discussion in this paragraph. In this regard, follow-up studies could provide further valuable insights to either disprove or confirm the possibility of a concerted mechanism and associated surface complexes, which may furthermore be exclusive for a specific catalytic system.

2.2.2 Anhydride mechanism

Acid anhydride molecules have been observed during ketonization reactions, opening up the possibility of these species being intermediates in the reaction mechanism.[34, 80-82] In early studies for example, Martens *et al*. observed time-on-stream dependent anhydride formation during acetic, propanoic and butyric acid ketonization on zeolite catalysts. The authors used triphenylchlorosilane to selectively occupy the external surface acid sites (Brönsted OH), after which the formation of anhydride was inhibited, while the ketone yield remained unchanged. This experimental evidence suggests that anhydride formation is rather a dehydration side reaction on the outer acid surface sites of zeolite H-T, while inside the erionite cavity selective ketonization took place.[81] More recently, Woo *et al*. have proposed an acid anhydride mechanism based on the ketonization of hexanoic acid to 6-undecanone on a zirconia aerogel catalyst.[80] Hexanoic acid and hexanoic anhydride were cofed in a fixed bed reactor system at 300-330 °C in various ratios (1:0, 0:1, 1:1, 2:1 and 1:2) and the 6-undecanone yield was quantified. In all scenarios, the authors observed the formation of 6-undecanone. The potential role of acid anhydride was then investigated via an experimental kinetic study comparing 3 models. In the first, acid anhydride was presented as competitive side product from acid conversion via dehydration on the catalyst acid sites (eq. 4). The second model considered acid anhydride as intermediate towards the final ketone via consecutive dehydration and decarboxylation reactions (eq. 5). Finally, the last model proposed acid anhydride as the final product with a ketone intermediate species via an initial ketonization step, followed by CO_2 addition (eq. 6). Based on their experimental results and kinetic modelling, the authors concluded that the second pathway with acid anhydride as intermediate species during ketonization is the most probable one. However, the authors state that other reaction mechanisms, such as the β-

ketoacid route (although not detected), could occur simultaneously. Additionally, the conclusion of this work seems rather unconvincing based on the provided evidence, as some additional remarks can be made regarding this particular study. First, the thermodynamics and energetics of the elementary steps of the proposed models are not discussed . Secondly, the hexanoic anhydride substrate that was used also contained 4% of hexanoic acid, which could initiate ketonization to 6-undecanone (regardless of exact mechanism) and produce water in the process. This could react with the anhydride to generate new acids. As such, the observed ketone yield may be entirely originating from carboxylic acid without anhydride being an actual reaction intermediate. Thirdly, negative conversion values between -3 and -270% were obtained for experiments with hexanoic acid co-feeding, depending on the exact substrate ratio. A brief and inconclusive explanation was provided here, which may indicate a need for refinement in analysis and calculation methods. Finally, while the second model described the kinetic experimental results better than the others, still a rather large deviation was observed between theoretic model and experimental results. For example, the means of absolute relative residuals (MARR) values were 17, 27 and 20 % for hexanoic acid conversion, hexanoic anhydride conversion and 6-undecanone yield, respectively. The relative standard deviation of individual errors (RSDE) were 18, 20 and 15% respectively. For the first model, which states anhydride formation as a competitive side reaction, the MARR values were 35, 19 and 35%, while the RSDE parameters were 22, 16 and 22%, respectively. In conclusion, the current evidence for an anhydride mechanism is scarce, and anhydride formation may rather be a competitive side reaction depending on the catalytic system and reaction conditions. More fundamental theoretical approaches, for example by DFT studies could provide further clarity.

$$\boldsymbol{RCOOCOR + H_2O \rightleftharpoons 2RCOOH \rightleftharpoons RCOR + CO_2 + H_2O} \qquad (\boldsymbol{eq.4})$$

$$\boldsymbol{2RCOOH \rightleftharpoons RCOOCOR + H_2O \rightleftharpoons RCOR + CO_2 + H_2O} \qquad (\boldsymbol{eq.5})$$

$$\boldsymbol{2RCOOH \rightleftharpoons RCOR + CO_2 + H_2O \rightleftharpoons RCOOCOR + H_2O} \qquad (\boldsymbol{eq.6})$$

2.2.3 Ketene mechanism

The possibility of a ketene ($R_2C=C=O$) mechanism was inspired by experimental observation of ketene species during ketonization reactions of carboxylic acids (with at least one α-H atom) on metal oxide catalysts at elevated temperatures.[65, 77, 78, 83-86] Pham *et al*. have visualized this potential reaction pathway that starts with adsorption on a coordinatively unsaturated cation (metal site) by deprotonation and α-H abstraction, followed by oxygen removal to form a surface hydroxyl and ketene intermediate (Figure 3).[33] Further reaction of this species with the alkyl group of another adsorbed carboxylate species would then lead to ketone formation.

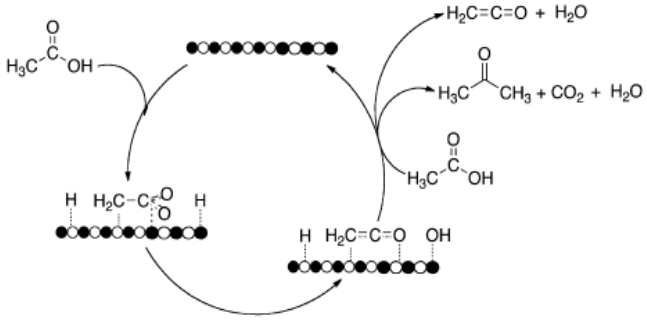

Figure 3: Ketene mechanism on metal oxide surface as proposed by Pham *et al*. Reprinted with permission from [33], Copyright (2013) American Chemical Society.

However, two groups have provided evidence against this ketene mechanism. First, Ponec *et al*. have shown via their isotopic experiments on cross-ketonization between ^{13}C labelled acetic and unlabelled pivalic acid that the ketene itself cannot be the reaction intermediate for ketonization.[84] Pivalic acid cannot form a ketene species as it does not have an α-hydrogen atom available for abstraction. Therefore, acetic acid would need to be the only source of the ketene intermediate, and ^{13}C should be detected in the 2,2-dimethyl-3-butanone product as it provides the carbonyl group for the ketone product. However, all of the ^{13}C was located in the CO_2 product rather than the ketone, which contradicts with the ketene mechanism as acetic acid would not be available to produce $^{13}CO_2$. Based on these results, the authors suggest that the observed ketene species during ketonization are rather in so called pseudo-equilibrium with the rate determining intermediate, which they considered to be an adsorbed methylene species that is formed after double hydrogen abstraction. Secondly, Barteau *et al*. have shown for the ketonization of acetic acid on titania-functionalized silica monolith catalysts that the ketone selectivity is complete and invariable for different degrees of conversion (3-100 %) at short contact times.[86] If ketene would be the intermediate in a sequential reaction sequence, it should have been present in significant amounts at low conversions, which was not the case, as the authors previously showed preservation of ketene products on silica monolith materials for short contact times. In conclusion, current evidence suggests that the ketene intermediate pathway is unlikely and should rather be viewed as a parallel route alongside ketonization.

2.2.4 β-ketoacid mechanism

The β-ketoacid mechanism will be discussed most extensively throughout this work, as this is currently the most plausible intermediate based on (very) recent experimental and theoretical evidence.[33, 35-37, 41, 60, 74, 76, 87-92] In contrast to acid anhydride and ketene species, no β-ketoacids have been observed experimentally during ketonization, which is a result of its highly

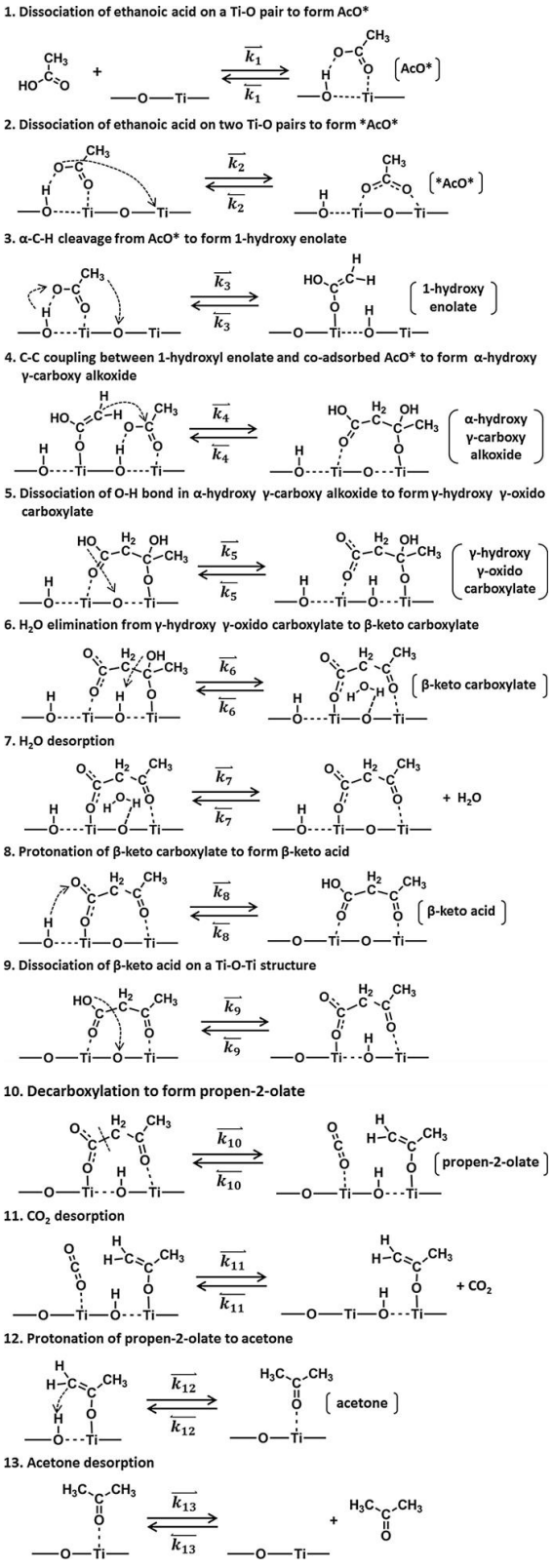

Figure 4: Ketonization mechanism on TiO_2 via β-ketoacid intermediate as proposed by Wang *et al*. Reprinted from [60], Copyright (2017) with permission from Elsevier.

reactive nature (and likely also the cause of the complexity to unambiguously invoke this pathway to explain the mechanism). Figure 4 illustrates the elementary reaction pathway for acetic acid ketonization on anatase TiO_2 via a β-ketoacid intermediate as presented by Wang *et al*.[60] Here, a first carboxylic acid is dissociatively adsorbed on the surface via its acid group, after which an α-H atom is abstracted by a surface lattice O with base character. The formed 1-hydroxyenolate is then coupled to a second adsorbed carboxylic acid in close proximity via nucleophilic attack on the carboxyl C, after which (following some elementary steps), H_2O is eliminated as side product with formation of the β-ketoacid. This reactive intermediate then decarboxylates via C-C bond cleavage to propen-2-olate and CO_2, the latter which desorbs as secondary by-product. To obtain the ketone product, the propen-2-olate intermediate is protonated by a surface hydroxyl, after which the metal oxide catalyst surface is regenerated and ketone desorption closes the catalytic cycle. Currently, some small variations on this scheme still exist between various DFT reports, which differ from each other regarding the specific type of carboxylic acid adsorption (complete O-H dissociation *versus* hydrogen bonding). However, this is rather a direct consequence of the use of different active materials (anatase and rutile TiO_2, monoclinic and tetragonal ZrO_2), indicating that similar but slightly varying β-ketoacid mechanisms may exist depending on the exact catalytic system used. This should be kept in mind when comparing and discussing different catalysts, substrates and reactor systems used. Rather than viewing this as inconsistencies, it reflects the intrinsic complex nature of both the C- C coupling reaction and associated metal oxide surface chemistry.

The critical parameter in the β-ketoacid mechanism, while also necessary for the formation of ketene side products (see section 2.2.3), is the presence of at least one α-H (step 3 in Figure 4). This refers to a hydrogen atom bound to a carbon atom in the alpha position with respect to the carbonyl group of the carboxylic acid. It is based on convincing experimental evidence provided by several studies that have screened acid substrates with different substitutions and numbers of α-H atoms. For example, the group of Oliver-Tomas *et al*. recently studied the ketonization of pivalic (2,2-dimethylpropionic acid) and 2,2,5,5-tetramethyladipic acid (a dicarboxylic acid), which both lack α-H atoms, with ZrO_2 and BaO catalysts at 350-550 °C to elucidate the role of α-H.[93] Under these conditions, the symmetrical ketone product from pivalic acid (i.e. 2,2,4,4-tetramethyl-3-pentanone) was not observed. However, some other (smaller) ketones were identified in the product mixture for temperatures above 500°C. The authors contribute this to initial skeletal rearrangements or fragmentations of pivalic acid at this very high temperature to generate new intermediate α-H species, after which ketonization via β-ketoacid intermediates can occur. The same rationale applies to the conversion of 2,2,5,5-tetramethyladipic acid, where the symmetrical ketone product was not formed via the classical ketonization pathway. This is analogous to the discussion of section 2.1 of this work, where it was shown that under severe conditions cracking and disproportionation side reactions can occur. Similarly, Nagashima *et al*. also reported zero symmetrical ketone yield from pivalic acid over a CeO_2–Mn_2O_3 catalyst at 375 °C.[43] Additionally, the necessity for α-H has been investigated and demonstrated through isotopic labelling experiments (H/D exchange between carboxylic acid and catalyst surface), such as those performed by Pestman *et al*.[84] and Gonzalez *et al*.[83].

Regarding the exact identity of the rate-limiting step in the β-ketoacid mechanism, separate research groups have proposed different options. For example, Pulido *et al*. have suggested the decarboxylation step (step 10, Figure 4) as the rate-determining step based on their DFT calculations.[76] With *m*-ZrO_2 as catalyst and acetic acid as substrate, the formation of the β-ketoacid was calculated to be an exothermic step (-93 kJ/mol) with an activation barrier of 57 kJ/mol. However, formation of acetone enolate and CO_2 by decarboxylation of the β-keto carboxylate intermediate had a significantly higher activation barrier (108 kJ/mol). Many have contested this argument however, based on DFT calculations and experimental data, in addition to the observation that decarboxylation typically transpires easily by heating and that the associated intermediates have not been detected experimentally.[33, 35] In the work by Wang *et al*. it was shown that the C-C coupling TS has the highest free energy along the reaction coordinate for acetic acid conversion on anatase and rutile TiO_2, as well as *m*-ZrO_2, indicating that coupling between the 1-hydroxyenolate and second activated acid is determining the reaction kinetics.[60, 87] Similarly, Shylesh *et al*. have very recently reported C-C coupling as the rate-determining step using isolated zirconia on a silica support.[94] Indeed, the C-C coupling step is acknowledged by most as the rate-determining step. While Ignatchenko *et al*. agree that C-C coupling is limiting the ketonization rate, they allude (based on their own research) to the possibility that enolization may also play a significant role, ultimately stating that the combination of enolization and the following C-C coupling step is kinetically relevant.[89] Clearly, C-C coupling is favoured as the rate-limiting step in the mechanism, while still subject to some (minor) discussion. This could potentially also be dependent on the combination of catalytic system, substrate and reaction conditions.

While in the past ketonization has been considered to be irreversible (ketone products are highly favoured thermodynamically), very recent work by the group of Ignatchenko *et al*. suggests that decarboxylative ketonization and (some of) its elementary steps should be considered to be reversible.[36, 95, 96] In vapor-phase scrambling experiments with ^{13}C labelled ketone species (acetone) in the presence of a ZrO_2 catalyst, CO_2 and H_2O in a small non-stirred autoclave, $^{13}C/^{12}C$ exchange between the ketone molecule and CO_2 was observed, which was attributed to scrambling between the two carboxylic acids (acetic acid) in a reversible process. Here, one of the acids goes through the enolization process (step 3 Figure 4) and ultimately loses CO_2, while the other is responsible for the carbonyl group of the ketone product. Furthermore $^{13}C/^{12}C$ exchange between carboxylic acid and CO_2 was observed, which was attributed to scrambling via a malonic acid intermediate. Perhaps the most convincing argument for the reversibility of ketonization is the disproportionation of methyl isopropyl ketone (MIPK) to di-isopropyl ketone (DIPK) and acetone in the presence of CO_2 and H_2O via isobutyric and acetic acid intermediates (Figure 5). It is noteworthy to point out that in these experimental studies, high pressures (~ 40 bar) and large amounts of CO_2 and H_2O (typically 10-20 excess factor) were used to test

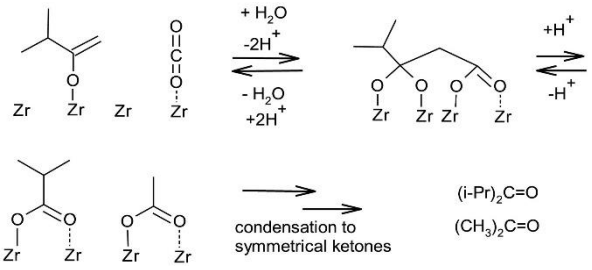

Figure 5: Reversibility of ketonization as demonstrated by Ignatchenko *et al*. via disproportionation of MIPK. Reprinted from [95], Copyright (2018) with permission from Elsevier.

the condensation between CO_2 and acetone, whereas practical application of ketonization processes may occur at much lower pressures under continuous gas flow, decreasing the likelihood of the reverse reaction under classic ketonization conditions. It is also important to mention that these concepts were specifically and exclusively postulated for the gas-phase. It is unclear whether such phenomena should be taken into account also in the condensed phase.

3. Catalysts

It is clear from Tables 1,3 and 4 of this review that many catalysts have been screened for the ketonization of carboxylic acids, with an obvious preference for metal oxides over others such as zeolites. In this section, both material types will be discussed in detail in terms of substrate-surface interactions, catalytic active sites, targeted modifications, selectivity and stability for carboxylic acid ketonization. This information will hopefully lead to targeted synthesis and/or modification of active materials to improve their overall ketonization performance for future biomass conversion.

3.1 Metal oxides

3.1.1 Substrate-surface interactions

To understand how metal oxides catalyse the C-C coupling of two carboxylic acids, it is paramount to discuss the initial adsorption interactions between the active sites and substrate molecules. Furthermore, also the association between the surface and reaction products (ketone, CO_2 and H_2O) yields valuable information to explain observed experimental data. To this end, the use of both experimental techniques (FT-IR, TPD, UV-vis DRS, DRIFTS, isotopic labelling) and theoretical modelling (DFT calculations) is invaluable.

Via surface adsorption studies, it has been found that carboxylic acids can adsorb both physically and chemically on metal oxide surfaces. Depending on the exact surface material and temperature conditions, various chemical dissociative adsorption modes can exist. For example, Panchenko *et al*. have visualized the potential interaction modes of valeric acid on a ZrO_2 surface based on DRIFTS and UV-vis DRS techniques (Figure 6).[91] These adsorption configurations, which result in adsorbed carboxylates ($RCOO^-$) and surface hydroxyls by deprotonation of the substrate, can be generalized to other carboxylic acids and metal oxide materials. They include chelating bidentate (I), bridging bidentate (II), monomolecular monodentate (III) and bimolecular monodentate (IV) modes. As shown, these adsorption modes differ from each other in both the amount of metal atoms involved per carboxylic acid, as well as the interaction between substrate oxygen and surface metal atoms. In general, the bridging bidentate configuration (II) is the most stable adsorption configuration for a carboxylic acid due to the simultaneous interaction with two metal atoms.[33] As already discussed in section 2.2.1 of this work, the possibility of a bimolecular monodentate (IV) adsorption mode seems highly unlikely based on current DFT evidence (too high steric repulsion) and the lack of convincing experimental data (allocation of IR vibrations for example). Regarding the ketone product, two different interactions with the catalyst surface have been proposed: (I) hydrogen bond formation between a hydroxylated surface and C=O carbonyl, or (II) direct interaction between a metal atom (Zr in this case) and the O atom of the carbonyl group (Figure 7).

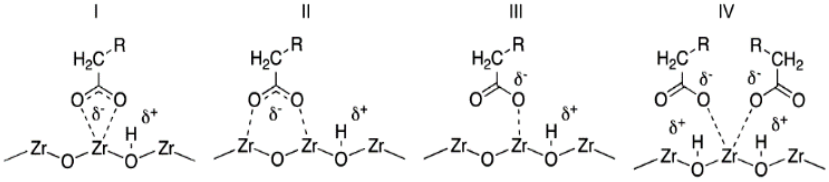

Figure 6: Potential interaction modes between monocarboxylic acid and ZrO_2 surface, Reprinted from [91], Copyright (2014) with permission from Elsevier.

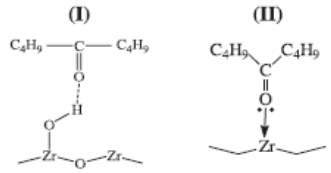

Figure 7: Possible interactions between ZrO_2 surface and 5-nonanone reaction product as presented by Panchenko *et al*. Reprinted from [91], Copyright (2014) with permission from Elsevier.

To determine which of these configurations are present and active for C-C coupling under ketonization conditions, Almutairi *et al*. have screened alumina, titania, zirconia and ceria for the gas-phase ketonization of acetic acid.[88] For all materials, DRIFT spectra of adsorbed acetic acid were measured at room temperature after initial evacuation at 130 °C, revealing a small amount of physisorbed acid in addition to bidentate bridging surface acetates. By isotopic labelling experiments, CH_3COOH/CD_3COOD exchange was shown to occur on all oxide surfaces at 130 °C, which is far below relevant ketonization temperatures on these materials. Furthermore, no exchange occurred between deuterated surface acetates and surface protons at this temperature. However, the opposite was shown for typical ketonization temperatures above 250 °C with TiO_2, where H/D exchange between bidentate bridging acetates and surface hydroxyls (for instance in presence of water) took place. Secondly, exchange between bidentate bridging acetate and a second co-adsorbed acetic acid molecule was also observed (even at 130 °C). First of all, these data show that under typical ketonization conditions the most stable bridging bidentate carboxylates can be in equilibrium with other surface acetate species (such as monodentate) and may be kinetically indistinguishable before the (rate-determining) C-C coupling step. This has also been proposed in earlier work.[84, 97] Secondly, the H/D exchange between carboxylate and surface hydroxyls supports a β-ketoacid mechanism with enolate formation (step 3, Figure 4) as discussed in section 2.2.4, after which this enolate may interact with a second bidentate or monodentate carboxylate.

Heracleous *et al*. have used DRIFTS-TGA-MS as an experimental tool to determine the active intermediates of nanostructured FeO_x and MnO_x catalysts during the ketonization of acetic and propionic acid, and aqueous pyrolysis bio-oil mixtures at 335 °C.[62] For both materials, bidentate acetate species were observed on the fresh surfaces, of which the concentration decreased for increasing temperatures (from 50 to 900 °C). Both desorption of unreacted carboxylate species and turnover via ketonization was observed, as evidenced by acetone and CO_2 evolution (between ~250-500 °C). While this does not directly indicate that bidentate species are the active configuration during ketonization, it shows that they are either in equilibrium with the actual active species (which were not detected or observable in this case) or that they are the genuine active precursors.

While the two experimental studies above have not directly observed monodentate carboxylate species, Wang *et al*. have reported the presence of both monodentate and bidentate carboxylates on the active surfaces of TiO_2 and ZrO_2 catalysts.[60] In their combined experimental and theoretical work, DFT calculations were used to estimate the vibration frequencies (cm^{-1}) of the different configuration modes, as well as their adsorption stability (~ bonding strength) on the surface. Afterwards, infrared spectroscopy of acetic acid at reaction temperature (250 °C) was used to investigate their presence on anatase and rutile TiO_2, and monoclinic ZrO_2. Firstly, IR spectra showed for anatase TiO_2 that two substrate molecules can either bind via a monodentate acetate configuration on one Ti-O pair each, or as bidentate carboxylates on two vicinal pairs. At reaction conditions, there is a marked preference for the first configuration, which is stable at most surface coverages due to the lack of steric repulsion as a consequence of the larger Ti-to-Ti distance on anatase (0.383 nm $d_{Ti5c-Ti5c}$). For the latter, bidentate acetate adsorption becomes less stable with increased coverage, owing to a discrepancy between reagent O-O and surface Ti-to-Ti bond distances. In contrast, the smaller Ti-to-Ti distance for rutile (0.299 nm $d_{Ti5c-Ti5c}$) promotes the coverage of the bidentate carboxylate species, while monodentate acetates on vicinal Ti-O pairs (0.360 nm dTi_{5c-O2c}) experience increased steric repulsion. For monoclinic ZrO_2, molecularly adsorbed acids (H-bonding with lattice O), monodentate and bidentate carboxylates were observed under ketonization conditions. These studies will be discussed further in more detail in section 3.1.2 of this review.

In conclusion, based on the current experimental and theoretical data available in the ketonization literature, we find the following mechanistic points to be most plausible. The C-C coupling is the rate-determining step during ketonization, which goes through a β-ketoacid intermediate formed by an adsorbed enolate and carboxylate. At this point, it cannot be unanimously stated whether the enolate is originating from either a monodentate or bidentate carboxylate, and whether the second carboxylate is in the monodentate or bidentate configuration for the C-C coupling step. More likely, this is situational and dependent on the exact catalytic material used (bond strength and bond distances), as well as the reaction conditions. Additionally, different carboxylate adsorption modes can be present simultaneously on the active surface and in equilibrium with each other under the ketonization conditions.

3.1.2 Active sites

Evidently, the identity of the active surface sites for ketonization on metal oxides is related to the discussion of the mechanism (section 2 of this work) and of the previous paragraph, as they are responsible for the interaction with the carboxylic acid substrate molecules and ketonization products in the numerous elementary steps. Therefore, it is clear that coordinatively unsaturated surface M-O pairs (or derivatives) are the catalytic active sites and they play a crucial role in the ketonization of carboxylic acids.

Still, many different correlations have been reported between the exact nature of these active sites and the physico-chemical characteristics (especially acid-base properties) of the catalysts in question. This debate is further amplified by the often widely varying reactor setups, reaction conditions, catalysts and substrates in these studies. As a result, the ketonization literature is embedded with few contradicting and sometimes confusing conclusions, as demonstrated below. Therefore the purpose of this paragraph is to critically evaluate the abundance of experimental and theoretical evidence regarding this subject and extract from there more general conclusions, as much as this is possible and reliable.

For instance, Ding *et al*. have proposed the significance of acid-base active site balance for the C-C coupling of biomass-derived propionic acid to 3-pentanone on $Ce_xZr_{1-x}O_2$ materials at 270-350 °C.[98] Via XPS, it was shown that the amount of Ce^{3+} and oxygen vacancies increased with Zr incorporation, with the highest ratio for $Zr_{0.5}Ce_{0.5}O_2$. Meanwhile, NH_3 and CO_2 TPD demonstrated that an increased amount of Zr incorporation resulted in an increase of medium Lewis acid site density and strength (coordinatively unsaturated cations). Simultaneously, the density of weak (surface -OH groups) and medium (O^{2-} species from M^{x+}-O^{2-} pairs) base sites increased for Zr loadings of up to 50%, while the density and strength of strong base sites (low-coordination O^{2-} ions) decreased when increasing the amount of Zr for all loadings. Furthermore, the catalyst materials showed different crystal structures depending on the elemental composition, as evidenced by XRD and Raman techniques. Pure CeO_2 and ZrO_2 consisted of fluorite cubic and monoclinic phases, respectively, while $Ce_xZr_{1-x}O_2$ showed cubic and tetragonal structures. Regarding their activity for ketonization, it was found that two maxima existed when plotted against the Zr content: $Ce_{0.9}Zr_{0.1}O_2$ (49.8 $mmol.g^{-1}.min^{-1}$) and $Ce_{0.1}Zr_{0.9}O_2$ (60.3 $mmol.g^{-1}.min^{-1}$). No positive correlations were found between the intrinsic reaction rates and the surface area, the concentration of Ce^{3+} or the concentration of oxygen vacancies, respectively. The same observations were made when correlating with the density of weak, medium, strong and total acid or base sites. However, the authors suggested that the ketonization rate could be related to the ratio of medium strength acid/base sites, with a maximum reaction rate for ratio values around 1, which is the case for $Ce_{0.1}Zr_{0.9}O_2$ only, while $Ce_{0.9}Zr_{0.1}O_2$ had a ratio of approximately 0.8. This would indicate the need for balanced acid-base pairs, both in strength and density, as active centres for carboxylic acid ketonization. Both monodentate and bridging bidentate acetate species were most abundant on the most active catalyst surfaces, with an increasing amount of monodentate species for increased Zr loadings and acidity. Additionally, the monodentate species were more weakly adsorbed on $Ce_{0.1}Zr_{0.9}O_2$. The authors suggest that the connection between these observations might explain the highest reaction rate for $Ce_{0.1}Zr_{0.9}O_2$, for which higher monodentate loadings favour the necessary enolate formation. However, as discussed in section 3.1.1 enolate formation from bidentate species cannot be dismissed yet. Too much and too strong acidity resulted in more and stronger adsorption of 3-pentanone reaction product, as determined via DRIFTS. For the materials with the strongest basicity, lower activity could be attributed to the stronger inhibiting adsorption of CO_2 during reaction. Some important remarks must be made at this point, however. First, the crystal structure may have a possible impact on the observed differences in ketonization activity, which the authors also briefly mention. In fact, we will discuss and demonstrate this in more detail in section 3.1.3 of this review. Indeed, in this study the correlation between activity and the ratio of medium strength acid/base sites was actually largely made for materials with different crystal structures, as mentioned above. Therefore, this direct comparison might not be strictly accurate, and a complex combination of these factors cannot be excluded based on the results. Secondly, the assignment of weak, medium and strong acid-base sites is based on deconvolution of the NH_3 and CO_2 TPD signals in certain temperature regions and therefore relative and based on indirect, if not subjective definition. In this regard, a follow-up study investigating more materials with similar crystal phases and different acid/base properties could provide the necessary ultimate evidence.

At first sight, other if not contrasting conclusions were drawn by Jahangiri *et al*. for the gas phase ketonization of acetic acid on ZrO_2 at 350-400 °C.[99] Here, the impact of calcination temperature during synthesis on the crystallization and ketonization activity was explored. Via calcination, amorphous $Zr(OH)_4$ starting material was converted into small tetragonal nanoparticles at 400 °C (~ 9 nm) and larger monoclinic particles at 600 °C (~15-48 nm). Via XPS and DRIFTS analysis, it was shown that the surface O:Zr atomic ratio decreased from 2.7 to 2.2 for increased calcination temperatures, which was attributed to de-hydroxylation of the surface and formation of anion vacancies (Lewis acidity). The acidity was further probed by both pyridine titration and propylamine temperature programmed reaction, confirming the Lewis acid nature of the materials. Furthermore, increased calcination temperatures led to a higher weak acid site density on the surface, while simultaneously decreasing the acid site strength of the strong acid sites. Interestingly, the acid strength of weak acid sites was not influenced by the calcination temperature. For the catalytic experimental results at 350 and 400 °C, a positive correlation was found between the acetone productivity on surface area basis and the weak acid site density. It was concluded that these weak Lewis acid sites (or their associated unsaturated Zr^{4+}-O^{2-} acid-base couples) are the active species for ketonization. For catalysts with a higher amount of strong Lewis acid sites, lower activity and selectivity was observed with increased formation of carbon cokes, which was attributed to active site blocking via firmly adsorbed bidentate acetate species and oligomerisation side reactions.

While the conclusions of this study might seem different than those of the study by Ding *et al*., both groups actually propose Lewis acid-base M^{x+}-O^{2-} pairs as the active sites for ketonization. Whereas one group used deconvolution of NH_3 TPD to distinguish between weak, medium and strong acid sites, the other used temperature programmed reaction of propylamine with TPD of reactively formed propene. As such an intrinsic difference exists between the terms to describe the acid-base strength. To resolve such issues, it would be interesting to characterize the cited materials in these studies with both techniques, which would allow for a more direct and correct comparison, assuming that other factors such as catalyst surface area, crystal structure, substrate and reaction conditions are adequately similar.

Deriving so-called composition-structure-function relations for carboxylic acid C-C coupling becomes even more complex when different reaction regimes and mechanisms may exist on the same catalyst materials, as suggested by the recent work of Ling *et al*.[74] Here, acetic acid ketonization was performed in a fixed bed reactor at 300-425 °C on Ca/Zn/AlO_x mixed metal oxides (CZA) with various Ca/Zn/Al ratios. For reaction temperatures of 300-350 °C, acetic acid conversion was higher for materials with a higher amount of Al, while between 375-425 °C the catalysts with higher Ca and Zn loadings showed a higher overall conversion rate. Furthermore, it was shown by CO_2 TPD that higher Al loadings resulted in a higher density of weak (surface -OH) and medium base sites (surface M^{n+}-O^{2-} pairs), whereas increasing the calcium and zinc content increased the density of strong base sites (isolated O^{2-} on surface). Based on these experimental observations and available literature, the authors propose that two different ketonization pathways can occur, depending on the reaction regime and catalyst material. At high temperatures (>375 °C) the materials catalyse the reaction via the earlier described bulk mechanism (section 2.1). This typically occurs on highly basic materials, in this case the materials with high Ca and Zn loadings as they provide the required strong base sites originating from CaO and ZnO (Figure 8 top). However, at lower temperatures (<350°C) surface Lewis acid-base pairs (e.g. amorphous calcium aluminates - CaO and Al_2O_3) catalyse the reaction via the β-ketoacid pathway towards ketone, water and carbon dioxide (Figure 8 bottom). It must be noted that the proposed pathways in Figure 8 are not based on experimental evidence provided in the study for the presence of the adsorbed species (by infrared spectroscopy for example). Additionally, no kinetic parameters were determined and no suggestion was made regarding the rate-limiting step in either pathway. It is also not entirely clear whether both pathways could occur simultaneously on the same material to a varying degree, depending on the reaction conditions. Still, these observations indicate surface M^{n+}-O^{2-} pairs as active sites for ketonization. Perhaps more importantly, it shows that the complexity of the surface chemistry involved in the C-C coupling reaction may increase even further when mixed metal oxides are used. Incorporation of metals with different acid-base properties opens up the possibility of different reaction regimes on the same material. More examples of experimental ketonization studies with determination of the active sites and derivation of their structure-function correlations will be discussed throughout this work in the next sections.

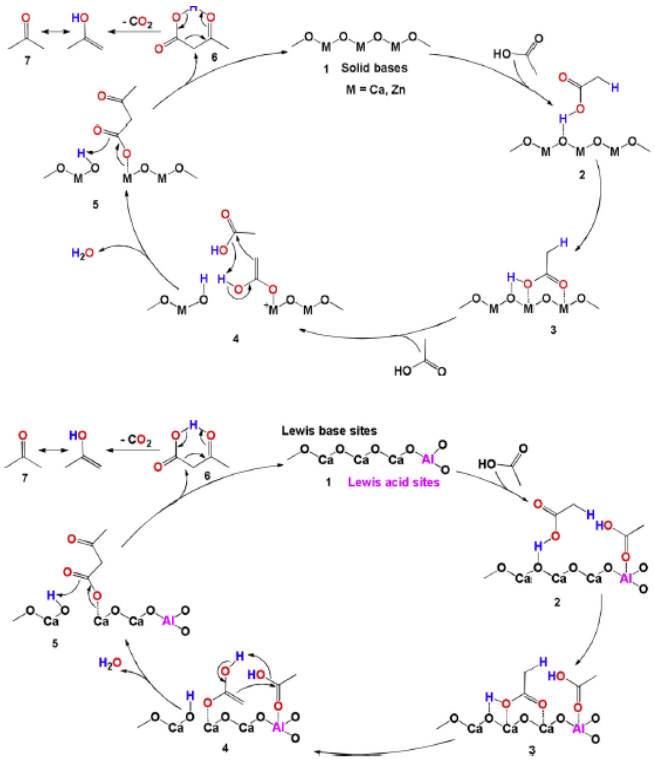

Figure 8: Proposed mechanism of ketonization on CZA catalysts at high (top) and low (bottom) temperatures as presented by Ling *et al*. Reprinted from [74], Copyright (2019)

As already partially discussed in section 3.1.1, extensive experimental and theoretical work has been done by the group of Wang *et al*. who studied the gas phase coupling of C_2-C_4 acids on anatase and rutile TiO_2[60], and monoclinic and tetragonal ZrO_2[87] at 230-260 °C. Unlike most studies, which almost exclusively discuss the differences in observed ketonization activity in terms of acid-base site density and/or strength, the Ti_{5c}-O_{2c} and Ti_{5c}-Ti_{5c} bond distances were also studied in this work as a potential contributing factor. Their experimental results showed that for TiO_2, the anatase material was more active for C-C coupling of acetic acid than rutile per acid-base pair (unsaturated Ti_{5c}-O_{2c}) with a factor of 5 for the initial turnover rate at 250 °C. Determination of the acid-base density of both catalysts was performed by titration with propanoic acid during acetone condensation reactions, which is different than the more common techniques such as NH_3 TPD and pyridine IR. Anatase showed the highest density of acid-base pairs with a value of 3.7 pairs per nm² *versus* 1.7 pairs per nm² for rutile TiO_2. However, it should be noted that these values are

based on the assumed difference in preferred adsorption configuration, as discussed previously in section 3.1.1. As a result, the authors used titrant stoichiometries of 1 (monodentate binding) and 2 (bidentate binding) Ti-O pairs per acid molecule for anatase and rutile, respectively. Therefore, the authors dismiss the possibility of interconversion between different configurations and their potential contribution to the observed ketonization rate. The observed differences in activity were further explored via DFT calculations for the most common (101) anatase and (110) rutile surfaces (Figure 9). The Lewis acid-base strength of both materials was evaluated by theoretical gaseous OH^- and H^+ affinity calculations by DFT. This study indicated that for anatase only Ti centres with fivefold coordination (Ti_{5c}) possess the necessary acid strength to bind with adsorbed species, while both O_{3c} and O_{2c} atoms can interact as base sites. The Ti_{5c} centers also have a weaker Lewis acidity (less negative OH^- affinity) compared to rutile, while in contrast the O atoms possess a stronger basicity. Due to the different crystal structure of rutile (Figure 9), the Ti_{5c} sites are only directly connected to O_{3c} atoms, shortening the distance between neighbouring Ti_{5c} while increasing the distance with O_{2c} atoms compared to anatase. Based on all experimental and theoretical evidence discussed, the higher activity of anatase compared to rutile was attributed to the preferential adsorption of active monodentate carboxylates and stronger transition state stabilization due to intermediate Lewis base-acidity and more favourable $d_{Ti5c\text{-}Ti5c}$ and $d_{Ti5c\text{-}O2c}$ bond distance values. respectively. This results in decreased steric hindrance of the C-C coupling transition state (TS) with additional stabilization due to hydrogen bonding with surface OH. The lower activity of rutile TiO_2 was explained by adsorption of stable, unreactive bidentate spectator species and increased steric repulsion of the C-C coupling TS with decreased stabilization due to stronger Lewis acidity, shorter $d_{Ti5c\text{-}Ti5c}$ and longer $d_{Ti5c\text{-}O2c}$ values. As such, it was concluded that the $Ti_{5c\text{-}O2c}$ and $Ti_{5c\text{-}Ti5c}$ distances (and also the Lewis acid-base strength) were the driving forces to explain the ketonization performance. To the best of our knowledge, no other groups have investigated or correlated the observed ketonization activity on the basis of (mis)match of substrate and lattice bond distances during adsorption and C-C coupling steps in this manner. The work on monoclinic and tetragonal ZrO_2 will be discussed in the next paragraph.
From these discussions of section 3.1.2 (together also with previous and next paragraphs) we may conclude that the active sites for ketonization of carboxylic acids on metal oxide surfaces are coordinatvely unsaturated M^{x+}-O^{y-} Lewis acid-base pairs. Regarding

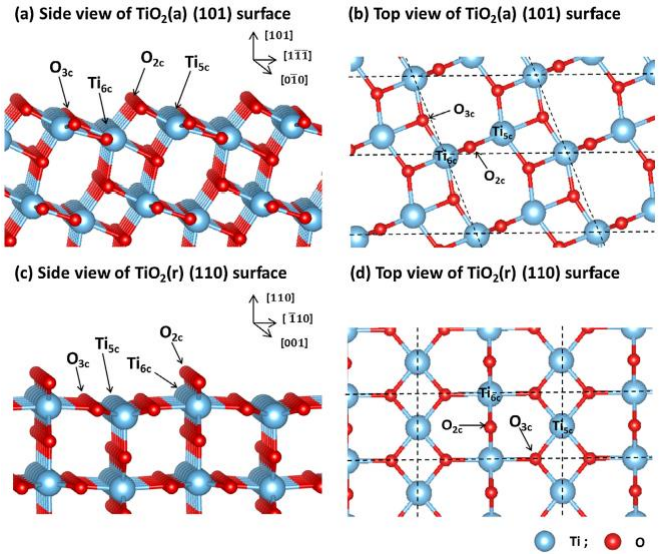

Figure 9: (101) anatase and (110) rutile surfaces of TiO_2 as drawn by Wang *et al.* Reprinted from [60], Copyright (2017) with permission from Elsevier.

material properties (and setting aside reaction conditions), the differences in activity, selectivity and stability between catalysts are related to atleast two and possibly three or more defining factors. The amount of active surface Lewis acid-base pairs determines among other factors the potential for substrate adsorption. Their acid-base strenght does not only determine the energy of the binding interaction with substrates, but also with the ketone product, CO_2, water and other side products (if present). While currently the amount of research and evidence is still scarce in literature, it seems reasonable to acknowledge that M-M and M-O bond distances could play a significant role given the nature of the C-C coupling reaction and its mechanism. This interesting research area could provide helpful insights in the future. A significant amount of confusion and (apparent) contradictions is still present, partially due to the difference in experimental determination of Lewis acid-base pairs and their strength. Different characterization techniques (TPD, TPR, titration, IR with different probe molecules) of similar materials yield different absolute values, without the possibility for interested readers to directly compare them between studies. This situation becomes even more problematic when the same techniques are used on similar materials which still yield different results. For instance, in the case of pyridine IR studies because different research groups use different extinction coefficient values based on reported literature values which may have actually been obtained under different experimental conditions (such as temperature). No general consensus exists on the assignment of the terms weak, medium and strong acidity and/or basicity, which further contributes to this discussion. Finally, as we will show in the next paragraph, metal oxides and their associated surface chemistry

are inherently complex topics because different synthesis methods may yield vastly different end products, even when starting from the same precursors.

3.1.3 Catalyst morphology, structure and crystal phase

To determine the influence of catalyst morphology, Lee *et al*. synthesized porous ZrO_2 aerogel materials with different specific BET surface areas by manipulating the calcination temperature (500-1200 °C).[38] An increase in calcination temperature led to a decrease in surface area (from 103 to 2 m^2/g), larger pore width, smaller total pore volume and varying acidity per surface area (5.1-7.0 $\mu mol/m^2$) as determined by NH_3-TPD. In the gas-phase ketonization of hexanoic acid, positive correlations were found between the 6-undecanone yield and BET surface area, total acidity and total basicity, with a large positive deviation (higher ketone yield than expected) from linearity for the material that was calcined at 800°C and showed larger mesopores (~35 nm). The authors therefore concluded that both higher surface area and improved mass transfer to the active sites via larger pores were the determining factors for ketonization performance. While the latter statement does sound reasonable for porous materials, we must note that it was also shown via XRD that the zirconia aerogels consisted of both monoclinic and tetragonal phases, with a larger amount of the monoclinic structure for higher calcination temperatures. Therefore, strictly speaking a 1:1 comparison cannot be made regarding the impact of pore structure on activity as materials with different crystal structures were compared. Furthermore, the sample size is too small as these conclusions were drawn based on one outlier (material calcined at 800 °C). Similarly, Wu *et al*. have reported on the effect of porosity and crystal morphology when studying the aqueous phase ketonization of acetic acid with $ZrMnO_x$ catalysts.[100] With Zr-O-Mn as proposed active sites, it was shown that increasing the oxidation temperature and time (up to 550 °C and 24 hours) during synthesis via a carbonization-oxidation method led to a higher amount of highly dispersed Mn^{4+} into smaller ZrO_2 catalyst crystals with a larger amount of exposed surface atoms. As a result, an accompanying increase in Lewis acidity had a positive effect on the ketonization performance of acetic acid in water at 340 °C and 190 bar. This extremely high reaction pressure was necessary to ensure liquid phase ketonization conditions. Furthermore, when changing from water to a water-ethanol mixture and ethanol as thermal treatment solvent during material synthesis, an increase in acetone yield was observed (52 *versus* 62 *versus* 64%, respectively) under identical reaction condition for the final materials. This was attributed to higher surface area (84, 106 and 147 m^2/g), Lewis acid density (0.089, 0.117 and 0.228 mmol/g) and larger pore volume (0.285, 0.376 and 0.719 cm^3/g) and average pore sizes (13.3, 13.7 and 16.2 nm). However, the catalytic results for the material synthesized in ethanol do not match/support these conclusions, as the acetone yield was nearly identical to that of the material synthesized in the water-ethanol mixture, which showed significantly different material properties. Limited substrate concentration and accessibility to the acid sites were proposed by the authors to explain this observation. However, it is not clear why this suggestion was made, and especially only for the material in question, since it showed the largest pore volume and average pore size of all materials. Bennett *et al*. have also investigated the importance of highly dispersed small active particles when using supported catalysts for carboxylic acid ketonization.[101] When employing Fe_3O_4/SiO_2 materials for acetic acid ketonization at 300-450 °C, an increase in magnetite loading from 4 to 63 wt% increased catalyst particle size, while simultaneously decreasing the surface area. An inverse relationship was found between acid site density per mass (as determined by propylamine TGA-MS) and particle diameter of the Fe_3O_4 phase. When correlating with the mass-based ketonization rate and acetone yield, it was found that larger Fe_3O_4 particles exhibited lower acetone production. Furthermore, no correlation was found between turnover frequency (TOF) per acid site and magnetite particle size, indicating the structure-insensitive nature of carboxylic acid ketonization on these materials.

As discussed, not only the active phase but also the support material and their interaction are important considerations that have to be taken into account when choosing appropriate supported catalysts for C-C acid coupling. Indeed, Wu *et al*. have shown the aqueous phase ketonization of acetic acid in a batch reactor on various ZrO_2/C catalysts, synthesized by either hydrolysis of organic zirconium in the presence of carbon nanotubes (CNT), carbonization of Zr-based UiO-66 metal organic framework (MOF) materials or carbonization after sol-gel synthesis with citric acid.[52] For the carbonized samples, a higher amount of carbon increased the amount of poorly crystallized tetragonal ZrO_2. Both the carbon content and nature of the crystal phase seemed to be important for the ketonization activity under reaction conditions (340 °C), with an increased acetone yield for carbonized catalysts. When comparing carbonized samples to ZrO_2/CNT, the authors found smaller and more active highly dispersed *t*-ZrO_2 phases on the carbonized supports. Furthermore, weaker interaction between the active phase and support was observed for the CNT materials. Thirdly, the higher aqueous phase ketonization activity of carbonized catalysts was linked to enhanced acetic acid adsorption and decreased water inhibition as a result of the more hydrophobic nature of the catalyst support. Likewise, Pham *et al*. have reported the liquid phase ketonization of acetic acid on $Ru/TiO_2/C$ catalysts in water, n-hexane and N-methyl pyrrolidine solvents at the remarkably low temperature of 180 °C.[64] For all reaction solvents, $Ru/TiO_2/C$ was more active than TiO_2/C and Ru/TiO_2 per mass TiO_2 in the catalyst material , while for all three catalysts acetic acid conversion was highest when organic solvents were used as reaction medium. Also in this case, the hydrophobic activated carbon support is suggested to increase acid adsorption and decrease deactivation caused by water inhibition, which is crucial when aqueous phase bio-oil ketonization is required. While these assumptions sound reasonable, as activated carbon is used to adsorb organic molecules from water media for example, no direct evidence was given to further support the claims of both studies. Related to this discussion, Lopez-Ruiz *et al*. reported the enhanced hydrothermal stability and activity for the aqueous liquid phase ketonization of acetic acid on $La_xZr_yO_z$ catalysts.[63] The activities ($mmol/g_{cat}*h$) of these mixed metal oxides were 265 and 45 times higher at 295°C than parent La_2O_3 and

ZrO_2,respectively. Interestingly, their activity initially increased with longer time-on-stream, while both parent materials showed faster deactivation (and therefore lower stability). It was shown via SEM, STEM, XRD and XPS techniques that under the hydrothermal reaction conditions, the original amorphous samples underwent crystallization to a stable phase, which was isomorphic to t-ZrO_2 (Figure 10). Via TPD-DRIFTS, it was shown that these active materials exhibited larger amounts of adsorbed acetate species under hydrothermal conditions than ZrO_2, which could explain their higher ketonization rates in hot liquid water. Additionally, not all band signal intensities remained constant for adsorbed species when comparing them in the presence and absence of water, suggesting the possibility that H_2O may inhibit adsorption/formation of specific adsorbed acetate species. It must also be noted that a decrease in La:Zr ratio was observed early on during reaction for catalysts with initial ratios higher than 0.17 due to solubilization of excess La.

The specific crystal phase composition and morphology of the active material can be important when selecting a suitable ketonization catalyst (evidenced by the discussion in section 3.1.2). Analogue to their work on anatase and rutile TiO_2, Wang *et al*. have studied the gas phase coupling of C_2-C_4 acids on monoclinic and tetragonal ZrO_2 at 230-260 °C.[87] Monoclinic zirconia is the

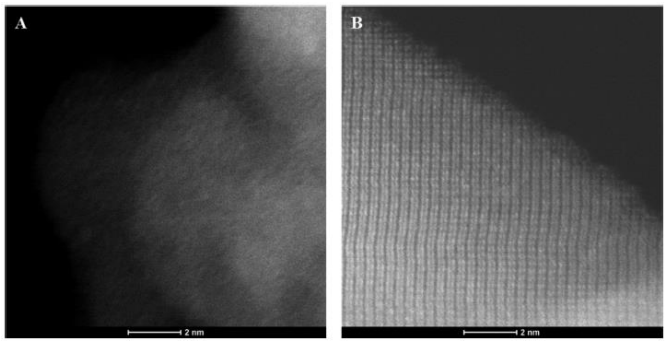

Figure 10: STEM of $La_xZr_yO_z$ materials before (A) and after (B) liquid phase hydrothermal ketonization conditions (10 wt% acetic acid in water, 9800 kPa, 295 °C) as reported by Lopez-Ruiz *et al*. Reprinted with permission from [63], Copyright (2017) American Chemical Society.

most stable phase at room temperature, with phase transformation to tetragonal ZrO_2 at ~ 1200 °C. Stabilization of the tetragonal phase at room temperature is possible, however, by addition of impurities such as divalent or trivalent cations (cfr. mixed metal oxides).[92] The ketonization rate of acetic acid was higher on *m*-ZrO_2 (1.43 ks^{-1}) compared to *t*-ZrO_2 (1.15 ks^{-1}) at 250 °C and 3 kPa acetic acid pressure. Unfortunately, this was not further investigated by the authors as the remaining part was solely dedicated to the monoclinic material and its comparison against anatase TiO_2. In a different study by Foraita *et al*., the conversion of stearic acid was ~1.3 times higher on *m*-ZrO_2 compared to *t*-ZrO_2 after 6 hours at 260 °C in dodecane solvent under 40 bar H_2 (29 *versus* 21% conversion).[102] The selectivity values to stearone (C_{35} ketone) were low, however, showing values of 18 and 22%, respectively. It was shown here that *m*-ZrO_2 had a higher concentration of adsorbed acid compared to *t*-ZrO_2, which was assigned to a higher number of defect sites (higher oxygen exchange ability as determined by temperature-programmed isotope exchange experiment). This limited amount of experimental results may indicate that, in addition to its higher crystal structure stability at typical reaction conditions, pure *m*-ZrO_2 is more active than pure *t*-ZrO_2 for carboxylic acid ketonization. Investigation of *t*-ZrO_2 is still valuable and necessary, however, as mixed metal oxides like CeO_2-ZrO_2 are (mainly) composed of tetragonal zirconia (nano)crystals.

Fernández-Arroyo *et al*. created highly faceted {001} anatase TiO_2 materials via hydrothermal synthesis with HF as capping agent, as determined by XRD, HRTEM and Raman techniques.[103] These catalysts were compared to commercial P25, anatase (mainly consisting of thermodynamically stable (101) phase) and rutile samples for the catalytic condensation (including ketonization) of an aqueous bio-oil model mixture containing acetic acid, hydroxyacetone, ethanol and propanal in a batch reactor at 200 °C and 13 bar N_2. Both initial activity and total organic product yield after a 7 hour reaction were highest for the (001) materials, which was attributed to their higher Lewis acid density originating from a higher concentration of unsaturated five-coordinated Ti_{5c} centres compared to the thermodynamically more stable (101) anatase facet. Furthermore, their stability in the aqueous reaction medium was enhanced compared to the commercial samples, which was assigned to their higher hydrophobicity due to the presence of (catalytically inactive) fluorine species originating from the HF treatment. These results indicate that tailored synthesis of specific crystalline structures and morphology may be a new approach to improve the performance of metal oxides. Whereas the catalysts of the previous study were still composed of multiple crystals, Kim *et al*. have studied the high temperature deoxygenation, dehydration and ketonization of acetic and propanoic acid on TiO_2 (001) single crystal surfaces via TPD in an older report.[79] These single crystals were synthesized via Ar^+ bombardment techniques. It was shown that the selectivity of acid conversion was dependent on both the structure and composition of the surface. After dissociative adsorption to a carboxylate, which was not influenced by the surface nature, direct deoxygenation occurred on the sputtered reduced surfaces with low valence Ti species and oxygen vacancies (determined by XPS). For oxidized surfaces with Ti^{4+} cations, unimolecular dehydration to ketene was observed on the {011} faceted surface with fivefold coordinated Ti ions, while ketonization was promoted on the {114} faceted

surface that consisted of stoichiometric fourfold coordinated Ti^{4+}. The authors proposed bimolecular monodentate adsorption for this crystal type, although we have already discussed in sections 3.1.1 and 3.1.2 that this is highly unlikely due too excessive steric repulsion. The authors also provided no experimental data to further support this claim (by IR, for instance). Furthermore, comparison between single and multi-crystal materials is not straightforward, and we have already pointed out the caveats and limitations of using TPD to study catalytic reactions. Still, the data indicate that different crystal surfaces show different catalytic activity. Heracleous *et al*. have used DRIFTS-TGA-MS as an experimental tool to determine the activity of nanostructured FeO_x and MnO_x catalysts during the ketonization of acetic and propionic acid, and aqueous pyrolysis bio-oil mixtures at 335 °C.[62] Interestingly, no correlation was found between surface coverage and ketonization activity, as the most active materials (nanocast Fe_2O_3 and hydrothermal MnO_2) showed lowest vibrational band intensities for adsorbate species. Therefore, it was postulated that the parent materials are not the actual catalysts but rather precursors, which are transformed to their active phases under reaction conditions. By TGA-MS, only unreacted acetate desorption was observed for MnO_2 with no acetone production, while both unreacted species and ketonization products were identified for the Fe_2O_3 materials. Via TPR and postreaction XRD and XPS, it was shown that unreactive MnO_2 undergoes complete in-situ reduction to the active MnO phase under reaction conditions, which showed a larger band intensity for adsorbed acetate species. Similarly, it has been shown before that Fe_2O_3 is (partially) reduced to (more) active Fe_3O_4 under reaction conditions.[104]
In conclusion, it can be stated that metal oxides can contain multiple crystalline surfaces with different reactivity. Additionally, local structures such as edges, steps, etc. result in a complex reaction environment due to the presence of point defects, vacancies, heteroatoms and trapped electrons. Single crystals and nanosized oxide materials can exhibit different properties compared to their bulk analogues as a result of their low dimensionality. This may impact their ketonization performance as they may expose other crystallographic surfaces.

3.1.4 Catalyst modification

Over the years, several synthesis methods, pre-treatments and post-synthetic modifications have been explored to further enhance the overall ketonization performance of (mixed) metal oxide catalysts, which can encompass improvement in activity, selectivity, stability or ideally combinations thereof. The main routes to achieve this will be discussed in this section and include doping with other transition metals and oxides, surface reduction and calcination pre-treatments and impregnation with (noble) metals that exhibit hydrogenation capacities to induce so-called hydrogen spillover effects.
When looking at Tables 1,3 and 4, it is obvious that doping of metal oxides to generate (supported) mixed metal oxides is the most common of these suggested strategies. The initial screening study by Glinski *et al*. can perhaps be viewed as the pioneering work in this field, in which the authors tested 20 different oxides supported on silica, titania and alumina for the gas-phase ketonization of acetic, propanoic and butyric acid.[105] In this work, CeO_2 and MnO_2 on silica were found to be the most active materials, with higher loadings leading to higher ketone yields. Although the positive effect of metal doping on ketonization activity was presented, no further discussion was conducted to link the observational work with the catalysts' properties and potential active sites. More recently, Lu *et al*. have for instance investigated the effect of Ti doping of CeO_2 materials via a homogeneous precipitation method for the gas-phase ketonization of acetic acid at 280-350 °C.[106] An increased conversion was observed at all temperatures for Ti loadings of 10 and 30%, compared to both pure CeO_2 and TiO_2 parent materials, although a further increase to 50 and 70% was detrimental for the catalytic activity. Furthermore, the most active $Ce_{0.7}Ti_{0.3}O_x$ material, the activity of which was also dependent on calcination temperature during synthesis, exhibited superior stability with time on stream compared to bare CeO_2 for at least 8 hours. Compared to the parent materials, the more active mixed metal oxides showed improved adsorption and facilitated activation of acetic acid molecules on the surface due to the higher amount of surface oxygen vacancies and higher surface density of weak acid-base Ce-O-Ti active pairs, as determined by TPD, FT-IR, TPR, XPS, Raman and XRD techniques. When too high Ti loadings were used, the ketonization activity was lowered due to a higher density of strong acid-base surface sites and breaking of desired Ce-O-Ti bonds due to formation of pure TiO_2 particles. Similarly, the same authors have also shown the promoting effect of Fe when preparing $Ce_{1-x}Fe_xO_y$ (x=0.1-0.7) catalysts for the gas-phase coupling of acetic and propionic acid with analogue conclusions in a different publication.[107] To further link ketonization performance and the impact of metal oxide doping, Sudarsanam *et al*. have performed the cycloketonization of dimethyl adipate to cyclopentanone on $Ce_xZr_{1-x}O_2$, $Ce_xZr_{1-x}O_2/SiO_2$ and $Ce_xZr_{1-x}O_2/Al_2O_3$ catalysts.[42] Here, dimethyl adipate conversion and cyclopentanone yield increased when incorporating Zr into CeO_2 materials, with the highest activity for alumina supported materials. The structural and textural properties and redox potential of $Ce^{3+/4+}$ were screened by Raman spectroscopy, Williamson-Hall analysis of XRD data and oxygen storage/release capacity (OSC) determination via thermogravimetric methods. It was shown here that ketonization activity was positively correlated with the amount of oxygen vacancy defects, crystal lattice strain and OSC as a result of structural defects arising from mixed metal oxide synthesis. Some interesting observations were made by Snell *et al*. for the liquid phase batch ketonization of acetic acid in toluene solvent with several $CeMO_x$ catalysts (M= Mn, Fe, Al, Zr).[46] After screening their ketonization activity, it was shown that there was no correlation between acid conversion and catalyst properties such as BET surface area, degree of reducibility, or Ce^{3+} content. Different ketonization regimes were observed, however (see also section 2.2), depending on the combination of reaction temperature and nature of the incorporated metal. For intermediate temperatures (230 °C) $CeZrO_x$ and CeO_2 showed the highest acid conversion, while at a higher temperature (300 °C) $CeMnO_x$ and $CeFeO_x$ were most active. Via post-reaction catalyst characterization, it was suggested that the activity was related to the susceptibility of metal acetate formation,

which is preferred at intermediate temperatures, *versus* the efficacy of further decomposition to ketone, which is favoured at higher reaction temperatures. These factors depend on the M-O bond strength and therefore on the identity of the incorporated metal. Interestingly, no mention is made of potential metal (dopant) leaching in these publications. This topic should not be ignored tough, and will be discussed further throughout this work. For additional literature on the effect of metal oxide doping for ketonization, the reader is amongst others referred to the collection of listed references.[43, 65, 70, 108-110]

Surface reduction via pre-treatment has been shown to be another strategy to improve the ketonization performance of metal oxide catalysts. Already in the 1970s, Jewur *et al*. have presented the impact of hydrogen pre-treatment on iron oxide materials for the gas-phase ketonization of acetic acid at 360-440 °C.[104] In this early work, a 15 minute hydrogen treatment at 500 °C doubled the acid conversion rate compared to the fresh parent material under similar reaction conditions. On the other hand, both air and oxygen treatments at 500 °C for 2 hours had a negative impact on the ketonization activity. The improved acetic acid conversion was linked to the partial/gradual transformation of the original hematite (α-Fe_2O_3) material to magnetite (Fe_3O_4) species, which was shown to be dependent on total reduction time. For long reductions (>3.5 hours), free iron (Fe) was also formed. Here an increase in activity was observed for increased Fe^{2+}/Fe^{3+} ratios, up to an optimal value of 0.5, after which acetic acid conversion dropped for higher Fe^{2+} loadings. Very recently, Weber *et al*. have studied the influence of reduction and the redox state of red mud and Fe/SiO_2-Al_2O_3 catalysts on the ketonization of pyrolysis bio-oil.[111] These red mud materials, which are waste products of the mining industry, are complex iron-based materials that also contain various other metal compounds such as Al, Ca, Na, Si, K and Mg. After reduction at 300, 400 and 500 °C, these catalysts were tested in the gas-phase ketonization of bio-oil at 400 °C in a fixed bed reactor. Via Mössbauer spectroscopy, it was shown that these reduction methods convert the parent hematite material into mixtures of goethite (FeO(OH)), magnetite and metallic iron depending on pre-treatment temperature. Furthermore, both the catalysts' surface areas and pore volumes were increased in all cases compared to the parent material. Based on NH_3-TPD analysis, it was shown that higher reduction temperatures increased the density of weak acid sites, while simultaneously reducing the amount of strong acid sites. Based on the catalytic results, the red mud material that was reduced at 300 °C showed the highest ketonization activity and selectivity. This was attributed to a combination of both a higher and lower amount of magnetite and metallic iron species, respectively. For higher reduction temperatures enhanced coking, reduced liquid carbon balance, and lower activity and selectivity were observed. According to the authors, these findings could be ascribed to the lower levels of strong acid sites, loss of strong basic sites and decreased amount of magnetite phase. As mentioned before, CeO_2, ZrO_2 and TiO_2 have often been proposed as the most suitable catalysts for carboxylic acid ketonization due to their high activity and selectivity. To investigate the potential of surface reduction and understand its effects on a molecular level, Tosoni *et al*. have performed DFT+U calculations for the ketonization of acetic acid on the tetragonal (101) ZrO_2 surface.[92] In this work, the energetics of the elementary steps in the β-ketoacid reaction mechanism were determined and compared for stochiometric and hydrogenated ZrO_2, as well as ZrO_2 with oxygen vacancies. The considered reaction pathway included the initial adsorption of acid and formation of the respective enolate intermediate ($\mathbf{CH_2COO^{2-}_{(ads)}}$), formation of the acyl intermediate ($\mathbf{CH_3CO^{-}_{(ads)}}$) from a second acid molecule, and finally the C-C coupling reaction between the acyl and enolate species to the β-ketoacid (see section 2.2.4 of this work for more details). Firstly, it was shown that on the non-reduced stochiometric *t*-ZrO_2 surface, the creation of enolate intermediate after acid adsorption is an uphill process (E_b of reactants is lower than E_b of products) with a high activation energy. Furthermore, stabilization of the acyl intermediate is hindered due to its oxygen and electron deficient nature, leading to the recreation of CH_3COO^-. Both phenomena lead to the overall lower ketonization performance on non-reduced ZrO_2. While the reduction of bulk ZrO_2 is difficult due to the high energy cost of oxygen vacancy formation (up to 6 eV), reduction of surface sites via strategies such as hydrogen spillover to produce protons and Zr^{3+}, reverse oxygen spillover and water desorption remain viable. For hydrogenated zirconia nanoparticle surfaces, the authors propose homolytic dissociation of hydrogen which leads to the formation of two protons (H^+ bound to O^{2-} ions) and two Zr^{3+} sites. This behaviour of nanoparticles is different than heterolytic dissociation of hydrogen, which leads to the formation of a proton and an hydride (H^- bound to a Zr^{4+} species). The presence of Zr^{3+} ions showed no significant influence on enolate formation. However in this case, an adsorbed acetate species can be moved to the vicinity of a Zr^{3+} cation, where the carboxyl C-O bond is cleaved and the O atom interacts with a surface proton. As a result, a stabilized adsorbed acyl radical fragment can be formed ($\mathbf{CH_3CO^{*}_{(ads)}}$) with a local potential energy minimum (+0.76 eV activation barrier) due to transfer of the unpaired electron of Zr^{3+} to the acyl fragment, which transforms the Zr^{3+} to Zr^{4+}. This results in a higher ketonization surface reactivity compared to that of non-reduced surfaces. The authors state that it remains to be understood how these Zr^{3+} active centres are re-generated during the catalytic cycle. Also, no mention is made regarding potential side reactions of the radical fragments, such as dimerization for instance. Surfaces with oxygen vacancies ($\boldsymbol{V_0}$), for example as a result of water desorption, showed high stabilization of the enolate fragment with a low energy barrier for enolization (+0.53 eV). Due to the excess electrons of the oxygen vacancy in this case, a H atom of $\mathbf{CH_3COO^{2-}_{(ads)}}$ is transferred to $\boldsymbol{V_0}$ with formation of a hydride species ($\mathbf{H^-}$) with -0.63 |e| Bader charge (eq. 7). The authors do not mention, however, whether this hydride could potentially recombine with the adsorbed surface proton to form hydrogen (H_2). Related to this, regeneration of the active centres (oxygen vacancies) and closing of the catalytic cycle is not yet fully understood, although some suggestions that relate to water desorption of hydroxylated surfaces under reaction conditions, were made by the authors. Elsewhere, it has been reported that some oxygen vacancies of ZrO_2 are highly reactive to homolytic H_2 dissociation via DFT calculations.[112] This may also occur if H_2 is formed, resulting in two hydride Zr-H species next to the vacancy. This may complicate the surface chemistry even further, and clearly more investigation is required on this subject to provide clarity. The materials with oxygen vacancies also had a dramatic

impact on the formation of the acyl intermediate (eq. 8) by rendering this step exothermic (-0.35 eV), which is impossible on stochiometric ZrO_2 surface and endothermic on hydrogenated *t*-ZrO_2 (+0.76 eV). Both effects ultimately result in a higher ketonization activity compared to bare ZrO_2. Finally, the authors calculated the lowest energy barrier for the C-C coupling step on the hydrogenated surface (0.4 eV) when compared to the surface with oxygen vacancies (1.03 eV), suggesting its higher overall reactivity. The same group has also discussed similar work on the positive impact of surface reduction of TiO_2 on the deoxygenation of phenol.[113]

$$CH_3COOH_{(g)} + V_O^0 \rightleftharpoons CH_3COO^-_{(ads)} + H^+_{(ads\ O)} + V_O^0 \rightleftharpoons CH_2COO^{2-}_{(ads)} + H^+_{(ads\ O)} + V_O^{2+}/H^- \qquad (eq.7)$$

$$CH_3COOH_{(g)} + V_O^0 \rightleftharpoons CH_3COO^-_{(ads)} + H^+_{(ads\ O)} + V_O^0 \rightleftharpoons CH_3CO^-_{(ads)} + OH^-_{(ads\ Zr)} + V_O^{2+} \qquad (eq.8)$$

The third route towards more active ketonization materials is related to the discussion above and involves the addition of (noble) metal species with hydrogenation capacities such as Ru, Pd, Pt or Ni on the active phase of the ketonization catalyst. Aranda-Pérez *et al*. have reported the liquid phase ketonization of acetic acid on 5% Ru/TiO_2 catalysts in a batch reactor at 200-220°C with *n*-hexane or water as reaction solvent.[53] Three different commercial TiO_2 materials were used: anatase, rutile and P25 (80:20 mixture). Via energy dispersive X-ray (EDX) and high-resolution transmission electron microscopy (HR-TEM) Ru particle sizes were determined to be 3-7 nm on average with smaller cluster sizes for the rutile support compared to anatase, and thus higher metal dispersion (31 *versus* 12%). These findings were attributed to the difference in metal-support interaction, as rutile and anatase possess different crystallographic structures and electronic properties (see section 3.1.2). Based on prior studies performed on Pt/TiO_2, the authors propose favourable interfacial lattice matching between RuO_2 and rutile TiO_2, resulting in more stable Ru-O-Ti bonds during calcination. Furthermore due to the lower energy of formation of oxygen vacancies for rutile, a stronger interaction between the metal and oxygen vacancy is achieved during the reduction step of the synthesis procedure. Via hydrogen consumption during TPR analysis the percentages of reduced TiO_2 were calculated to be 20 and 35% for anatase and rutile, respectively, indicating higher intrinsic reducibility and density of unsaturated Ti^{3+} cations on the rutile surface, in addition to the favourable Ru nanocluster interactions for hydrogen spillover. However, at this point it is important to point out that the X-ray microfluoresence (XRMF) results also showed that the actual Ru loading of both materials differed from the target 5%, with values of 3.9 and 6.9% for the anatase and rutile support, respectively (the authors used these actual values to determine degree of reduction). As such, strictly speaking this does not allow a direct 1:1 comparison between both TiO_2 support materials. Ultimately, these factors led to a higher acid site density per surface area for 5% Ru on rutile, corresponding to 12.48 v*ersus* 5.47 μmol NH_3/m^2 respectively, as opposed to the higher acid density per catalyst mass for anatase due to its higher initial surface area, viz. 23 *versus* 114 m^2/g. When comparing catalytic activity, TOFs of acetic acid coupling in liquid hexane were highest for 5% Ru on rutile for all reaction temperatures between 200-220°C (factor 1.5-4 compared to anatase), which was suggested to be a result of the combination of the higher density of Ti^{3+} active sites and the reduced Ti-to-Ti distances. Because C-C coupling is a bimolecular reaction between two adjacent adsorbed substrates, a decrease in intermolecular distance could improve the ketonization activity according to the authors. However, the work of Wang *et al*. (that was discussed in sections 3.1.1 and 3.1.2) argued the exact opposite, i.e. the reduced Ti-to-Ti distances were used to explain the lower ketonization activity of rutile TiO_2 compared to anatase, due to increased steric repulsion of the substrate molecules and less stabilization of the transition state. Clearly, both studies are significantly different from each other on at least two crucial points. First, the reaction medium is different, i.e. gas phase *versus* condensed phase ketonization chemistry. Secondly, in the study by Wang *et al*. pure TiO_2 materials are used, while in this case 5% Ru/TiO_2 catalysts are employed (although it was shown that Ru is not intrinsically active for ketonization). These contradicting conclusions drawn from catalytic studies under different conditions do not allow us to directly state whether anatase or rutile TiO_2 is the most active crystal phase for carboxylic acid ketonization at this point. Unfortunately, the intrinsic activities of anatase and rutile without Ru loading were not reported, as this could have provided additional information on this topic. Further research is therefore required in this area to possibly generate more general conclusions in the future. When the same materials were tested in the aqueous phase, no ketonization activity was observed for the anatase and P25 materials, while 5%Ru/TiO_2 (rutile) preserved 87% of its activity compared to the results in *n*-hexane. This was linked to the higher hydrophobicity of rutile (as shown by contact angle measurements) compared to anatase, which can be more prone to both water inhibition and water-induced structural collapse at high temperatures. While the authors did not provide direct evidence, they suggest that the higher hydrophobicity of rutile may be the result of a lower surface -OH concentration. Finally, the stability of the 5% Ru/TiO_2 rutile catalyst was demonstrated as it could be reused at least 3 times in the aqueous phase reaction without significant loss of activity or selectivity. Pham *et al*. have also used Ru/TiO_2 and Ru/TiO_2/C catalysts for the aqueous phase ketonization of acetic acid.[41, 64, 90] Via EPR, XPS and TPR techniques, it is suggested in these publications that, in general, incorporation of Ru facilitates and accelerates the formation of active Ti^{3+} species. For additional literature on the deposition of Ru clusters on TiO_2 and ZrO_2 for biomass conversion reactions, its electronic effects and hydrogen spillover, the reader is referred to the work of Tosoni *et al*.[113] To the best of our knowledge, no reports have been published on the use of Pd, Pt or Ni on metal oxides with ketonization as main target reaction.

3.1.5 Side reactions and catalyst stability

While materials such as ZrO_2, TiO_2 and CeO_2 can (often) catalyse the ketonization of carboxylic acids with full selectivity to the target ketone product, several side reactions can occur simultaneously on metal oxide surfaces depending on the identity of the catalyst and substrate, in combination with the applied process conditions and reactor system. Consequently, these side products may not only impact the reaction selectivity, but also the stability of the active material, as will be shown specifically in this paragraph (and further throughout the review). This includes both adsorption on the active sites (coking), but also more permanent deactivation mechanisms such as structural disintegration. Despite their high importance, it is clear that both catalyst stability and regeneration of the active materials are two topics that have not received adequate attention yet in this research field after surveying the available ketonization literature.

As discussed in section 2.2, anhydride and ketene molecules have been observed during ketonization. Rather than intermediates, they should be viewed as products from competing side reactions. In the aforementioned study by Wang *et al*. the more active anatase TiO_2 and ZrO_2 catalysts were also more prone to deactivation.[60] Based on infrared spectroscopy and DFT results, this was ascribed to the presence of unreactive (towards ketonization) bidentate carboxylate spectator species that occupy active acid-base pairs. Furthermore, it was shown that the bidentate species can dehydrate to a ketene molecule and water in a reversible reaction. The deactivation of catalysts could be countered by using a Cu/SiO_2 co-catalyst (20 wt% Cu) and constant H_2 atmosphere (20 kPa) during ketonization. Under these new ketonization conditions, the positive co-catalyst effect on stability was attributed to the slow and continuous hydrogenation of these ketene molecules under hydrogen pressure to ethanal and ethanol side products. As a result the ketene does not undergo the reverse reaction back to the unreactive bidentate species, limiting the competitive adsorption on the active catalytic sites by these spectator. This results in improved stability and retention of a higher reaction rate. It must be noted that the addition of the co-catalyst and hydrogen also impacts the product selectivity in this system, as ethanal and ethanol products are also formed (albeit to a minor extent).

As shown throughout this work, the choice of metal oxide material will determine the required temperature for ketonization, which in turn will also influence the selectivity and occurrence of side reactions. For instance, it has been reported multiple times that very high reaction temperatures (>350 °C) can promote cracking side reactions of intermediates, and decomposition of the primary ketone product. As a result, a mixture of lower molecular weight ketones, alkenes, alkanes and gaseous products is obtained.[32, 72] While we will discuss the subject of fatty acid ketonization with metal oxides in more detail in sections 4.2 and 6 of this review, these substrates are prone to deoxygenation side reactions via decarboxylation and decarbonylation, resulting in C_{n-1} hydrocarbons. Additionally, when polyunsaturated substrates are present in the feedstock, skeletal C=C migration via the Lewis acid sites of amphoteric oxides may lead to conjugated diene species and further possible cokes formation via oligomerisation side reactions.[114] In the re-ketonization side reaction, which is discussed extensively in section 5, the primary ketone target can undergo condensation with a carboxylic acid to water and an unstable β-diketone intermediate.[96] The latter can then undergo a cleavage reaction (catalyzed by surface -OH) to yield a different carboxylic acid and ketone molecule. Depending on the initial composition of the feedstock (single *versus* multiple carboxylic acids), this may result in a lower selectivity towards a single target ketone and as such it should be categorized as a side reaction.

Regarding catalyst stability, Almutairi *et al*. have screened alumina, titania, zirconia and ceria for the gas-phase ketonization of acetic acid.[88] At 300 °C, the activity increased in the order $Al_2O_3 < TiO_2 < ZrO_2 < CeO_2$, while stability decreased following $TiO_2 > ZrO_2 > CeO_2$. The latter was attributed to the presence of cokes, as determined by chemical analysis after combustion of the spent catalysts. The carbon contents on spent TiO_2, ZrO_2 and CeO_2 were 1.2, 1.2 and 5.6%, respectively. The exact nature of the coke species was not determined however. The authors did show that both CeO_2 and ZrO_2 could be regenerated by a calcination treatment in air (500 °C for 3 hours), nearly regaining full initial activity. This may be attributed to the surface area of the calcined CeO_2 material, which was slightly lower than the fresh parent material (73 m^2/g *versus* 85 m^2/g). Similarly, others have also reported on the deactivation of metal oxides by coke formation. For example, 5 wt% carbon was found on Fe_3O_4/SiO_2 after 8 hours during acetic acid ketonization[101], while the activity of $Co\text{-}Mo/Al_2O_3$ for pentanoic acid coupling decreased during 15 hours on stream, after which 2.7 wt% carbon was found on the spent catalyst.[109] Lee *et al*. also found cokes on their ZrO_2 aerogel catalyst during hexanoic acid ketonization.[38] While XRD did not show a crystal structure change after reaction, both the surface area and pore volume decreased with increasing time on stream due to coke deposition. Jiang *et al*. have shown that doping of Mg-Al hydrotalcite materials with Ce could increase the catalyst stability. The "$Mg_3Al_{0.9}Ce_{0.1}$" catalyst showed higher activity and stability for at least 7 hours on stream during propanoic acid ketonization at 350 °C, compared to the reference "Mg_3Al" material.[110] Post-reaction XRD analysis showed that the structure of $Mg_3Al_{0.9}Ce_{0.1}$ was maintained, while new diffraction peaks were observed for Mg_3Al, possibly indicating lower structural stability.

Finally, the impact of water on the stability of ketonization catalysts is complex and can be dependent on both the active material and reaction conditions. Hydrothermal breakdown of the metal oxide surface may occur under severe reaction conditions, resulting in a permanent loss in activity.[106] As discussed in the previous paragraph, the stability of metal oxides in aqueous reaction media (such as bio-oils) may be enhanced by increasing its hydrophobicity (for example by adding a carbon support).[52] In contrast, water can also enhance the ketonization stability (while lowering activity) by competing for adsorption on the active sites. As a result, the presence of other side products with a stronger negative impact on the stability are reduced on the active surface. This has been observed for zeolite materials for instance, which will be discussed in the next section.[115]

3.2 Zeolites

3.2.1 Mechanism and active site

Although already reported over 30 years ago, only few studies have investigated the use of zeolites for carboxylic acid ketonization. This trend is changing however, as this topic has regained new momentum in the last few years.[47, 48, 69, 116-118] A critical first aspect for discussion is the nature of the catalytic active sites, the reaction mechanism and how these differ from metal oxide materials. While there seems to be a general consensus regarding the active sites and activation of the first carboxylic acid, uncertainty still surrounds the exact nature of the rate-limiting step and activation of the second acid molecule. Brönsted acid sites (BAS), which are acidic Al-$O^-(H^+)$-Si protons generated via isomorphic substitution of Si^{4+} by Al^{3+} in the zeolite structure, are the active sites based on temperature programmed desorption and infrared spectroscopy studies.[81, 82, 119] In the first step of the reaction mechanism, a carboxylic acid molecule is adsorbed on the zeolite surface and protonated on the oxygen of its -OH group by BAS, after which dehydration occurs with release of H_2O to form an acylium species ((eq. 9). The latter is in equilibrium with an acylium cation intermediate, which plays a central role in the overall reaction pathway. Hence, in comparison to carboxylic acid activation on metal oxides, no carboxylate is initially created. It is also possible for this acylium intermediate to deprotonate and desorb from the zeolite surface as a ketene side product (R-C=C=O), which is a parallel pathway that was discussed earlier for metal oxide catalysts. To proceed via ketonization, it is believed that a second acid molecule must be adsorbed and activated on the surface in close proximity to the first acylium cation. However, the exact adsorption and activation type of this second substrate on zeolites is not yet fully understood currently and subject to debate. Similar to the metal oxide mechanism, some groups have proposed that an adsorbed carboxylate is formed via deprotonation due to interaction of the acidic substrate proton and a basic lattice oxygen of the zeolite (eq. 10). This would consequently result in a nucleophilic carboxylate anion species that can attack the acylium cation to form a new C-C bond. According to Martens *et al*., this would either yield an anhydride (RCOOCOR') (eq. 11a) or a ketone (RCOR') and CO_2 (eq. 11b).[81, 117] For the latter however, it remains unknown which elementary steps, reaction intermediates and transition state take part in the reaction mechanism. It has been proposed that the C-C coupling could occur via a β-ketoacid intermediate, but activation of the α-H of the carboxylate has not been explained yet on zeolites.[33] In any case, carboxylic acid activation and ketone formation could be dependent on the acidity of the substrate molecule and the acid-base properties (strength and density ~ Si/Al ratio) of the catalyst material.

$$\boldsymbol{RCOOH + HZ \rightleftharpoons RC^{+}O + H_2O + Z^{-}} \qquad (\boldsymbol{eq.9})$$

$$\boldsymbol{R'COOH + Z^{-} \rightleftharpoons R'COO^{-} + HZ} \qquad (\boldsymbol{eq.10})$$

$$\boldsymbol{RC^{+}O + R'COO^{-} \rightleftharpoons RCOOCOR'} \qquad (\boldsymbol{eq.11a})$$

$$\boldsymbol{RC^{+}O + R'COO^{-} \rightleftharpoons RCOR' + CO_2} \qquad (\boldsymbol{eq.11b})$$

Other groups remain inconclusive on the nature of the second intermediate, and describe the ketonization mechanism in a more general way as coupling of an adsorbed acylium species with a second activated acid, for which the elementary steps currently remain unkown. The main reason behind this approach is the lack of ketonization studies on zeolites where carboxylate species have been detected directly by techniques such as infrared spectroscopy for example. The actual reaction network and mechanism could be more complex than presented by equations 9-11 and more research in this particular field is required.

In the work by Gumidyala *et al*. for example, it is suggested that the C-C coupling step is rate-determining based on infrared, TPD and kinetic data.[47] Note that this is similar to the most accepted rate-determining step of ketonization on metal oxide catalysts. To confirm the role of BAS as the active sites, the authors employed two different strategies. First, an ion exchange protocol with Na^+ was performed to remove the H^+ sites in various amounts, which indeed showed that the ketonization rate dropped in proportion to the degree of cation exchange on the BAS. Furthermore, the Lewis acidity introduced via Na^+ incorporation did not promote ketonization in this instance. Secondly, silicalite-1, which is an all silica MFI zeolite with no Al substitution, showed no activity for acetic acid ketonization at 300 °C. While acyl species were identified in this ketonization study, the presence of carboxylates was not reported. Despite these experimental results, the nature of the active sites and mechanism of zeolite ketonization may be dependent on the specific reaction conditions and catalysts involved (pure zeolite *versus* bifunctional catalyst), as very recently Jahangiri *et al*. reported the gas-phase ketonization of acetic acid over Ga/HZSM-5 catalysts.[116] The incorporation of Ga species into the zeolite framework introduced Lewis acidity, as probed by DRIFTS after pyridine adsorption, while the acid strength was determined via temperature-programmed reaction spectroscopy of propylamine. Increased Ga loading (0.5-10 wt%) resulted in a decrease of total acid site loading and acid strength compared to HZSM-5, and an increase of weak/strong acid site ratio. At 350 °C in a fixed bed reactor, turnover frequencies were similar for different Ga loadings and the parent zeolite, while at 400 °C a proportional increase in TOF was observed in relation to the incorporated Ga content. Given the correlation of ketonization activity and the ratio of weak/strong acid sites, as was also the case for the acetone selectivity (~13-30% with maximum for 10% Ga loading), the authors suggested that ketonization transpires preferentially on weak Lewis acid sites for these materials. This concurs with ketonization on metal oxide catalysts. Another mechanistic pathway may be present here which is different from that of pure zeolites: first, a surface acyl intermediate is formed via BAS from a first acid molecule, while a neighbouring carboxylate species is formed on a nearby LAS from a second reagent molecule, after which nucleophilic attack forms

an intermediate that decomposes into acetone and CO_2. Similarly, Yan *et al*. have very recently investigated the conversion of acetic acid over metal containing (Y, Sc, La, Ce, Pr, Sn and Ti) Beta zeolites.[69] All materials (5% metal loading) were active for gas-phase ketonization at 450 °C, although large differences in yield were observed. While 5% Y/Beta only yielded ~25% acetone, up to ~65% ketone yield was achieved over Ti/Beta at full conversion. At lower temperatures of 350 and 400 °C, the ketone yield increased for Y/Beta. Furthermore, it was also dependent on the metal loading, with a negative impact for 10 and 15 wt% Yttrium loadings. These catalysts exhibit both BAS and LAS, and the ketonization activity was attributed to both weak acidic silanol groups of Beta (BAS) and weak Lewis acid-base pairs (confined Y clusters). Furthermore, Palizdar *et al*. have reported the upgrading of beech wood pyrolysis oil with Fe and Zn containing hierarchical MFI zeolites, which includes carboxylic acid ketonization, that was promoted on hierarchical Zn/HZSM-5.[120]

In conclusion, Brönsted acid sites are active for carboxylic acid ketonization on zeolite catalysts. Currently, the most plausible mechanism involves the C-C coupling between an acylium cation and a second activated acid (of which the exact nature is unknown). No theoretical studies have been performed to provide additional insight into this topic, which also holds true regarding kinetics and the identity of the rate-limiting step. The small amount of available experimental data suggest that the C-C coupling step is kinetically relevant, which sounds reasonable based on our current understanding. For bifunctional zeolites, incorporation of metals with Lewis acid properties can result in active materials containing both BAS and LAS which are active for ketonization.

3.2.2 Side reactions and catalyst stability

The main reason for the low number of ketonization reports with zeolites as catalysts is perhaps the reaction selectivity, which is typically significantly lower compared to metal oxide catalysts. This can be attributed to the nature of the active sites (BAS) and the acylium intermediate, giving rise to several possible side reactions. Indeed, already in the 1980s, Vervecken *et al*. studied the gas-phase conversion of C_2-C_4 acids on HZSM-5 zeolites with different Si/Al ratios, as well as on other catalysts such as L, Y, BETA, MOR and ERI zeolites.[82] For acetic acid ketonization on HZSM-5 (Si/Al= 100), low acetone yields of 23% and 15% were achieved at 320 °C and 360 °C for conversions of 47% and 97%, respectively. High yields of other side products such as xylenols, phenols and hydrocarbons were reported. These originate from a diacetone alcohol intermediate, that is formed via aldol condensation of the primary acetone ketonization product, which is catalysed by BAS. When comparing the products originating from the different acids (C_2-C_4), the typical defining property of zeolite catalysts, namely shape-selectivity, was observed. For propionic acid, lower phenol yields were observed due to the bulkier intermediate transition state, a consequence from transition state shape-selectivity. For butyric acid ketonization on ERI materials, the cage-effect was observed, resulting in no yield of phenols due to the geometrical constraints, where the bulky transition state cannot be formed, ultimately leading to higher selectivity towards ketonization. Later, the same group suggested anhydride formation as a side reaction on the outer surface acid sites of zeolite T, while inside the erionite (ERI) cavity selective ketonization for butyric and propionic acid took place. For large pore zeolites, aldol condensation of the primary ketone product is the main pathway, ultimately resulting in isophorone, mesitylene or 1,3,5-trimethylbenzene, depending on acid site strength. For pentasil zeolites with intermediate amount of BAS, mainly xylenols were formed.[81] Therefore, the main factors directing the reaction selectivity were the nature of the zeolite (topology/pore structure), the acid strength and the acid site density.

Low ketonization selectivity (maximum ~ 30%) was also observed by Gayubo *et al*. for acetic acid conversion at 400 °C with HZSM-5, which dropped even lower after longer time on stream due to aforementioned consecutive side reactions of acetone towards hydrocarbons and aromatics.[115] Wang *et al*. showed a linear correlation between 3-pentanone conversion and BAS density on HZSM-5 for propionic acid ketonization and the same group very recently visualized the major reaction routes of carboxylic acids on acidic zeolites, including initial aldol condensation, followed by cracking, aromatization, etc. (Figure 11).[117, 119] Clearly, aldol condensation of the primary ketone product must be quenched if high ketonization selectivity and yield are to be achieved on zeolites. On a catalyst design level, this can possibly be realized by tuning BAS density, BAS strength and geometrical material structure. It must be noted that high ketonization selectivity on zeolite catalysts is possible, as shown by the work of Gumidyala *et*

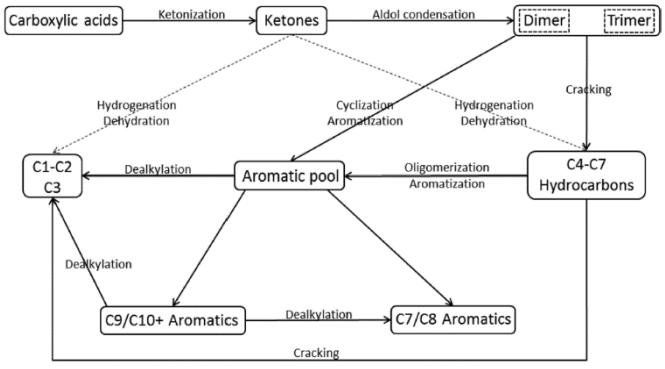

Figure 11: Main reaction routes for carboxylic acid conversion on acidic zeolites. Reprinted with permission from [117], Copyright (2019) American Chemical Society.

al., where acetone was (almost) exclusively formed at temperatures between 270-330 °C on a HZSM-5 zeolite. However, in contrast to the previous studies, which mostly reported full carboxylic acid conversion, only 10-20% of acetic acid was converted at 300 °C.[47] Obviously, the resulting low yield of acetone will also reduce the following side reactions, and selectivity values cannot be compared at different conversion values. At higher temperatures (340 °C), lower carbon balances were observed (~77 %), which was ascribed to the occurrence of acetone side reactions. Therefore, moderating operating conditions can form a second viable strategy to optimize ketonization selectivity on zeolite catalysts.

Evidently, both the target ketonization coupling as well as the numerous side reactions may have an impact on the catalyst stability, its deactivation mechanism and potential for regeneration. Wang *et al*. showed that the activity of HZSM-5 zeolite decreased with time on stream (up to 5 hours) for both propanoic and 3-pentanone conversion.[119] Deactivation was faster for the carboxylic acid substrate, which was attributed to a higher amount of coke formation (5 *versus* 2.5% respectively, as measured by TOP). Furthermore, analysis of the coke composition revealed that the coke from propanoic acid conversion had a higher H_2O/CO_2 ratio. The faster deactivation was explained by a stronger adsorption of carboxylic acid on the active sites compared to the ketone (-130 kJ/mol *versus* -61 kJ/mol adsorption energy, respectively), while more aromatics in the coke for 3-pentanone conversion could explain the difference in H_2O/CO_2 ratio. For regeneration, the authors showed that a calcination procedure at 550 °C could restore the original activity for propanoic acid conversion with preservation of the MFI structure (measured by XRD). Similarly, others have also shown that calcination of the spent zeolite catalyst is an appropriate strategy to regain original activity.[47, 117] Specifically for zeolite catalysts, pore/channel blockage by larger coke species such as oligomers may be a secondary contributor to deactivation (in addition to outer surface deactivation).

Others have also proposed coke deposition to be the main origin for zeolite deactivation.[115-117, 120] Palizdar *et al*. have shown that the amount and/or type of coke is influenced by both the incorporation of metal species (Zn, Fe) and hierarchization to generate mesoporous materials.[120] Addition of Zn and Fe to hierarchical ZSM-5 reduced the amount of strong acid sites responsible for side reactions to heavy cokes, reducing the peak temperature necessary for regeneration. Hierarchization of microporous ZSM-5 may also influence both the coke yield and composition. Here, the mesoporous material showed a higher amount of coke formation than the parent, which was attributed to increased accessibility to the strong acid active sites. However, the type of coke may be altered as the increased transport rate of substrates, intermediates and products could result in lower residence times, reducing the potential for extensive oligomerization reactions.

Besides material properties, the presence of water in the substrate feed (typical for bio-oil) can also impact the catalyst stability and coke formation. For example, Gayubo *et al*. have observed a reduction in the amount of cokes by competition between water and substrate/side products for adsorption on the active sites.[115] It must be noted that while this increased the stability, competitive adsorption of water evidently resulted in decreased activity. Regarding the reactor system, the authors also found that the amount of cokes was higher at the inlet of the fixed bed system due to a higher initial substrate concentration. Accordingly, a higher concentration of primary ketone product at the inlet is readily available to undergo aldol condensation and further side reactions. Others have also observed that water negatively impacts carboxylic acid conversion, while simultaneously increasing zeolite stability.[47]

4. Substrate

As can be derived from this review so far, most ketonization studies have been performed on single short-chain model compounds (mainly acetic and propionic acid). However, some groups have investigated more complex substrates or mixtures to simulate real biomass feedstocks. Indeed, whether the goal is to valorise pyrolysis bio-oil or upgrade (fatty) acid feedstocks, industrial application of ketonization will require an understanding of the influence of different substrate properties. Therefore, the impact of carbon chain length, degree of (un)saturation, degree of branching and presence of other functional groups will be reviewed in this section.

4.1 Carbon chain length

Several groups have reported on the impact of the carbon chain length on carboxylic acid ketonization.[40, 43, 58, 62, 68, 90, 117, 121, 122] These findings have been mostly observational, although recently more fundamental in depth analysis has been performed. Pham *et al*. have studied the gas-phase ketonization of acetic, propionic and butyric acid on a Ru/TiO_2 catalyst at 275-335 °C.[90] Based on their experimental kinetic data and Langmuir-Hinshelwood (LH) model, rate and adsorption constants, adsorption enthalpies and entropies, activation enthalpies and entropies, and true activation energies were determined for each acid, which are summarized in Table 2. While all three acids had nearly identical heats of adsorption (-134 kJ/mol), the adsorption entropy increased (decreased in absolute value) with increasing carbon chain length (from -198 to -178 J/mol.K). Furthermore, the activation enthalpy and entropy, as well as the true activation energy (from 161 to 225 kJ/mol) increased with the acid carbon number. Quite surprisingly, however, are the reported positive activation entropy values in this study, which implies an increase in the degrees of freedom for the transition state compared to the two adsorbed carboxylate species. This is more probable for a dissociative mechanism and thus seems rather unlikely for the C-C coupling reaction, as two substrate molecules are required to form one activated complex in an associative type of mechanism. To explain these positive values, the authors have suggested the possibility of either a transformation of the transition state to a more loosely bound state, or an increase in entropy due to

intramolecular configurational contributions. Others have not observed such positive activation entropy values, and more clarity on this topic is certainly desirable. In any case, based on these results it was concluded that the carboxylic acids adsorb on the catalyst surface via the acid group and that they do not interact with the surface via their alkyl groups. Furthermore, the formation of the C-C bond, which is assumed to be rate limiting in the LH model, can be obstructed for larger alkyl groups, as a bulkier transition state is more sterically demanding at the catalyst surface for the bimolecular reaction.

A second publication by Cao *et al*. also looked at C_2-C_4 acids to determine the impact of carbon chain length on ketonization performance, albeit here on a HZSM-5 catalyst at 350 °C.[117] Again, a decrease in intrinsic reaction rate (0.96, 0.44 and 0.28 mmol/g_{cat}.min, respectively) was observed for increasing carbon number, as well as a decrease in TOF based on the density of BAS (2.64, 1.21 and 0.77 min^{-1} respectively). For a temperature of 350 °C, true activation enthalpy ΔH, entropy ΔS, and activation energy ΔG were determined. Similarly, these 3 parameters increased with increasing chain length and as a consequence a nearly identical conclusion was drawn as in the previous work. Larger carboxylic acids impose increased steric hindrance for the C-C coupling reaction, which enlarges the energy requirement for this rate-determining step. Here however, the entropies of activation were negative for all acids (between -325 and -290 kJ/mol), which is also the case for other gas-phase studies. For example, values of -90 and −135 J/mol.K were reported for pentanoic and 2-methylbutanoic acid ketonization on ZrO_2.[123] Based on both experimental data and DFT calculations, Wang *et al*. have reported $\Delta H^{\ddagger}$, $\Delta S^{\ddagger}$ and $\Delta G^{\ddagger}$ values for the ketonization of C_2-C_4 acids on anatase and rutile TiO_2[60] and ZrO_2[87] in the presence of hydrogen and a 20% Cu/SiO_2 co-catalyst. For TiO_2 the $\Delta G^{\ddagger}$ values varied between 166-176 kJ/mol for the C-C coupling step of C_2-C_4 acids at 250°C. For ketonization of acetic acid on the anatase catalyst, $\Delta H^{\ddagger}$ was determined as 137 kJ/mol with a $\Delta S^{\ddagger}$ of -56 J/mol.K at 230 °C. For ZrO_2, $\Delta G^{\ddagger}$ values varied between 157-168 kJ/mol for the different substrates. As a general consensus, it can be stated that under identical reaction conditions, an increased carbon number results in lower ketonization activity. This may be (partially) explained by the increased steric hindrance for the C-C coupling during the rate-determining step of the reaction mechanism.

Table 2: Summary of thermodynamic and kinetic parameters of carboxylic acid ketonization on Ru/TiO_2 at 275-335°C as determined by Pham *et al.*[90]

	Acetic acid (C_2)	Propionic acid (C_3)	Butyric acid (C_4)
Adsorption enthalpy ΔH (kJ/mol)	-134	-134	-135
Adsorption entropy ΔS (J/mol.K)	-198	-190	-178
Activation enthalpy $\Delta H^{\#}$ (kJ/mol)	156	182	220
Activation entropy $\Delta S^{\#}$ (J/mol.K)	3	32	78
True activation energy E_a (kJ/mol)	161	186	225

4.2 Degree of (un)saturation

Very few studies have been published on the impact of unsaturated feedstocks on catalyst performance for ketonization (activity, selectivity and stability). Given the dominance of bio-oil model compounds as substrates in ketonization research and the absence of unsaturated carboxylic acids in such feedstocks[124], this has been in fact only explored for fatty acids from oleochemical biomass to the best of our knowledge. Due to this exceptional case, further discussion in this paragraph will focus exclusively on fatty acid coupling. Lee *et al*. have recently investigated the ketonization of C_{18} fatty acids with different degrees of unsaturation, *viz*. stearic acid ($C_{18:0}$), oleic acid ($C_{18:1}$) and linoleic acid ($C_{18:2}$), on a P25 TiO_2 catalyst in a fixed bed reactor system at 380 °C and atmospheric pressure.[114] While not specifically mentioned by the authors, these conditions suggest gas phase reactions as the normal boiling points of all three substrates are ≤ 360 °C. First of all, these three substrates showed rather similar conversion profiles after 12 hours as a function of WHSV, indicating no significant impact of unsaturation on the overall average conversion rate. In contrast, significant differences in ketonization selectivity were observed. At (near) full conversion, C_{35} ketone yields of 89, 83 and 75% were achieved for $C_{18:0}$, $C_{18:1}$ and $C_{18:2}$, respectively. These results show a lower selectivity for the higher degree of unsaturation, and thus simultaneously higher yields of unwanted side products. The latter included shorter C_{16} olefins and C_{19} methyl ketones as main by-products, in addition to smaller amounts of hydrocarbons ($<C_{15}$) and C_{20}-C_{30} ketones. Based on these results, a decomposition pathway was proposed where a so-called McLafferty rearrangement -a β-cleavage of fatty ketone product with γ-hydrogen transfer- occurs (Figure 12). Both enol and alkene fragment species are generated, after which the first can undergo keto-enol tautomerization towards the C_{19} methyl ketone side products. Since the olefin by-products had a carbon

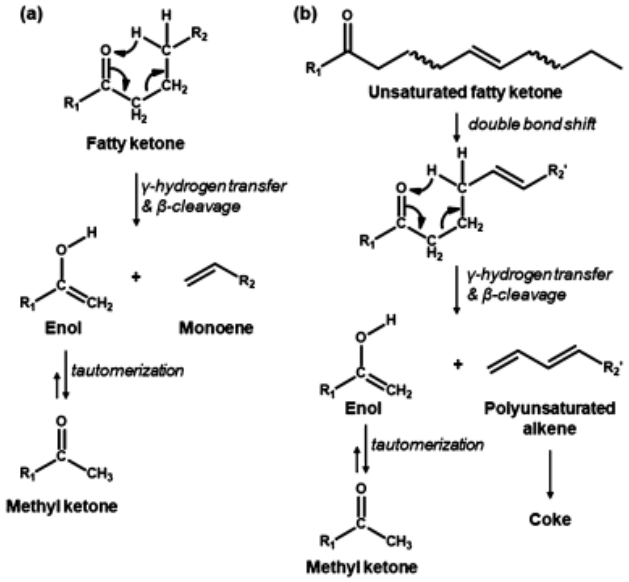

Figure 12: Side reactions of saturated (a) and unsaturated (b) fatty ketones as presented by Lee *et al*. Reprinted with permission from [114], Copyright (2018) American Chemical Society.

number of 16 and no C_{17} species were detected, decarbonylation of C_{18} fatty acids was discarded. Interestingly, via a control experiment with pure C_{11} ketone, the authors only observed McLafferty rearrangement in presence of the TiO_2 catalyst, while no thermal reaction took place, indicating the catalytic nature of this rearrangement pathway. Based on side product distribution for the unsaturated fatty acids in particular, additional skeletal C=C migration via the Lewis acid sites of the amphoteric TiO_2 was proposed, leading to polyunsaturated conjugated 1,3-diene species and further possible cokes formation (0.33, 0.56 and 1.25 wt % for stearic, oleic and linoleic acid, respectively based on post-reaction TGA). Finally, a higher degree of unsaturation resulted in a higher amount of cracking towards lower molecular weight species ($<C_{15}$ hydrocarbons and C_{20}-C_{30} ketones). Unfortunately, the authors did not report the impact of reaction conditions (in particular temperature) on product selectivity, as the balance between primary ketonization and secondary reactions will likely be temperature dependent. This aspect will hopefully be addressed in future ketonization studies. It must be noted that in earlier work by Glinski *et al*. mixtures of acetic/10-undecenoic acid and hexanoic/oleic acid were used for ketonization on CeO_2/Al_2O_3 and MnO_2/Al_2O_3 catalysts at 300-450 °C. However, only brief notice was made of C=C bond migration and decomposition with coke formation when unsaturated feedstocks were used.[125]
One strategy to combat this lower ketonization selectivity of (poly)unsaturated carboxylic acids for overall higher ketone yields is to perform a prior hydrogenation step, after which highly selective ketonization of the saturated fatty acids can occur. Indeed, when looking at patent literature concerning triglyceride and fatty acid ketonization, this has proven to be a viable solution (see section 6 of this review). Additionally, finetuning the reaction temperature and conditions could potentially play a significant role as well, although currently the necessary data is lacking in literature.

4.3 Degree of branching

Unlike unsaturation, the effect of substrate branching has been elaborately investigated.[39, 43, 85, 89, 93, 123] When discussing the β-ketoacid surface mechanism in section 2.2.4, some examples of branched-chain carboxylic acid experiments were already mentioned as these were used to establish the necessary requirement of an α-H atom. Therefore, ketonization does not readily occur when using branched substrates such as pivalic (2,2-dimethylpropanoic acid) and 2,2,5,5-tetramethyladipic acid.[85, 93] Pestman *et al*. performed ketonization of isobutyric acid at 350 °C on a Fe_2O_3 catalyst and observed significantly lower ketone yield when compared to a non-branched acid such as propionic acid, regardless of the small difference in carbon number.[85] One postulated argument was the increase in steric hindrance for a branched carboxylic acid for the bimolecular C-C coupling on the catalyst surface compared to the linear substrates. Note that this is also one of the primary suggested reasons for slower ketonization reactions of longer carboxylic acids (section 4.2). Later, Nagashima *et al*. screened various branched carboxylic acids for ketonization in a mixture with propionic acid on CeO_2-Mn_2O_3 at 375 °C.[43] These included 2-methylpropanoic, 2,2-dimethylpropanoic, 3-methylbutanoic and 3,3-dimethylbutanoic acid. When looking at the ketone product distribution of these mixtures, it is clear that both branched α-substituted as well as β-substituted acids are less reactive for ketonization, with a larger decrease in activity for increased number of methyl groups. While in both publications an increase of steric hindrance was central to explain the experimental results, they were rather observational in nature, and no hard evidence was given for the branching effect. Recently however, thanks to the work of Oliver-Tomas *et al*.[123] and Ignatchenko *et al*.[89] a more fundamental understanding of the origin of the influence of branching has been established. In the first study, ketonization was performed on linear pentanoic and branched 2-methylbutanoic acid with a ZrO_2 catalyst at 350-425 °C. At all reaction temperatures, conversion

of pentanoic acid was significantly higher (100% *vs*. 30% for 2-methylbutanoic acid at 425 °C for example), with initial reaction rates that were approximately 30 times higher for pentanoic acid. Interestingly, while the apparent activation energies based on transition state theory were nearly identical (116 kJ/mol for pentanoic and 105 kJ/mol for 2-methylbutanoic acid, respectively), a large(r) difference in the change in entropy of the transition state was obtained (-90 and -135 J/mol.K respectively). Based on these findings, entropic effects seem to determine the difference in carboxylic acid reactivity. More specifically, the degrees of freedom of the system are reduced for bulkier side groups with hindered rotation of methyl groups. In the second recent study, Ignatchenko et *al*. performed DFT modelling for the ketonization of acetic acid with isobutyric acid on the *m*-ZrO_2 (111) surface. Here, the decarboxylation step (loss of CO_2), was determined to also be kinetically relevant for the bulkier isobutyric acid, besides the C-C coupling step. Both electronic and steric effects of the methyl substituent were found. More specifically, the alkyl group impacts the activation energy of decarboxylation by altering the C-C sigma bonding and antibonding orbitals, and the bond strength via electron delocalization. Furthermore, steric effects play a significant role for the bimolecular reaction on the catalyst surface.

4.4 Presence of other functional groups

Suitable substrates for ketonization do not exclusively comprise of monofunctional carboxylic acids as various multifunctional molecules can be used for C-C coupling. Firstly, dicarboxylic acids (and derivatives) can be converted, which form a special class of ketonization substrates as they open up the possibility for both internal self-ketonization towards internal cyclic C_{n-1} ketones, as well as typical ketonization towards C_{2n-1} products. In the first case, the reaction becomes monomolecular rather than the bimolecular coupling that has been discussed in this work so far. Indeed, Renz *et al*. studied the cycloketonization of adipic acid ($(CH_2)_4(COOH)_2$) to cyclopentanone ($(CH_2)_4CO$), a valuable fine chemical, over base catalysts.[126] For instance, a cyclopentanone yield of 90% was achieved after dry distillation of adipic acid in a round bottom flask in the presence of $Ba(OH)_2$ at 350 °C. Furthermore, also β-substituted branched derivatives of adipic acid could be converted via internal cycloketonization. In this study, the possible occurrence of classical C-C ketonization towards a C_{11} product was not mentioned. Later, Sudarsanam *et al*. studied the gas-phase cycloketonization of dimethyladipate (diester derivative of adipic acid) on $Ce_xZr_{1-x}O_2$ catalysts at 300-450 °C.[42] Depending on the applied process conditions and catalyst, high ester conversions (up to 100%) and cycloketone yields (up to 75%) were achieved. Regarding reaction selectivity however, no further details were given besides the mention of "trivial products", leaving open the possibility for typical C-C ketonization as "side reaction". A lot of early observational work has also been done on this subject by Liberman *et al*., who screened dicarboxylic substrates with different carbon numbers for linear and cycloketonization.[127-131] Based on the conversion of the zinc salts of adipic (C_6), pimelic (C_7), suberic (C_8), azelaic (C_9), and sebacic (C_{10}) acids, it was observed that lower carbon numbers (C_{6-8}) preferentially undergo cycloketonization, whereas for larger acids (C_{9-10}) the linear ketonization reaction was dominant.

Besides dicarboxylic acids, other multifunctional carboxylic acid substrates have been used in ketonization studies, such as levulinic acid for example. This keto acid (4-oxopentanoic acid) is considered to be an important platform molecule and can be derived from lignocellulosic biomass. Karimi *et al*. have studied the ketonization of an aqueous levulinic acid solution (50 wt%) on a red mud catalyst (mixed iron oxide material) and detected the direct 2,5,8-nonatrione ketonization product at 200 °C.[40] Although the results were only semi-quantitative, activity was low (even at the high operating temperature of 365 °C) and low selectivity was observed due to side reactions of reactive levulinic acid to γ-valerolactone (GVL) and pentanoic acid via dehydration-hydrogenation, and to Angelica-lactone decarbonylation and coking products. More recently, Lilga *et al*. have investigated the ketonization of aqueous levulinic acid on Ce- and La-doped zirconia materials at 380-400 °C in presence of formic acid or ethylene glycol as reducing agents.[132] No mention of 2,5,8-nonatrione product formation was made, as a complex biphasic mixture was obtained from various (side) reactions. It must be noted that levulinic acid has also been used indirectly as a ketonization substrate, via its initial conversion to pentanoic acid (via GVL intermediate in presence of hydrogen and formic acid as reducing agents)[133, 134], which can then be converted into 5-nonanone, as demonstrated by the work of Serrano-Ruiz *et al*.[135] Another bio-based multifunctional carboxylic acid that is presented as an important platform chemical is lactic acid (2-hydroxypropanoic acid), which is an alpha-hydroxy acid that can be produced from lignocellulosic biomass.[136] Hence, this molecule has also been screened for upgrading via ketonization, as in the work by Serrano-Ruiz *et al*.[137, 138] Lactic acid conversion was tested in aqueous solution (30 wt%) over a Pt/Nb_2O_5 catalyst at 300 °C, after which an organic product phase was obtained. This phase contained a mixture of C_4-C_7 ketones, C_1-C_7 alkanes, acetaldehyde, propanoic acid, etc., which was explained by the initial formation of acetaldehyde and propanoic acid intermediates from the reactive lactic acid substrate via hydrogenation and CO cleavage or dehydration-hydrogenation, respectively. These intermediates can then undergo aldol condensation and ketonization reactions on the catalyst surface towards C-C coupling products, such as 3-pentanone. Similar to levulinic acid, lactic acid can also be regarded as an indirect substrate for ketonization. Interestingly, it is important to note that in contrast to levulinic acid, no direct ketonization product of lactic acid - 2,4-dihydroxy-3-pentanone - was observed.

Aromatic carboxylic acids can be regarded as another class of multifunctional carboxylic acids with potential use as ketonization substrates. Accordingly, Gooßen *et al*. have reported the cross-ketonizaton of mixtures of aliphatic and aromatic acids towards aryl alkyl ketones, which are important intermediates in the chemical industry.[44] This pathway was presented as a sustainable alternative for typical Friedel-Crafts acylation reactions. In this work, a library of various aliphatic and aromatic acids were screened under different process conditions (250-340 °C) with multiple metal oxide catalysts (MgO, ZrO_2, MnO_2, Fe_3O_4) in several reaction solvents (e.g.,Dowtherm A, N-methyl pyrrolidon, sulfolane, and tetraglyme). A reaction mechanism for this particular type of cross-ketonization was proposed, which is shown in Figure 13. Carboxylate formation from the aromatic acid (5) should be favored because of its higher acidity compared to the proton of the aliphatic acid. However, these species do not possess the necessary α-H atom for homo-ketonization. Therefore, an activated aliphatic acid (2) is required at the catalyst surface for further cross-ketonization (6) via a β-ketoacid intermediate (7) to maximize the yield of the aryl alkyl ketone target (3). Additionally, it was verified via ^{13}C-labelled aromatic acids that the final ketone function originates from the aromatic acid, while CO_2 is formed from the aliphatic substrate. Furthermore, it was concluded that electron-poor as well as electron-rich aromatic and heteroaromatic acids are suitable ketonization substrates, even when combined with other functionalities such as halogens, amines, ethers and phenols. Finally and perhaps most importantly, the C-C coupling towards aryl alkyl ketones was highly selective when using magnetite nanoparticles, producing only CO_2 and H_2O as expected ketonization by-products, indicating no reactive behavior of the aromatic acid towards undesired side reactions. For example, 3-toluic acid was coupled with phenylacetic acid resulting in an 80% yield of cross ketonization product 2-phenyl-1-(3-tolyl)-ethanone and 9% yield of 1,3-diphenylacetone, which is the homo-ketonization product of phenylacetic acid. It must be noted that also other non-aromatic cyclic carboxylic acids have been used as ketonization substrates. While not multifunctional in nature by definition, Dooley *et al*. have performed the cross-ketonization of cyclopropanecarboxylic acid with acetic acid towards methylcyclopropylketone (MCPK), a useful chemical intermediate, with high conversion on CeO_2-based catalysts at 400-450 °C.[65, 77]

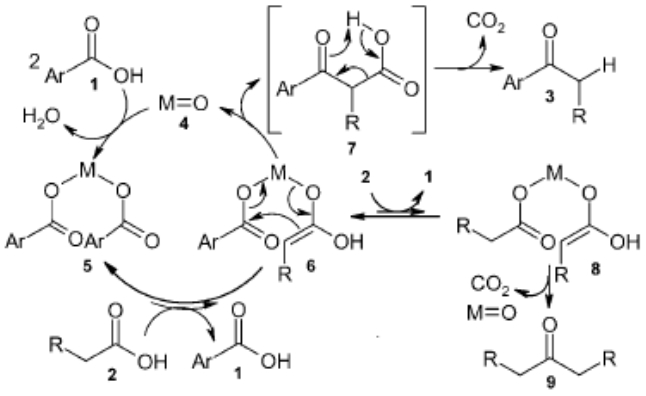

Figure 13: Mechanism for cross-ketonization of aliphatic and aromatic carboxylic acids as proposed by Gooßen *et al.* Reprinted from [44], Copyright (2010) with permission from Wiley.

Wrzyszcz *et al*. have reported the gas-phase ketonization of various oxidized derivatives of n-decane such as decanol, decanal, decyl decanoate and 3-hydroxy-octyl-dodecanal on a Fe_3O_4 catalyst in a fixed bed reactor at 310-400 °C.[67] Although differences in substrate reactivity and reaction pathways were observed, 10-nonyldecanone was the main ketonization reaction product for all substrates. When utilizing alcohol or aldehyde substrates, the proposed catalytic sequence was alcohol → aldehyde → hemiacetal → ester → ketone with a higher ketone yield for decanal compared to decanol. Others have also concluded the general reactivity of oxygenates towards ketonization to decrease in the order acid > aldehyde > alcohol > ester.[37]

5. Kinetics & thermodynamics

Numerous publications have touched on the subject of ketonization kinetics, albeit to various degrees of depth. These range from pure observational description of conversion to combined (theoretical) kinetic modelling, correlation to the active sites and elementary reaction steps. These kinetic models have been presented under many different forms such as power laws, LH expressions, Eley-Rideal (ER) type mechanisms, etc. In this section, an update on the current state of the art regarding ketonization kinetics will be provided to the reader, which to the best of our knowledge, has not been covered in such manner in earlier reviews before.

Given that ketonization is a bimolecular coupling reaction between two carboxylic acids towards a ketone, carbon dioxide and water, the influence of concentration of both reactants and products on the reaction rate has been investigated by several groups.

Pham *et al*. have studied the gas-phase kinetics of acetic acid coupling on a Ru/TiO_2 catalyst at 275-285 °C and used a classic power law for their kinetic model (eq. 12)[41]:

$$\boldsymbol{r = k_0 e^{\frac{-E_a}{RT}} P_{AA}^a P_{Ac}^b P_{CO2}^c P_{H2O}^d} \qquad (\boldsymbol{eq.12})$$

with k_0 the reaction rate constant, E_a the apparent activation energy, $P_{AA}^a, P_{Ac}^b, P_{CO2}^c, P_{H2O}^d$ the partial pressures of acetic acid, acetone, carbon dioxide and water, respectively, and a,b,c and d the accompanying reaction orders for each compound. Based on experimental results (after verifying the absence of diffusion limitations), reaction orders of 1.6, -0.4, -0.2 and -0.1 were obtained for acetic acid, acetone, carbon dioxide and water, respectively. These values were explained by a second order rate limiting step (C-C coupling) with competitive adsorption that includes product inhibition from all three reaction products. It was proposed that competitive adsorption of products occurs on the same surface active sites, with decreasing inhibition strength in the order of acetone > carbon dioxide > water. Additionally, it was also demonstrated via co-feeding experiments that product inhibition of the catalyst was reversible. Similarly, Lu *et al*. also performed co-feeding experiments with water (10 mol%) and carbon dioxide (50 mol%) during the gas-phase ketonization of acetic acid on a $Ce_{0.7}Ti_{0.3}O_x$ catalyst at 315 °C.[106] In this study, however, the influence of acetone was not investigated and a different outcome was observed. Indeed, the original activity was only regenerated in the case of CO_2 after suspension of co-feeding, whereas the original activity was not obtained after experiments with H_2O co-feeding. Three different explanations were provided by the authors for the inhibition results of water. While no additional experimental or theoretical data were added to support these claims specifically, they seem plausible based on the currently available literature. Firstly, water can adsorb competitively on the surface active sites via its -OH groups and thereby hinder carboxylic acid adsorption. Secondly, it can also act as a reagent and hydrolyse reaction intermediates during ketonization. Finally, hydrothermal breakdown of the catalyst (surface) may explain the permanent loss in activity after water co-feeding. The negative impact of reaction products on the ketonization rate has been known for many years, as already in the 1970s Jewur *et al*. performed gas-phase ketonization experiments of acetic acid on an iron oxide catalyst in the presence of acetone, water and carbon dioxide.[104] Interestingly, inhibition orders which were dependent on the reaction conditions, were observed. At 375°C, the strength of inhibition decreased in the order water > acetone > carbon dioxide, while at 440 °C this shifted to water > carbon dioxide > acetone. At the higher reaction temperature, the overall inhibition strength was decreased while conversion was increased. Clearly, adsorption and desorption of substrates and products, as well as the catalyst surface properties, are temperature dependent and this may be regarded in view of differences in adsorption enthalpy.

Gaertner *et al*. studied the kinetics of hexanoic acid ketonization on a $Ce_{0.5}Zr_{0.5}O_2$ catalyst in a fixed bed reactor with 2-butanone or hexane as reaction solvent.[139] A varying dependence on the hexanoic partial pressure was observed for the reaction rate, which increased up to 0.1 atm., after which it remained constant at all reaction temperatures between 275-350 °C for partial pressures up to 0.75 atm. The former indicated a second order dependence in the Henry pressure range, while the latter indicated saturation of the surface active sites and therefore a zero order reaction regime. For this particular reaction, both CO_2 and H_2O product inhibition were investigated. The ketonization rate decreased from 12.6 to 3.7 $\mu mol.min^{-1}g_{cat}^{-1}$ at 325 °C for 56 mol% co-feeding of CO_2 in the gas phase, whereas these values dropped from 17.7 to 6.7 $\mu mol.min^{-1}g_{cat}^{-1}$ for 5 mol% co-feeding of H_2O in the reaction solvent. Interestingly, the inhibitory effect was not reversible for CO_2, although some of the original activity was regained afterwards. The authors rejected product inhibition from the ketone product (6-undecanone), based on the observation that the ketonization rate did not change when switching from 2-butanone to hexane as reaction solvent. As a result, the following rate expression was proposed based on a LH model for an irreversible forward reaction with no ketone inhibition and competitive adsorption of all species on the same active sites (eq. 13):

$$\boldsymbol{r = \frac{k_f P_{HA}^2}{\left(1 + K_{ads,HA} P_{HA} + K_{ads,H2O} P_{H2O} + + K_{ads,CO2} P_{CO2}\right)^2}} \qquad (\boldsymbol{eq.13})$$

with k_f the forward reaction rate constant, P_x the partial pressures of hexanoic acid (HA), water and CO_2 and $K_{ads,y}$ the corresponding adsorption constants. From this kinetic model, the so called binding energies (cfr. adsorption enthalpies) of HA, CO_2 and H_2O on the active sites were found to be -81, -138 and -96 kJ/mol respectively, indicating the strong bonding tendency of CO_2 on the active sites of $Ce_{0.5}Zr_{0.5}O_2$. In a follow-up publication, however, this LH model was modified to incorporate separate acidic and basic active sites on the catalyst surface, because ketonization rates were overestimated and the previous model did not accurately describe the transition from second to zero order dependence for the acid partial pressure.[121] Unfortunately, no further (mechanistic) insights were provided by the authors to support this distinction between acidic and base sites on a molecular level. Their exact identity was not addressed, and it is unclear how and why they interact differently with the substrate and products, in addition to being insensitive for ketone inhibition. Therefore this new expression, with one type of surface site for the adsorption of carboxylic acid and another for both H_2O and CO_2 adsorption, is purely anecdotal and to the best of our knowledge, others have not proposed similar models (eq. 14):

$$r = \frac{k_f P_{HA}^2}{\left(1 + K_{ads,HA} P_{HA}\right)^2 \left(1 + K_{ads,H2O} P_{H2O} + + K_{ads,CO2} P_{CO2}\right)^2} \quad (eq.14)$$

Asymptotic ketonization rates as a function of acid concentration have been observed by others, for example in the work of Ding *et al*., where the observed reaction order for propionic acid ketonization at 270°C on $Ce_{0.1}Zr_{0.9}O_2$ was 0.38 for an acid partial pressure up to 1.2 kPa.[98] For ZrO_2, the observed order was 0.55 up to 0.3 kPa partial pressure. For higher acid partial pressures, zero order dependence was observed. Kulyk *et al*. used a TPD-MS experimental setup to investigate the reaction kinetics of valeric acid pyrolysis and ketonization to 5-nonanone on nanosized CeO_2/SiO_2 and γ-Al_2O_3 materials.[78] In this work the reaction order, apparent activation energy, pre-exponential factor and activation entropy were determined by a custom software and experimental setup. Because no shape change or shift of the T_{max} desorption peak of the ketone ion to a lower temperature occurred for increasing concentrations of valeric acid, the authors suggested a first order reaction. Furthermore, the Arrhenius plot method based on experimental results showed higher correlation (R^2= 0.96-0.99) for a first order reaction compared to the expected theoretical second order dependence for the bimolecular coupling (R^2= 0.92-0.94). Contrary to most ketonization studies, however, this pyrolysis reaction was studied for conversion of pre-adsorbed valeric acid by ramping the system temperature to 750 °C and collecting the different mass fragments as a function of temperature/time. This set-up implies non-equilibrium conditions without continuous addition of substrate, for which it was also not specified whether or which of the different valeric acid loadings used (0.3-1 mmol/g) could coincide with full monolayer coverage. As such the measured kinetic parameters might not accurately represent the bimolecular surface reaction, but possibly desorption limitations because insufficient acid molecules can adsorb in close proximity to each other, which is a necessary requirement for the ketonization reaction. If this is the case, acids must desorb and re-adsorb near an adsorbed substrate before ketonization can occur, which could influence the determination of the observed reaction order. Therefore, a follow-up study addressing these topics could provide useful insights into using this kind of experimental set-up to study heterogeneously catalyzed reactions.

The group of Murkute *et al*. proposed an irreversible second order reaction for the ketonization of propionic and butyric acid on MnO_x/CeO_2 supported on wormhole hexagonal mesoporous silica (HMS) and MCM-41 catalysts in gas phase at 410 °C via the rate expression (eq. 15)[68]:

$$kC_0 \tau \rho_{cat} = 2\epsilon(1+\epsilon)\ln(1-X_A) + \epsilon^2 X_A + (\epsilon+1)^2 \frac{X_A}{(1-X_A)} \quad (eq.15)$$

with k the reaction rate constant, C_0 initial reagent concentration, τ residence time, ρ_{cat} catalyst bulk density, ϵ the expansivity as a result of the net change of moles during reaction and X_A the fractional acid conversion. When plotting the right side of the equation *versus* residence time, a linear plot was observed for both materials for propionic acid ketonization, indicating indeed the second order reaction behavior. Furthermore, the reaction rate constant can be obtained via the slope of these curves. Gumidyala *et al*. studied the kinetics of acetic acid ketonization on HZSM-5 at 270-330 °C and observed reaction orders of 1.6 and -0.46 for acetic acid and H_2O, respectively, with a reversible inhibition effect of water after co-feeding.[47] It was proposed, based on the zeolite ketonization mechanism (section 3.2.1), that water either interacted with the acyl intermediate in a reversible way back to acetic acid, or that it adsorbed competitively on the active surface sites. This inhibition effect was also found to be less at higher temperatures (320 *vs*. 300 °C). Interestingly, here the authors also mentioned a varying reaction order of water from -0.46 to -0.2 with respect to increasing time-on-stream (TOS), indicating a higher inhibiting effect in the initial state. This may be due to the fact that the catalytic system is not yet in a steady state modus operandi, or that water induces changes of the surface. The decay of ketonization rates for different H_2O loadings was used to calculate deactivation coefficients k_d. Based on these findings, the authors suggested a positive impact of water on catalyst stability, while simultaneously negatively impacting its activity. The proposed rate-limiting step in this study was the second order coupling of an acyl intermediate with a second adsorbed carboxylic acid, for which LH type kinetic equations were formulated. Similarly, Pham *et al*. studied the kinetics of C_2-C_4 carboxylic acid gas-phase ketonization on Ru/TiO_2 with a conventional second order LH model that includes product inhibition and competitive adsorption of all products on the same active site as the carboxylic acid substrates (eq. 16)[90]:

$$r = \frac{kK_{acid}^2 P_{acid}^2}{(1 + K_{acid} P_{acid} + K_{ketone} P_{ketone} + K_{H2O} P_{H2O} + + K_{CO2} P_{CO2})^2} \quad (eq.16)$$

An important observation was made with regard to the adsorption constants, which decreased in value in the following order acid > ketone > H_2O > CO_2 for all acids. Furthermore, they decreased in value for all species with an increase in temperature between 275-335 °C. Accordingly, the enthalpies of (the exothermic) adsorption were highest (i.e. most negative value) for all acids, followed by ketone, carbon dioxide and water respectively. The results indicated a catalyst surface which was almost exclusively covered

with acids at low conversions, while only at higher conversions a stronger impact of product inhibition from ketones was observed. In all cases, the surface coverages and thus the impacts of CO_2 and H_2O were very low. One of the most elaborate studies on ketonization kinetics, which combines both experimental kinetic data as well as associated theoretical DFT modelling for all proposed elementary steps of the mechanism (Figure 4), has been performed by Wang *et al*. on gas-phase ketonization of C_2-C_4 acids on TiO_2 and ZrO_2 in a 1:1 physical mixture with a 20% Cu/SiO_2 catalyst.[60] As mentioned earlier in section 3.1.5, both the presence of H_2 and the Cu/SiO_2 catalyst in the reaction mixture ensured stable ketonization rates for the different TiO_2 materials (anatase and rutile) with time on stream. Based on the experimental results for anatase TiO_2, the adsorption constant values of all reaction products H_2O, CO_2 and acetone were very low, indicating negligible surface coverage of these species. Furthermore, it was concluded that the C-C coupling (Figure 4, step 4) is the rate-determining step. Based on the proposed mechanism and the assumptions of pseudo-steady-state for all bound species, quasi-equilibrium for all reaction steps except for C-C coupling and irreversible decarboxylation, and with AcO* and * (free Ti-O pairs) as the most abundant surface intermediates (MASI), the following rate expression was proposed (eq. 17):

$$\frac{r}{[L]} = \frac{\overrightarrow{k_4} K_3 \overrightarrow{k_{10}} K_1^2 P_{acid}^2}{\left(\frac{\overleftarrow{k_4} P_{H2O}}{\prod_{z=5}^{9} K_z} + \overrightarrow{k_{10}}\right)(1 + K_1 P_{Acid})^2} \qquad (eq.\,17)$$

with [L], $\overrightarrow{k_x}$, $\overleftarrow{k_x}$ and K_x the catalytically active acid-base pairs (Ti-O), the forward and reverse rate constants and equilibrium constant for step x, respectively (Figure 4).

Most kinetic studies have been performed in the gas-phase. However recently, an elaborate theoretical kinetic study based on ab initio molecular dynamics (AIMD) simulations and DFT calculations was published by Cai *et al*. on the ketonization of acetic acid on monoclinic zirconia $(\bar{1}11)$ surface, where the novelty lies in the comparative investigation of both vapor and condensed aqueous phase ketonization.[140] Opposed to the classic LH mechanisms that have often been suggested, in this work an alternative LH model was proposed for the vapor phase, while a different ER mechanism was postulated for the aqueous phase (Figure 14). Regarding the interaction between water molecules and the catalyst surface for the condensed phase, it was found by calculation that nearly 2/3 of Zr_{6c} are occupied sites as a result of both H_2O adsorption and dissociation by reaction with lattice oxygens to form surface hydroxyls. Simultaneously, all the O_{2c} active sites are taken by hydroxyl species at equilibrium, resulting in very limited accessibility of active sites for ketonization under relevant reaction conditions (such as 277°C). Additionally, the interaction between catalyst surface and water molecules was thermodynamically more favorable for the condensed phase, as reflected by the stronger adsorption energy (-212 *versus* -125 kJ/mol for vapor phase). While in the vapor phase bonding strength decreased in the order, acid (dissociative) > water > acid (molecular), equal binding strengths for the acid substrate and water were found in the condensed phase, implying more competitive adsorption. In contrast, the adsorption energies for acetone were lower than those of acid and water for both phases, showing values of -107 and -141 kJ/mol for vapor and condensed phase, respectively, resulting in less 'occupation' of the active surface sites. For the particular case of the aqueous phase, the authors found interaction energies (i.e. adsorption energy of aqueous phase minus adsorption energy of vapor phase) of -133 and -34 kJ/mol for acetic acid and acetone, respectively, showing thus preferable interaction of the substrate via hydrogen bonding with surrounding water molecules. This is likely due to the more hydrophilic nature of acetic acid. The alternative vapour phase LH mechanism was based on direct coupling of acetic acid and di-anion intermediates, which was found to be both kinetically and thermodynamically more

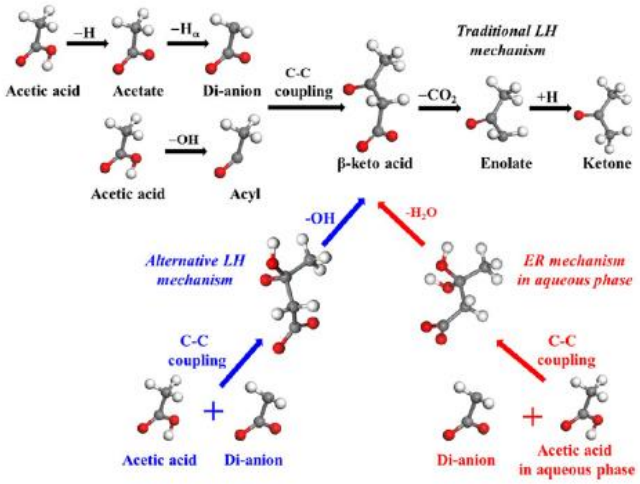

Figure 14: Reaction mechanisms for ketonization of acetic acid in gas and condensed aqueous phase via β-ketoacid as discussed by Cai *et al.* Reprinted with permission from [140], Copyright (2018) American Chemical Society.

favourable than the generally assumed LH mechanism, with a calculated activation energy of 27 *versus* 184 kJ/mol, respectively. The Gibbs free energy profiles of all studied pathways in the aqueous phase were constructed, as shown in Figure 15. Besides site blockage and hydroxylation of catalyst surface, an additional exclusive effect of water molecules in the aqueous condensed phase is the Grotthuss proton transfer mechanism. This encompasses proton transfer from O_{2c} sites to O_{3c} sites with the aid of surrounding water molecules. The result is contribution of H_2O in the (de)protonation steps via this Grotthuss mechanism, which results in a reduction of ketonization rate compared to the vapor phase (47 kJ/mol activation energy). Furthermore, due to the low availability of active sites on the surface because of multiple water effects, the DFT calculations propose a more suitable Eley–Rideal mechanism pathway for the condensed phase (with lower calculated 27 kJ/mol activation energy,). The effects of the dynamic water environment on the surface steps were verified via configuration sampling, showing its impact on the reaction energetics, even when not directly engaging in the reaction itself. Clearly, this study shows the added complexity of liquid-solid interfaces for catalytic ketonization compared to strict gas-phase coupling of carboxylic acids.

To conclude this section, a final remark should be made with regard to the so-called re-ketonization side reaction, which recently has been reinvestigated by the group of Ignatchenko and co-workers, and may occur simultaneously during ketonization under reaction conditions.[96, 141] Therefore, this pathway may also have a significant impact on the (observed) ketonization kinetics. Although both pathways can yield the same products, it should not be confused with the work on the reversibility of the ketonization reaction (which was reported by the same group), as the reverse and re-ketonization reactions are not the same. In the reverse reaction (see Section 2.2), which is an integral part of the ketonization mechanism, the ketone product may disproportionate back to two carboxylic acid molecules by reaction with CO_2 and H_2O. These carboxylic acids may be the same or different, depending on if the ketone was a product of homo- or cross-ketonization. In the re-ketonization reaction however, a ketone molecule (which may be a direct ketonization product) undergoes condensation with a carboxylic acid molecule (a ketonization substrate) to water and an unstable β-diketone intermediate. The latter can then undergo a cleavage reaction (catalyzed by surface -OH) to yield a different carboxylic acid and ketone molecule. For example, during the ketonization of acetic acid to acetone, the acetone product may react further with acetic acid substrate to the corresponding β-diketone, which decomposes back into acetone and acetic acid. Because in this case only a singular carboxylic acid and the corresponding ketone are present in the mixture, the reverse ketonization reaction and re-ketonization reaction cannot be distinguished from each other as they yield the same acid (acetic acid) and thus also ketone product (acetone). In this case, the re-ketonization reaction (if it occurs) may also be called a hidden degenerate pathway as it cannot be readily observed by the product distribution. In another example, ketonization of isobutyric acid was conducted in the presence of acetone, which yielded methyl isopropyl ketone and acetic acid in the product mixture. This is a consequence of the re-ketonization reaction, in which isobutyric acid reacts with acetone to methyl isopropyl ketone (MIPK) and acetic acid. The latter can then undergo homo-ketonization to acetone, or cross-ketonization with isobutyric acid. Here, the re-ketonization reaction can readily be observed by the formation of MIPK and acetic acid. The reaction rate of this side reaction during ketonization was studied by ^{13}C isotopic labelling by Ignatchenko *et al*. They have very recently shown that for ^{13}C acetic and decanoic acid coupling in the presence of unlabeled acetone, both labeled and unlabeled 2-undecanone was formed. Based on the relative product distributions and deviation from the statistically expected ratios, it was concluded that the ketonization reaction is significantly faster than the re-ketonization side reaction. With in-situ and

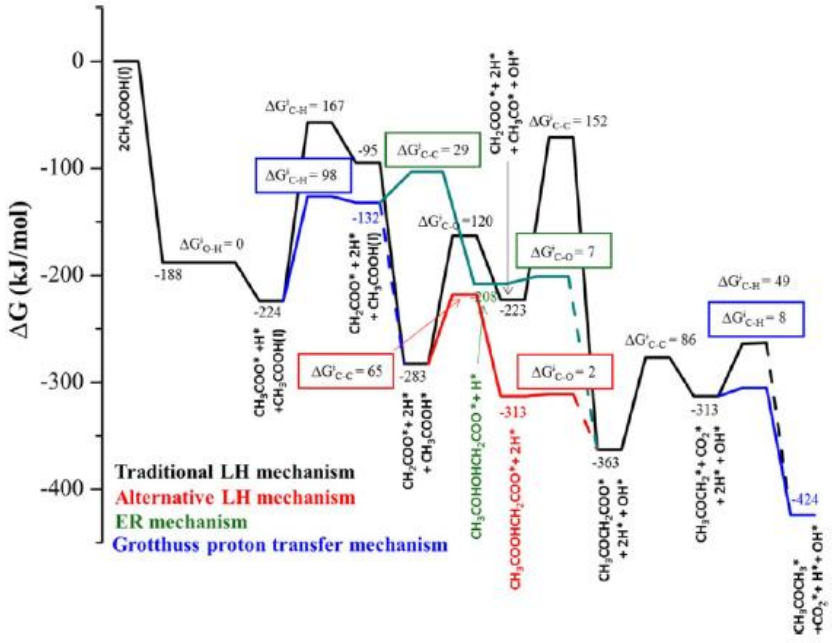

Figure 15: Gibbs free energy profile in the aqueous phase ketonization of acetic acid on $(\bar{1}11)$ zirconia as determined by Cai *et al*. Reprinted with permission from [140], Copyright (2018) American Chemical Society.

operando IR, the authors showed that at reaction conditions, no acetone was adsorbed on the available active surface, while acetic acid coverage was high. Therefore, the re-ketonization reaction rate is limited by the weaker adsorption of ketone compared to the carboxylic acid. Nevertheless, these results suggest that future kinetic studies on ketonization should investigate this side reaction, as well as the reversibility concept under reaction conditions.[36, 39, 89, 95, 96, 141] It is important to note once more that these concepts were specifically and exclusively postulated for the gas-phase under specific conditions at a very high reaction temperature (400 °C). It is unknown whether such phenomena should be taken into account also in the condensed phase.
In conclusion, the ketonization rate can be increased by increasing the initial carboxylic acid concentration up to the point of surface saturation, after which a further increase in substrate concentration does not further improve the reaction rate. Product inhibition by all three products can reduce the ketonization rate, depending on both the catalytic system and reaction conditions. While competitive adsorption on the active sites is one aspect of the possible inhibition mechanisms, the reaction products may also interact with available surface species. This can include hydrolysis of reaction intermediates by water and/or re-ketonization of the primary ketone product with carboxylic acid. Furthermore, the inhibition may be irreversible due to structural changes/damage to the active material. Increasing the reaction temperature can improve the ketonization rate while simultaneously decreasing product inhibition due to easier desorption of reaction products. A delicate balance must be maintained here as to ensure that also the ketonization selectivity remains high, as the occurrence of side reactions is typically also promoted at higher reaction temperatures. For C-C coupling in the condensed phase, the reaction environment can become even more intricate due to participation of the solvent, as evidenced by the Grotthuss mechanism in aqueous media.

6. Biomass valorisation via ketonization

6.1 Lignocellulose carboxylic acids (≤C_{10})

As discussed in this review, the recent surge in ketonization studies is dominated by the coupling of short-chain lignocellulosic biomass derived carboxylic acids. These (pyrolysis) bio-oil compounds typically require chain length extension, primarily for fuel applications. Although in many cases pure model substrates are employed, some groups have studied the additional complexity of valorising “realistic” feedstocks mimicking a commercial industrial situation. This includes for example the presence of various oxygenates in an aqueous environment, other metal and salt impurities, etc. Additionally, further upgrading and/or characterization of the physicochemical properties of the (ketone) product have been explored towards possible future commercial processes and applications.

6.1.1 Ketonization in the lignocellulose bio-refinery

Jackson *et al*. have studied the ketonization of acetic acid on $Fe_{0.2}Ce_{0.2}Al_{0.6}O_x$ in water (16 vol%) in the presence of other bio-oil organic components originating from sugar and lignin such as hydroxyacetone, furfural, phenol, guaiacol, cresol and eugenol.[50] In this case also other ketone products were formed (besides acetone), such as 2-butanone and 3-pentanone, as a result of hydroxyacetone conversion to propanoic acid/propanal intermediates under the reaction conditions (400-430 °C). Perhaps more importantly, a significant temperature dependent adverse impact of eugenol, guaiacol and furfural on the catalyst activity was observed. For example, the ketonization rate almost halved after adding 1 vol% eugenol to the reaction mixture. Besides this drop in activity, the non-acid bio-oil components proved to be reactive under the coupling conditions, resulting in formation of cokes and lower mass balances. Similarly, Mansur *et al*. performed ketonization with ZrO_2–FeO_X catalysts on pyroligneous acid from Japanese cedar woodchip biomass.[51] This consisted of many organics apart from acetic and propionic acid, such as hydroxyacetone, phenols, ethers, ketones, heavies, etc. Besides the aforementioned ketone yield from hydroxyacetone, the authors showed the negative effect of metal impurities such as K and Mg, which are inherently present in the bio-oil feedstock. Ion-exchange resins are able to remove these potential poisons prior to ketonization, resulting in significantly higher ketone yield. This suggestion of a pre-treatment step to improve downstream ketonization is not unique. A different kind of pre-processing has been proposed by Deng *et al*. who reported the inhibition effects of phenol and furfural on acetic acid ketonization in terms of activity and selectivity for multiple mixed metal oxides.[142] Especially for furfural, a steep decline of activity (95 and 44% conversion with 2.5 and 10 wt% furfural under identical conditions, respectively) was observed, possibly due to formation of humin-like decomposition products. As such, prior removal of these compounds is advised. An example of raw biomass pre-treatment for ketonization is presented in the work of Funai *et al*., who subjected livestock manure waste to a hydrothermal treatment to yield a carboxylic acid enriched slurry liquid which was subsequently converted via catalytic ketonization on iron oxide.[54] Due to the high compositional complexity and low mass balance, however, total ketone yields were low with a maximum of ~20 C-mol%, producing mainly gaseous products.
In most research articles that focus on lignocellulose based carboxylic acid valorisation, a so-called integrated or cascade scheme is envisioned with ketonization as one of the key processes. Davidson *et al*. for example, have shown that ketonization can be integrated in a 2-bed catalytic system in one reactor, combining acetic acid ketonization (eq. 18) and consecutive steam reforming of acetone (eq. 19) for hydrogen production via CeO_2 and Co/CeO_2 catalysts, respectively.[61] With this particular system, the authors have developed a setup that improves upon the one-bed direct steam reforming of acetic acid to H_2 (eq. 20) with regard to stability and inhibition of coke formation. This was attributed to the difference in direct decomposition side reactions of acetic acid and acetone during steam reforming on the supported Co material. DFT calculations showed that the most likely pathway of

direct acetic acid degradation on Co involved $CH_3COOH^* \rightarrow CH_3COO^* \rightarrow CH_3CO \rightarrow CH_3^*$, rather than degradation into CH_3CO^* and O^*. Additionally, at high temperatures the following decomposition route also becomes possible $CH_3COOH^* \rightarrow CH_3^* + COOH^* \rightarrow CH_3^* + CO^* + OH^*$. Higher amounts of adsorbed CH_3COO and CO species resulted in lower water adsorption and activation on cobalt, which is necessary to remove coke precursors such as CH_x (x = 0–3). For acetone, the most favorable decomposition is $CH_3COCH_3^* \rightarrow CH_3COC^* \rightarrow CH_3CO^* \rightarrow CH_3C^* \rightarrow CHC^* \rightarrow CH^* \rightarrow C^*$. As a result, no accumulation of adsorbed CH_3COO and CO species occurs in this case. Therefore, water adsorption and activation on Co is enhanced, which in turn increases removal of surface C and CH species via CO_2 formation. For all supported Co materials, viz. 15 wt% on $MgAl_2O_4$, ZnO, CeO_2, and activated carbon, the methane selectivity was significantly lower (0.6% for Co/CeO_2 for example) than the predicted thermodynamic CH_4 equilibrium selectivity (16.2%) at complete conversion. This was also true for the bare oxide support materials.

$$\mathbf{2\ CH_3COOH + 4\ H_2O \rightleftharpoons CH_3COCH_3 + CO_2 + 5\ H_2O} \qquad (\boldsymbol{eq.18})$$

$$\mathbf{CH_3COCH_3 + CO_2 + 5\ H_2O \rightleftharpoons 4\ CO_2 + 8\ H_2} \qquad (\boldsymbol{eq.19})$$

$$\mathbf{2\ CH_3COOH + 4\ H_2O \rightleftharpoons 4\ CO_2 + 8\ H_2} \qquad (\boldsymbol{eq.20})$$

An alternative integration of ketonization with a second chemical reaction has been explored by Weber *et al*. who combined C-C coupling of bio-oil oxygenates with subsequent aqueous phase hydrogenation of the intermediate ketones.[143] In this work red mud was used as ketonization catalyst in a packed bed reactor to convert a water mixture containing 4 wt% of acetic acid, formic acid, hydroxyacetone and levoglucosan at 400 °C, followed by hydrogenation at 180 °C and 20 bar H_2 using commercial Pd on (activated) carbon monoliths. It was noted that under ketonization conditions on the red mud catalyst, side reactions such as transfer hydrogenation, aldol condensation, dehydration and dehydrogenation could occur. Besides residual ketones, the complex final upgraded bio-oil (> 20 different oxygenated compounds) contained isopropyl alcohol, 2-butanol and cyclopentanol from their respective ketone precursors. Two different groups have reported the conversion of carboxylic acids to olefins via ketonization without the need of an additional (noble) metal containing hydrogenation catalyst, as was the case in the previous example. In the first, Oliver-Tomas *et al*. have reported the direct transformation of decanoic acid over TiO_2 to 10-nonadecanone and 10-nonadecene in inert N_2 atmosphere at 300-450 °C.[49] At 400 °C a maximum olefin yield of 35% was obtained, suggesting the consecutive hydrogenation and dehydration of the 10-nonadecanone ketonization intermediate product on the same TiO_2 material. To elucidate the origin of the reductant, the authors proposed a reaction scheme based on observed products in which after ketonization, the ketone product can undergo further aldol condensation and subsequent side reactions such as cyclization, aromatization, dehydrogenation, isomerization and hydrogen transfer (cfr. Figure 11). These steps can provide the hydrogen required to complete the cascade ketonization-hydrogenation-dehydration from carboxylic acid to olefin on TiO_2. Finally, the complex product mixtures after ketonization were further treated via hydrodeoxygenation on a Pt/Al_2O_3 catalyst to gasoline, kerosene and diesel biofuel fractions. In the second study, Baylon *et al*. researched the cascade conversion of acetic and propanoic acid to C_3-C_6 olefins using a $Zn_xZr_yO_z$ catalyst via a ketonization, aldolization and deoxygenation sequence.[45] Here, co-feeding of H_2 had a significant impact on product distribution, with increasing yields of propene, butene, and pentene for higher partial pressures of H_2, indicating the potential of hydrogen activation on the Lewis acid-base pairs of the catalyst at the elevated temperature towards these valuable precursors of fuels and chemicals.

Most research papers in this field ultimately suggest pyrolysis bio-oil acids as substrates for valorisation towards gasoline, kerosene and diesel biofuels. Gasoline components can be synthesized from the carbohydrate fraction without C-C coupling[144-147], although production of the higher boiling components of gasoline or diesel/kerosene requires chain extension. As such Serrano-Ruiz *et al*. have presented a process scheme which gradually deoxygenates solid cellulose biomass towards liquid hydrocarbon fuels.[148] In a first step, cellulose is decomposed into levulinic acid and formic acid in a H_2SO_4 solution, after which this product mixture is hydrogenated on a Ru/C catalyst to GVL. As described earlier, GVL can be converted into pentanoic acid, which in turn can be used as ketonization substrate towards 5-nonanone, which is achieved via Pd/Nb_2O_5 and CeO_2-ZrO_2 catalysts, respectively. Finally, the ketone is converted to gasoline and diesel hydrocarbon fuel species via hydrogenation, dehydration and isomerization reactions using a USY zeolite catalyst. Using wheat straw lignocellulosic biomass as raw feedstock, Hernando *et al*. have very recently applied an integrated cascade process to a second-generation biofuel oil via thermal pyrolysis followed by a 2-bed single reactor catalytic section with ZrO_2/HZSM-5 and K/USY catalysts to generate bio-oil with low oxygen content (12 wt%) and high energy yield (32% of raw biomass) via C-C coupling strategies such as ketonization and aldol condensations.[149] As shown in Figure 16, Shylesh *et al*. have presented an integrated multistep process including ketonization (step 2) for the production of linear and branched alkanes, aromatics and cycloalkane derivatives for bio-based fuels, fuel additives and lubricant applications via carboxylic acid feedstocks.[150] Via this multistep approach, a gradual decrease in oxygen content is established, while simultaneously enhancing the energy density by increasing carbon chain length. Here, additional condensation of C_3-C_9 ketone intermediates with an acidic Nb_2O_5 catalyst (step 4) is proposed to further enhance the carbon number to C_{10}-C_{18} diesel and jet

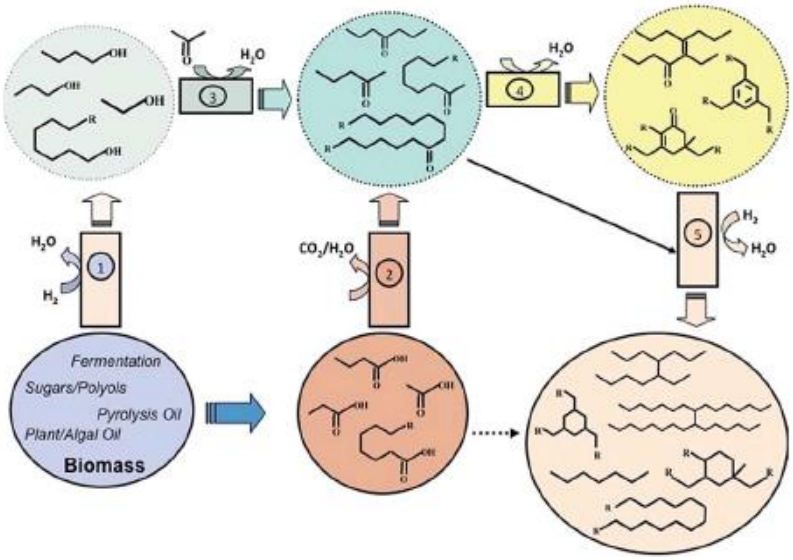

Figure 16: Converting biomass-derived carboxylic acids to liquid alkanes. (1) Alcohol synthesis from fermentation of sugars and by hydrogenation of carboxylic acids. (2) Self- and cross-ketonization of carboxylic acids to ketones. (3) Production of ketones by alkylation of alcohols with acetone. (4) Aldol-type condensation of ketones to dimer/trimer enones and alkylated aromatics. (5) Hydrodeoxygenation of enones, ketones and aromatics to fuel and lubricant alkanes. Reprinted from [150], Copyright (2017) with permission from Royal Society of Chemistry.

fuel precursors when starting from C_2-C_5 lignocellulose acids. Finally, total hydrodeoxygenation with a $Pt/NbOPO_4$ catalyst (step 5) results in bio-based hydrocarbon fuels that are compatible with current petroleum derived products.

6.1.2 Applications, economics and environmental sustainability

Huo *et al*. have very recently taken a so-called "fuel property first" approach towards biofuel production from carboxylic acids.[151] In this work, biological and chemocatalytic processes were combined as the butyric acid substrate was first produced by fermentation of corn stover using *Clostridium butyricum*, after which it was converted towards a drop-in bio-based diesel product with desirable physicochemical properties in a cascade integrated process. After a sequence of bio-derived butyric acid ketonization on ZrO_2, ketone condensation using Nb_2O_5 and catalysed hydrodeoxygenation with Pt/Al_2O_3, a hydrocarbon mixture was obtained in 88% C-yield with 56% C-yield of the C_{14} compound 5-ethyl-4-propylnonane. Fuel properties such as cloud point (CP), cetane number (CN), viscosity, density, heating value (HV), normalized soot concentration (NSC) and yield soothing index (YSI) were then determined and compared to base petroleum diesel. While the bio-based diesel demonstrated adequate performance for all investigated properties, an added benefit was shown concerning soothing tendency, which was much lower (< 50%) compared to conventional base diesel.

Davidson *et al*. have later elaborated their previously discussed concept even further by incorporating a third potential route for valorising the hydrothermal liquefaction of biomass feedstock. This comprises the catalytic production of H_2 via prior anaerobic digestion to CH_4, followed by steam reforming.[152] A techno-economic analysis (TEA) was carried out to compare these three different scenarios for the upgrading of organics in the condensed aqueous phase. An initial clean-up treatment, including activated carbon adsorption and liquid-liquid extraction to eliminate (in)organics, proved to be necessary in this case in order to avoid catalyst deactivation. It was concluded that liquid-phase ketonization provided the lowest minimum fuel selling price per gasoline gallon equivalent (GGE) of the three strategies ($3.49/GGE), with steam reforming and anaerobic digestion showing higher minimum selling prices. The economic advantage of the ketonization technology was attributed to the simultaneous production of valuable co-products such as olefins, while also showing improved energy and carbon efficiencies compared to the other two upgrading pathways. As is evident from the discussion in section 6, many efforts have been made towards bio-based fuels and chemicals from lignocellulose biomass acids via ketonization. These include usage of raw feedstock, concepts of integrated cascade processes, development of TEA and determination of physicochemical product properties towards actual application. To conclude this paragraph, it is of utmost importance to also consider the topic of (environmental) sustainability and biomass carboxylic acid ketonization. To this end, Vienescu *et al*. have performed a life cycle assessment (LCA) consisting of 6 different scenarios for pyrolysis bio-oil upgrading to liquid hydrocarbon fuels (Figure 17).[153] In this study the expected global warming potential (GWP) values ranged between ~ 2-6 kg CO_2 eq./kg upgraded fuel depending on the scenario. Regarding energy requirements, the authors calculated an electricity cost of 0.25 kWh/kg of light oxygenates for the ketonization step, while using a $Ru/TiO_2/C$ catalyst and assuming 46% ketone yield, based on previous work by Pham *et al*. For both scenarios that involve ketonization (3 and 6), it was shown that the global warming potential originating from ketonization and/or esterification was the lowest of all process steps. High contributions were calculated for feedstock cultivation, collection and biomass pre-treatment before the upgrading stage. Furthermore, both the pyrolysis and hydroprocessing steps had the highest overall contribution to CO_2 emissions due to high hydrogen consumption and electricity cost. Overall it was shown that in specific cases (scenario 1) lower CO_2 output (g CO_2 eq./kg

upgraded fuel) can be obtained for synthetic biofuel compared to conventional petroleum diesel (3 *versus* 3.5 kg CO_2 eq./kg fuel). However, inefficient implementations of proposed technologies will result in a low quality and high impact end product, reaching up to three times higher GWP than current diesel fuel. Other impact categories such as resource depletion, eutrophication and acidification should be considered as well when designing new process technologies based on raw biomass feedstock. Therefore, based on their findings the authors proposed scenarios 2 and 4 as reasonable trade-offs between final product quality (a result of the number and nature of intermediate steps involved) and final environmental burden.

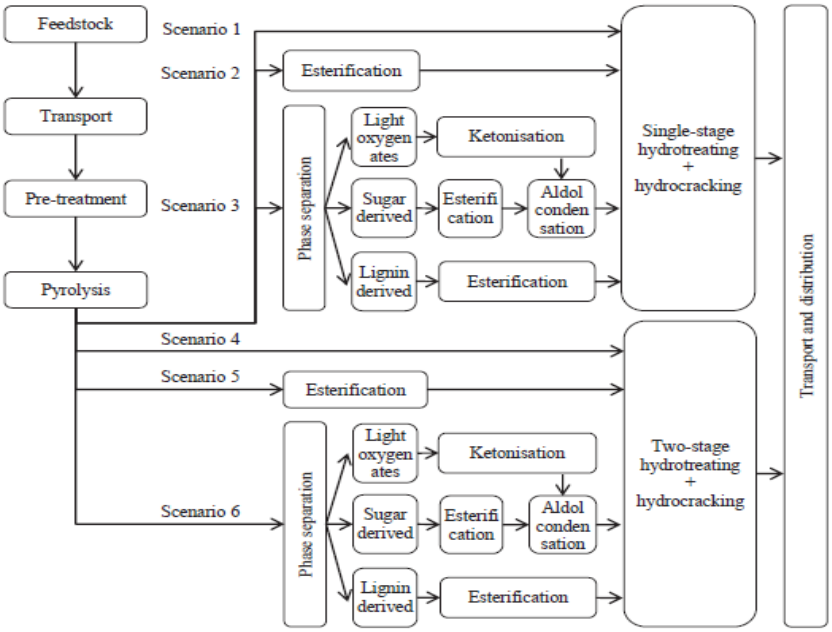

Figure 17: Life cycle assessment scenarios of pyrolysis bio-oil upgrading to liquid fuels as investigated by Vienescu *et al.* Reprinted from [153], Copyright (2018) with permission from Elsevier.

6.2 Oleochemical fatty acids (≥C_{12})

In this section, a collection of both academic and patent literature covering oleochemical biomass ketonization will be discussed. As vegetable oils, animal fats and algal oils are comprised of triglycerides, and both fatty acids and fatty acid methyl esters can be easily derived, these three feedstock groups each require examination as potential C-C coupling substrates. Although far less reported than short-chain acid ketonization, some newer studies have been published lately with a higher prevalence of patent applications in this domain. This warrants the need for an updated systematic survey. In most cases, the long-chain ketones (C_{23}-C_{35}), while valuable (end) products themselves, are considered as intermediates to corresponding (branched) hydrocarbons for fuel, lubricant and other chemical applications by applying consecutive downstream processing technologies such as hydrogenation, hydrodeoxygenation and hydro-isomerisation.

As was the case for short-chain carboxylic acids, an overview of selected ketonization research is presented in Table 3, showcasing the prevalent use of model compounds and (mixed) metal oxides as suitable substrates and catalysts. Fatty acid ketonization has been reported as early as the beginning of the 1900s. The initial studies predominantly used stochiometric amounts of metal carboxylate salts, (iron) metal catalysts or alkaline oxides to promote (solid) bulk ketonization using air bath or flask equipment as reactor setups.[73, 154] Due to the higher activity of amphoteric oxides however, these catalysts and accompanying reaction setups have been largely abandoned.

Table 3 Overview of selected fatty acid ketonization in academic literature.

Substrate	Catalyst	Reactor	T (°C)	P (bar)	X (%)	Y (%)	Ref
Rapeseed oil methyl esters	Zr-Mg-Y-O	Fixed bed	395	1	96	61	[155]
Hexanoic + Oleic acid	MnO_2/Al_2O_3	Fixed bed	425	/	91	/	[125]
Palm oil	MgO/Al_2O_3	Batch	420	/	100	69	[48]
Lauric acid	MgO	Fixed bed	400	/	96	94	[156]
Oleic acid + Iron oleate	Fe	Flask	~320	/	/	82	[157]
Cerotic acid	Fe	Air bath	360	/	/	70	[154]
Stearic acid	Fe	Air bath	365	/	100	80	[154]

Cuphea oil + acetic acid	$Fe_{0.5}Ce_{0.2}Al_{0.3}O_x$	Fixed bed	400	2.4 (N_2)	/	94	[158]
Stearic acid	TiO_2	Fixed bed	380	1 (N_2)	100	89	[114]
Linoleic acid	TiO_2	Fixed bed	380	1 (N_2)	100	75	[114]
Stearic acid	-	Batch	365	10 (Ar)	86	10	[159]
Stearic acid	$Mg_xAl_yO_z$	Batch	250	17 (N_2)	100	97	[160]
Stearic acid	$MnCO_3$	Flask	~335	/	100	~94	[73]
Methyl laurate	Sn-Ce-Rh-O	Fixed bed	410	1	99	60	[161]
Animal fat butyl esters	Fe-Si-Cr-K-O	Fixed bed	390	/	93	68	[162]
Sunflower Oil	ZrO_2	Fixed bed	400	1 (H_2)	100	58	[163]

/: Not mentioned; ~: Approximately; -: none

6.2.1 Fatty acids

Glinski *et al*. studied the conversion of 2:1 and 3:1 hexanoic (C_6) and oleic ($C_{18:1}$) acid mixtures on a 20 wt% MnO_2/Al_2O_3 catalyst at 300-450 °C in a fixed bed system towards a maximum yield of the cross-ketonization product (Z)-14-tricosen-6-one.[125] Additionally, the respective homo-ketonization products, 6-undecanone and 9,26-pentatriacontadien-18-one (oleone), were formed. Increasing the reaction temperature from 350 to 450 °C enhanced the acid conversion from 48 to 94% with a maximum yield of 56% for the cross-ketonization product at 425 °C and 87% conversion when starting from a 3:1 substrate mixture. At these high temperatures, cis-trans isomerisation towards (E)-14-tricosen-6-one and pyrolytic decomposition side reactions with coke deposition were also observed. The (Z)-14-tricosen-6-one target is a valuable chemical intermediate towards muscalure ((Z)-9-tricosene) after reduction of the carbonyl group, the latter which is used as a sex attractant hormone for the male house fly.

Very high ketone selectivity was achieved by Corma *et al*. for the gas-phase coupling of pure lauric acid ($C_{12:0}$) with a MgO catalyst in a fixed bed reactor at 400 °C.[156] Increasing the contact time (W/F) from 2.2 to 46.3 min increased acid conversion from 26 to 96%, with accompanying laurone selectivity of 78 and 98%, respectively. Regarding catalyst lifetime, 90% of initial activity remained after 7.5 hours on stream without any loss in selectivity. Afterwards, the hydrogenation of laurone to the corresponding alcohol was investigated in a second catalytic bed at 400-420 °C and 30 bar H_2 with Pt, Ru and Pd on MgO or Al_2O_3. For all experiments, C_{23} alkane yields were higher than those of the target alcohol, indicating a reaction pathway where the ketone is initially hydrogenated to the desired alcohol by the metal part of the catalyst, which then undergoes fast dehydration to the alkene analogue on the acid sites of the catalyst support with further rapid consecutive hydrogenation to the final alkane. In all cases significant yields of C_{10}-C_{22} alkanes and other hydrocarbons were detected, indicating simultaneous (undesired) hydrocracking side reactions, which may be catalysed by the bifunctional hydrogenation catalyst.

The most common ketonization temperatures often greatly exceed 300 °C and can go as high as 450 °C. However, Smith *et al*. have recently reported the liquid-phase ketonization of stearic acid in dodecane solvent on solid base Mg-Al layered double hydroxides (LDH) and their calcined mixed metal oxides (MMO) at the much lower reaction temperature of 250°C.[160] Under these conditions complete selectivity towards stearone (18-pentatriacontanone) was observed for all materials, i.e. a total of 20 different LDHs and MMOs with varying Mg/Al ratios and synthesis methods (co-precipitation and co-hydration). After 24 hours under 17 bar N_2 pressure, stearic acid conversion ranged from 60-100% depending on the specific catalyst. To explain the observed variety in catalyst activity, catalyst characterization via PXRD, TGA, SEM, ICP, N_2 physisorption and FTIR was performed. No significant difference in stearic acid conversion was observed when comparing LDHs and their respective calcined MMOs, which was also the case for MMOs synthesized by co-precipitation *versus* co-hydration methods, which resulted in less and more ordered crystalline structures, respectively. Additionally, the presence of NaOH impurities from the co-precipitation method did not seem to have any influence on the overall ketonization performance. When relating the stearic acid conversion to the average pore size of the materials, the authors found the occurrence of steric (hindrance) effects as materials with pores sizes >14 nm showed significantly higher stearone yields. The required presence of two large C_{18} substrate molecules in close proximity on the catalyst active sites (here -OH surface groups were assumed) could be inhibited when employing materials with too small pore sizes. However, no additional data was provided in this study to further support this claim.

While kinetic studies are prevalent for short-chain acid ketonization (section 5), no kinetic studies have been published on the catalytic ketonization of fatty acids, to the best of our knowledge. However, Murzin *et al*. have recently described the "catalyst-free" kinetics of stearic acid ketonization to stearone.[159] At first sight this seems rather surprising, as it is clear from reviewing past research that in almost all cases no thermal ketonization is reported to occur. Naturally, this depends on the applied process conditions and reactor setup, as ketonization requires high reaction temperature for energetic (endotherm) and kinetic (high activation energy) reasons. As described before, thermal palm oil ketonization has been reported at a temperature of 420 °C, which is at the high end when looking at Tables 1 and 3. In this work, the authors reported the catalyst-free ketonization of stearic acid in dodecane solvent in a 500 ml pressurized stainless steel batch reactor at 350 °C under 10 bar Ar pressure. Under these conditions, nearly 100% selectivity to stearone was obtained for initial substrate concentrations of 0.01-0.12M and reaction times

up to 2 hours. It is postulated here that the reactor wall, which consists of multiple different metal compounds, acts as a source of catalytic active sites for ketonization. When simultaneously increasing the initial concentration, temperature and reaction time to 1.75 M, 365 °C and 96 hours, the fractions of stearic acid, stearone and heptadecane in the final product mixture were 10, 14 and 48 wt% respectively, indicating low ketonization selectivity and the significant occurrence of fatty acid deoxygenation side reaction via decarboxylation. As shown in this review, many groups have proposed second order LH reaction kinetics to describe the heterogeneous C-C coupling of carboxylic acids. In this case however, the authors observed that second order kinetics were not able to fit the experimental results for an initial stearic acid concentration of 0.01M. A reaction mechanism was proposed which involves acid adsorption on the reactor wall active site in step 1, followed by its enolization in step 2, and finally fast coupling with an adjacent carboxylate to ultimately yield the ketone product in step 3. Combining the experimental data and proposed mechanism resulted in a kinetic model with zero order kinetics for high substrate concentrations and a first order dependence for lower concentrations, indicating the difference in availability of catalytic active reactor wall sites depending on initial stearic acid loading (eq. 21):

$$\boldsymbol{r = \frac{k_1 k_2 C_{acid}}{k_1 C_{acid} + k_2 + k_{-1} C_{H2O}} C_{cat}} \qquad (\boldsymbol{eq.21})$$

with r the reaction rate and k_1 and k_2 the forward reaction rate constants of the adsorption and enolization step, respectively. The reaction rate constant of acid desorption is expressed by k_{-1} and C_x represents the concentrations of component x (acid, water and catalyst). To the best of our knowledge, no other group has reported on the potential catalytic activity of reactor material for ketonization of carboxylic acids.

6.2.2 Fatty acid esters

The Polish research group of Klimkiewicz and Syper *et al*. have published several studies on the gas-phase ketonization of fatty acid esters using multiple different mixed metal oxides, which include for example Sn-Ce-Rh-O, Zr-Mg-Y-O and Fe-Si-Cr-K-O.[59, 155, 161, 162, 164, 165]. The C-C coupling of methyl laurate was studied at 350-410 °C with a Sn-Ce-Rh-O catalyst (10:1 molar ratio of Sn to Ce with 0.05 mol% of Rh) in a fixed bed reactor system with toluene as inert carrier solvent to produce laurone (12-tricosanone).[161] The ester conversion rose from 2 to 99% when increasing the reaction temperature from 350 to 410 °C, while the highest ketone yield of 63% was obtained at 400 °C. The main liquid side products were dodecane and dodecene (22% yield), with dodecanol and dodecanal as additional by-products at lower reaction temperatures (2-9% yield). No gaseous products were analysed. A similar catalyst was also tested for the ketonization of a mixture of FAMEs after transesterification of non-erucic rape oil feedstock with methanol, which consisted of 87% methyl stearate, 7% methyl palmitate, 3% methyl arachidate and 2% methyl behenate.[164] Interestingly, a large effect on ketonization selectivity was observed when switching from methanol to hexane as "inert" diluent, while maintaining similar ester conversion. In the case of methanol, ketone and hydrocarbon yields of 63 and 14% were achieved, respectively, at 96% conversion and 385 °C. Under similar conditions, less than 40% ketone yield was achieved when using hexane, with a simultaneous increase in hydrocarbon yield. No further explanation was given by the authors to explain clarify said (reactive) diluent behaviour. In follow-up papers, also technical waste feedstock such as butyl esters of animal fatty acids were successfully converted to fatty ketones, as well as using other complex mixed metal oxides such as Zr-Mg-Y-O (100:10:1 molar ratio) and Fe-Si-Cr-K-O (100:2:1:0.1).[155, 162] With isopropyl caprate as substrate, the only C-C coupling ketone product was 10-nonadecanone (28% yield at 91% conversion), indicating the exclusive ketonization of the acid moiety of the ester.[59] Simultaneously, high acetone and propylene yields were obtained from the alcohol fragment of the ester, alongside smaller amounts of alcohol, aldehyde and other ketones. For all these examples a maximum ketonization selectivity of 60% was observed when starting from fatty acid methyl esters, whether as model compounds or as transesterification products from (waste) triglycerides. Unfortunately, the authors have not provided any clear explanation as to why such multicomponent oxide catalysts are the materials of choice in all of the referenced studies above, compared to more simple and common metal oxides. This is reinforced by the lack of physicochemical characterization of the chosen materials and correlation between catalyst properties and observed ketonization activity, selectivity and stability. However, later the same research group has addressed some of these remarks by reporting on the use of Zr-Mg-O and Zr-Mg-Y-O for *n*-butanol conversion to aldehyde and ketone.[166] Here, it was shown that both materials exhibited higher *n*-butanol conversion (88 %) and 4-heptanone selectivity (80 %) compared to MgO, ZrO_2 and Y_2O_3 catalysts, which showed varying ketone selectivity between 0-41 % at the very high reaction temperature of 450 °C. This was attributed to a higher density of Lewis acid sites which are active for ketonization, induced by oxygen vacancies as a direct result of metal admixturing in these materials. While there was no difference in catalytic performance between Zr-Mg-O and Zr-Mg-Y-O, the inclusion of Y might enhance the mechanical durability of the catalyst material. It was postulated that similarly for Fe-Si-Cr-K-O and Sn-Ce-Rh-O, the multicomponent materials induce modification and stabilization of the oxide crystal structure, accompanied by an increase in Lewis acidity due to oxygen vacancy formation. Depending on the specific oxide formulation, these multicomponent materials are p- or n-type semiconductor like materials. At this point, we refer to section 3.1.4 of this work, where we have elaborately covered the topics of metal doping and addition of metals with redox activity for enhancement of the overall ketonization performance, which partly coincides with this discussion. For the specific materials above, addition of Fe and Rh

incorporates (de)hydrogenation capacity, which also opens up new pathways to the desired ketone products from alcohol substrates as described in the next paragraph.

Depending on the reaction conditions and specific catalyst, a multitude of parallel and sequential reactions can occur during fatty ester ketonization, which results in a complex reaction network and product distribution. Two esters can initially condense into an alcohol and β-ketoester according to a Claisen-Dieckmann reaction (eq. 22). This alcohol can be dehydrated to alkene and water (eq. 23), or dehydrogenated to aldehyde and hydrogen (eq. 24) if the catalyst has (de)hydrogenation capacity (for example the aforementioned Sn-Ce-Rh-O material). The aldehyde can then undergo further condensation towards the symmetric ketone of the alcohol parts of the original ester substrate (eq. 25). The β-ketoester can be hydrolysed in the presence of water to form a reactive β-ketoacid species and alcohol (eq. 26). This unstable β-ketoacid intermediate can then decarboxylate into ketone and CO_2 (eq. 27). Furthermore, the original ester molecules may be hydrolysed to the corresponding carboxylic acid and alcohol molecules (eq. 28), after which the carboxylic acids can undergo direct ketonization (eq. 29).

$$\mathbf{2\ RCOOCH_2R' \rightleftharpoons R'CH_2OH + RCORCOOCH_2R'} \quad (\boldsymbol{eq.22})$$

$$\mathbf{R'CH_2OH+ \rightleftharpoons R'' = CH_2 + H_2O} \quad (\boldsymbol{eq.23})$$

$$\mathbf{R'CH_2OH \rightleftharpoons R'CHO + H_2} \quad (\boldsymbol{eq.24})$$

$$\mathbf{2\ R'CHO \rightleftharpoons R'COOCH_2R' \rightleftharpoons R'COR' + CO + H_2} \quad (\boldsymbol{eq.25})$$

$$\mathbf{RCORCOOCH_2R' + H_2O \rightleftharpoons RCORCOOH + R'CH_2OH} \quad (\boldsymbol{eq.26})$$

$$\mathbf{RCORCOOH \rightleftharpoons RCORH + CO_2} \quad (\boldsymbol{eq.27})$$

$$\mathbf{RCOOCH_2R' + H_2O \rightleftharpoons RCOOH + R'CH_2OH} \quad (\boldsymbol{eq.28})$$

$$\mathbf{2RCOOH \rightleftharpoons RCOR + CO_2 + H_2O} \quad (\boldsymbol{eq.29})$$

6.2.3 Triglycerides

Although most studies in this field focus on the use of fatty acids and fatty acid esters as ketonization substrates, both are only present in minor amounts (i.e. few wt%) naturally in the raw biomass vegetable oil and animal fat feedstock, which are mainly comprised of triglycerides. One of the first studies to perform the "direct ketonization" of triglycerides was published by Jackson *et al.*, where refined seed oil of *Cuphea* sp. was used in the cross-ketonization coupling with acetic acid (Figure 18).[158] This feedstock has an interesting fatty acid distribution profile in the triglycerides (71% $C_{10:0}$, 3% $C_{12:0}$, 4% $C_{14:0}$, 6% $C_{16:0}$, 10% $C_{18:1}$ and 5% $C_{18:2}$), which differs from most other plant oils due to the higher amount of medium-chain compounds. Therefore, its volatility is also lower, lending itself to the potential of gas-phase coupling with acetic acid towards 2-undecanone, which has value due to its fragrance and insect repellent properties. The highest target yield of 91% was achieved after 21 hours at 400 °C over $Fe_{0.5}Ce_{0.2}Al_{0.3}O_x$ and an excess of acetic acid (23:1 molar ratio). Additionally, small amounts of the homo-ketonization product 10-nonadecanone (3% yield) were also found. When other materials such as Al_2O_3 and ZrO_2 were used as catalysts, lower target yields were achieved with a simultaneous increase in decanoic acid yield (up to 35%). These (intermediate) free fatty acids can originate from hydrolysis of the triglyceride substrate using water from the ketonization reaction or from the transesterification reaction between *Cuphea* oil and acetic acid. Interestingly, opposed to the suggested reaction equation (Figure 18), no glycerol by-product was obtained. After analysing the amount and H/C ratio of coke formation on the catalyst during TOS with TPO, it was suggested that glycerol is lost under the applied conditions via (cracking) side reactions.

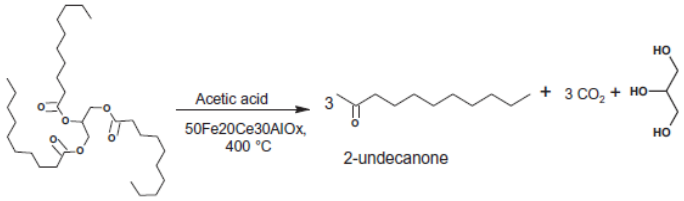

Figure 18: Cross-ketonization of *Cuphea* sp. oil with acetic acid as drawn by Jackson *et al.*
Reprinted from [158], Copyright (2012) with permission from Elsevier.

A more conventional triglyceride biomass source was used by Phung *et al.*, who studied the thermal and catalytic pyrolysis of palm oil, which has the largest production volume of all major vegetable oils worldwide.[48] Hereto, a batch reactor setup was used to

screen several catalysts, including Al_2O_3 and MgO-Al_2O_3 (calcined hydrotalcite), and zeolites HZSM-5 and NaX. After two hours of thermal reaction (no catalyst) at 420 °C, palm oil conversion was complete with 7% selectivity towards gaseous products such as CO, CO_2, light alkanes/alkenes (C_1-C_5) and acrolein, 47% liquid hydrocarbons and 31% ketones. When employing MgO-Al_2O_3 under identical conditions, the selectivity values were changed to 18, 28 and 69%, respectively, showing the increased tendency towards ketonization with accompanying gas production in the presence of a mixed metal oxide. Still, deoxygenation and cracking side reactions were significant under the applied process conditions. Here, it was suggested that glycerol is the main contributor to the overall CO, CO_2, acrolein and light hydrocarbon yield, formed via cracking reactions. The intermediate fatty acids are prone to both deoxygenation (via decarbonylation and decarboxylation) and cracking reactions. Alternatively when zeolite materials were added as catalysts, hydrocarbon and other oxygenate selectivity values rose at the expense of ketone yield with increased formation of olefins, oligomers and aromatics. While the recent work of Lee *et al.* is already described extensively in section 4.2 regarding the impact of unsaturation on ketonization (Figure 12), they have also tested non-model compounds by coupling of fatty acids originating from palm oil hydrolysis (44% palmitic acid, 42% oleic acid, 8% linoleic acid) in a fixed bed reactor at 380 °C on a TiO_2 catalyst.[114] After 40 hours on stream, a significant amount (> 20%) of side reactions such as cracking and McLafferty rearrangements occurred, resulting in a decreasing C_{31}-C_{35} ketone yield from ~ 75 to 50%, and catalyst deactivation due to coking. To combat this loss in selectivity and stability, the authors proposed a "hydrogenative hydrolysis" strategy of the palm oil feedstock, which combines the triglyceride hydrolysis and hydrogenation of unsaturated fatty acid species via the presence of a 5% Pt/C catalyst under a 15 bar H_2 reaction atmosphere. Consequently, the fully pre-saturated fatty acid mixture achieved a higher total ketone yield of 91%, with higher selectivity and time-on-stream stability. Evidently, it must be noted that in this case the resulting product mixtures are not the same as no unsaturated ketones can be formed. Finally, the fatty ketones were subjected to a hydrodeoxygenation step using Pt/Al_2O_3 at 300 °C under 20 bar H_2, resulting in ~ 83% C_{31}-C_{35} alkanes and smaller amounts of C_{14}-C_{30} hydrocarbon side products with a broader C-number distribution.

Oliver-Tomas *et al*. have further explored the impact of feedstock type (TG *vs*. FFA *vs*. FAME) on ketonization selectivity by carrying out isotopic labelling experiments.[163] Here, sunflower vegetable oil was used as triglyceride feedstock (93% C_{18} and 7% C_{16} fatty acids) for the ketonization on ZrO_2 in a fixed bed reactor system at 400-550 °C under atmospheric H_2 pressure. Under these conditions, full conversion resulted in a complex product mixture, which was divided into gasoline, diesel and wax fractions based on simulated distillation results. For all temperatures between 400 and 500 °C, selectivity towards the wax fraction (and thus ketonization) was low, decreasing from 43 to 11% for increasing temperature. After hydrodeoxygenation of the crude product mixtures on a Pt/Al_2O_3 catalyst, the liquid fraction mainly consisted of alkanes (72 wt%), monoaromatics (16 wt%) and cycloalkanes (5 wt%) with gasoline, diesel and wax yields of 6, 43 and 47%, respectively, for a reaction temperature of 400 °C. Clearly, side reactions such as cracking, Diels-Alder coupling, deoxygenation and aromatization occurred significantly, and was attributed to the presence of both unsaturated fatty acids species as well as the glycerol part of the original triglyceride. A reference experiment was therefore conducted with oleic acid as model fatty acid compound ($C_{18:1}$), which showed that cracking and fragmentation reactions are likely originating from the ester (glycerol) moiety, because wax and diesel yields were very high. When using methyl stearate as ketonization substrate, higher wax yields were obtained compared to similar experiments with sunflower oil. To elucidate the origin of side reactions, the gaseous output was analysed when regular sunflower oil and isotopically ^{13}C-labelled methyl stearate were used as substrates, indicating high yields of CO_2, CO and methane alongside other short-chain hydrocarbons

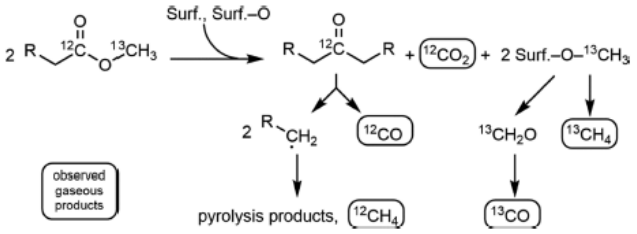

Figure 19: Formation of (un)labelled gaseous products from labelled methyl stearate ketonization as presented by Oliver-Tomas *et al*. Reprinted with permission from [163], Copyright (2017) American Chemical Society.

in both cases. When employing ^{13}C labelled methyl stearate, it was shown that labelled methane and CO originated from the labelled alcohol part of the ester (Figure 19). The authors proposed a conversion pathway of surface methoxy groups that are formed during ketonization into carbon monoxide by consecutive dehydrogenation to formaldehyde, followed by its oxidation to formic acid in the presence of water and further dehydration to CO. Furthermore, their unlabelled analogues could be formed by C-C bond cleavage of the ketone, where the resulting alkyl chains can undergo further radical chain reactions to short-chain pyrolysis products and additional methane. The presence of (un)labelled CO for both substrates indicate free radical mechanisms, with glycerol splitting into methanol and C_2 fragments under ketonization conditions as a potential, important initiator when starting from triglyceride biomass feedstock.

6.2.4 Patent literature

To conclude this section, patent literature regarding oleochemical biomass ketonization will also be discussed. Interestingly, compared to academic research papers many (recent) applications have been published, of which a selected overview is given in Table 4. Neste Oil and Rhodia Operations (Solvay) are clearly two major contributors, who have claimed several processes and/or catalysts for triglyceride, fatty acid and fatty acid ester ketonization. As expected, amphoteric (mixed) metal oxides are the preferred catalytic materials employed. As discussed earlier, glycerol and unsaturation in the original biomass feedstock result in lower ketonization selectivity and catalyst deactivation. Therefore, pre-hydrogenation of the fatty acids derived from initial vegetable/animal triglyceride hydrolysis may be preferable depending on required conditions. Besides the use of renewable biomass, which could potentially reduce CO_2 emissions, additional end-product advantages such as absence of sulphur, nitrogen and aromatic compounds are targeted compared to classic petroleum base oils. These ketonization reactions are often further combined with commercially available hydroprocessing technologies such as hydrodeoxygenation and hydro-isomerisation towards branched long-chain paraffins, which are valuable base oil compounds to replace current petroleum-derived products (Figure 20).

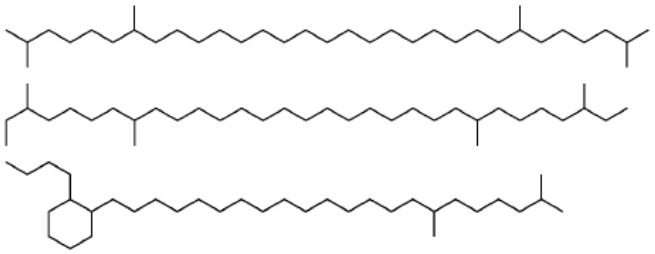

Figure 20: Target base oil molecules after consecutive fatty acid ketonization, hydrodeoxygenation and hydro-isomerisation. Reprinted from[167].

An alternative pathway towards these target molecules via ketonization has been employed by Myllyoja *et al*. In this example, distilled tall oil fatty acids were first isomerised via a mordenite zeolite catalyst, followed by hydrogenation on Pd/C resulting in the formation of a branched isostearic acid mixture. This was further used as substrate for ketonization on MnO_2 at 370 °C in a fixed bed reactor to the corresponding branched ketones, which were finally hydrodeoxygenated to the target paraffins.[167]
As mentioned, the follow-up hydrotreating technologies are commercially available as they are currently employed to remove heteroatoms such as O, N and S from petroleum products, often using sulphidized NiMo or CoMo on alumina support as catalysts.[168] Therefore, Kettunen *et al*. have proposed the combined production of base oils and fuels by performing the ketonization reaction under hydrotreating conditions (365 °C, 20 bar H_2, H_2/Hydrocarbon 500 Nl/l) with sulphidized K_2O/TiO_2-$NiMo/Al_2O_3$ as dual catalyst system to limit catalyst deactivation and oligomerization side reactions.[29] When starting from a mixture of palm oil and palm oil fatty acids, total base oil yield is low, however, compared to the obtained diesel fraction (31 *versus* 69%, respectively). In a different application, the sole use of a sulphidized $NiMo/Al_2O_3$ hydrotreating catalyst for both ketonization and hydrotreatment was demonstrated, eliminating the strict need for a dedicated ketonization catalyst.[31] Here, up to 30% base oil yield was achieved when starting from a feedstock mixture containing stearic acid and rapeseed oil biomass. As discussed in the metal oxide paragraph of this work, catalyst doping with (earth) alkali metals has been proposed as one of the potential modifications to enhance ketonization activity. In a recent patent application by Myllyoja *et al*., however, it was shown that the yield of undesired heavy products due to trimerization side reaction increased from 2 to 12 wt% when employing TiO_2 and K_2O/TiO_2 catalysts, respectively.[181] In the same work, ICP analysis was performed during the first 4 weeks of a 10 month operation to determine the degree of metal leaching. Full leaching of K combined with high levels of Na and Ca leaching were observed in the final ketone product for the K_2O/TiO_2 catalyst, indicating a second drawback compared to the regular TiO_2 material. Interestingly, here the C-C coupling of palmitic acid was conducted in the liquid phase at 18 bar under constant CO_2 flow at 360 °C. Later the

Table 4: Overview of selected fatty acid ketonization in patent literature.

Substrate	Catalyst	Reactor	T (°C)	P (bar)	X (%)	Y (%)	Ref
Hydrogenated palm fatty acids	MnO_2	Fixed bed	370	1	/	96	[167]
Stearic acid + rapeseed oil	$NiMo/Al_2O_3$	Fixed bed	365	7 (H_2)	/	30	[31]
Lauric acid	Al_2O_3	Fixed bed	410	1	~64	/	[169]
Cuphea oil + acetic acid	$Fe_wCe_xAl_yO_z$	Fixed bed	400	2.4 (N_2)	/	94	[170]
Palm oil fatty acid + palm oil	K_2O/TiO_2 – $NiMo/Al_2O_3$	Fixed bed	365	20 (H_2)	/	31	[29, 171]
Coconut fatty acids	Iron powder	Flask	300-320	/	100	79	[172]
Oleic acid	Iron powder	Batch	330-340	/	100	90	[173]
Oleic acid	Mn_2O_3	Fixed bed	350	5 (N_2)	100	100	[174]

Oleic acid	ZrO_2	Fixed bed	500	~257	/	/	[175]
Distilled animal fatty acids	Iron powder	Batch	590	3	98	90	[176]
Linoleic acid	MgO	Flask	310	0.01	99	86	[177]
Stearic + palmitic acid	Bauxite	Fixed bed	385	/	93	82	[178]
Sperm oil + acetic acid	Manganese oxide	Fixed bed	350	~0.04	/	60-70	[179]
Benzoic acid + palmitic acid	Fe	Flask	315	/	/	91	[180]
Palmitic acid	TiO_2	Fixed bed	360	18	99	/	[181]
Palmitic acid	K_2O/TiO_2	Fixed bed	350	13-17	99	82	[182]
Coconut fatty acids	Fe_3O_4	Batch	330	/ (Ar)	100	96	[183]

/: Not mentioned; ~: Approximately

same group published an extended liquid-phase ketonization process in which multiple sequential trickle bed reactors are proposed that utilize CO_2 as carrier gas, generated by the C-C coupling reaction.[182] Here carbon dioxide is separated from the reactor effluent, recycled and used as carrier for H_2O that is stripped from the liquid phase. Furthermore, due to the endothermic nature of the reaction, the advantage of this setup lies in the possibility to use intermediate heating units to maintain the required reaction temperature and combat the adiabatic decrease. As was mentioned in the kinetics part of this review, CO_2, H_2O and ketone have been established as catalyst inhibitors by competitive adsorption in many cases. In this patent application, only mention of H_2O inhibition in the liquid phase was mentioned, with no comments on the potential negative impact of using CO_2 as carrier gas or of the ketone product.

To combat catalyst deactivation when using alumina for the ketonization of fatty acids, Hommeltoft *et al*. have patented the use of an oxidative catalyst regeneration technique incorporating both a coke oxidizing step (2% oxygen in N_2 at 482 °C for 15 hours-3 days) and simultaneous or following steam treatment (410 °C for 2 hours).[169] When studying lauric acid ketonization to laurone, a gradual increase in reaction temperature from 410 to 432 °C was first applied to combat catalyst passivation, with a resulting catalyst activity of 50% after 700 hours. Then, three different calcination techniques were applied: without steam, with steam after calcination and with steam during calcination. It was observed that initial catalyst activity could be regenerated for both techniques including steam treatment, while only applying calcination recovered 70% of initial catalyst activity. This was attributed to the possible regeneration of Al-OH active sites when exposing the catalyst to water at elevated temperatures.

Although in most cases alkane compounds are the desired end-products, some alternative target molecules have been synthesized from the ketone intermediates. Back *et al*. have for example reported the stepwise ketonization of coconut fatty acids with iron powder via intermediate metal salt formation, followed by hydrogenation of the ketone products to secondary fatty alcohols.[172] Additionally, these alcohols can be dehydrated to internal olefins, which in turn can be sulfonated to yield internal olefin sulfonates, which are valuable targets in surfactant industry. According to the authors an additional advantage of using this type of catalyst is related to its ferromagnetic properties, which provide the possibility of using magnetic fields to recycle and separate the active material from the product mixture. However, recuperation of the metal salts after reaction is not disclosed further in the description part. More detailed synthesis procedures for said secondary fatty alcohols, internal olefins and olefin sulfonates from fatty acid derived ketones have recently been reported by the same group.[183] Because of the natural fatty acid composition of vegetable oils and animal fats, ketonization research has primarily focussed on C-C coupling of aliphatic carboxylic acids. However, it has been reported that cross-ketonization of aliphatic and aryl carboxylic acids can be an attractive upgrading pathway towards aryl aliphatic ketones.[180] These molecules are valuable intermediates and can be further processed into a wide variety of functionalized chemicals such as monomer building blocks, branched acids, polyamines, esters, amides, oximes, alcohols, olefins, sulfonates, etc.

7. Future perspectives

As shown in this work, many catalytic advancements have been achieved in the field of carboxylic acid ketonization. An increasing number of experimental and theoretical studies have shed light on some important questions regarding this heterogeneously catalysed reaction. However, it is also abundantly clear that at this stage an overwhelming majority of publications has focussed on the gas-phase coupling of model short chain C_2-C_4 carboxylic acids in the context of bio-oil upgrading.

As of today, the debate about the exact ketonization mechanism(s) and the identity of catalytically active sites involved during reaction is still ongoing, which warrants the need for additional experimentally derived structure-function correlations and theoretical modelling on a molecular scale. Related to this, the topics of side reactions, catalyst stability and regeneration have not been covered sufficiently yet in the available literature. These aspects are of the utmost importance, before being able to translate this C-C coupling reaction to commercial implementation in the future.

The transition towards any future ketonization technology that utilizes lignocellulose biomass derived substrates requires further research. As such, some groups have started to incorporate more complex starting mixtures to imitate more realistic pyrolysis bio-oil feedstock. However, these mixtures were simplified by combining several model compounds, while industrial streams often

contain hundreds if not more of different (oxygenated) compounds. Therefore a large information gap remains in this particular field in terms of feedstock and analytical complexity. The interaction between such bio-derived streams and the applied catalysts needs further investigation, especially regarding the impact of different (inorganic) impurities and spectator species on their performance and stability. Additionally, no comparisons or suggestions have been made on the most suitable ketonization methodology, i.e. conventional gas-phase fixed bed reactor setups or (aqueous) condensed phase (batch) reactions. More kinetic and thermodynamic questions come into play here, at both the catalyst and process design/engineering levels. Future development of targeted catalyst modifications could also be of large interest in this area to obtain more insight.

While ketonization is often proposed as a viable strategy towards biofuels and/or chemical precursors from short-chain acids, up to this point almost no information exists in academic or patent literature regarding its techno-economic feasibility and/or (environmental) sustainability. The need for both TEAs and LCAs seems crucial in this regard to gain more insight into the possible validity of ketonization as an effective valorisation process in future biorefineries. Furthermore, this work also encompasses critical selection of feedstock, while taking into consideration important sustainability aspects such as (local) availability, avoiding competition with the food industry, e.g. by use of waste streams.

For oleochemical biomass ketonization, even more unanswered questions remain as the amount of (academic) literature on this topic is much smaller. Interestingly, some crucial information may be deducted from the (very) recent patent literature. Experimental mechanistic and kinetic studies are nearly non-existent for these feedstock, while simultaneously no detailed modelling data or theoretical calculations are available for the interaction between these long chain C_{12}-C_{18} carboxylic acids and typical ketonization catalysts. Due to their vastly different physicochemical properties (acidity, boiling point, melting point, …) compared to short-chain acids, ketonization process design and engineering are important considerations for future research work. As the apolar triglycerides and fatty acids are likely to be in the condensed phase without water as possible reaction solvent at suitable C-C coupling conditions, the impact of this different reaction environment for substrate and catalyst should be investigated, preferably when no solvent is utilized. As is the case for lignocellulose biomass, also here the importance of different feedstock types such as animal, vegetable or algal sources, and the possible impact of their impurities and composition should be considered further. Meanwhile, to the best of our knowledge, no TEAs or LCAs have been performed on the ketonization of fatty acid (derivatives) which is crucial for evaluating its application potential and (environmental) sustainability in terms of carbon dioxide footprint. Lastly, characterization of the physicochemical properties of the final ketone products is an interesting topic that has not received much attention, as these molecules could serve as potential end products themselves in existing and future applications. Indeed, any further downstream processing technologies that can be omitted will result in stronger (economic) cases for ketonization in future biorefineries.

8. Conclusion

The C-C coupling ketonization reaction of carboxylic acids is increasingly showing its potential as a valuable upgrading strategy to convert both lignocellulose and oleochemical biomass into renewable fuels and chemicals. This is emphasized by the large amount of recent publications on this topic, which mainly focus on the gas-phase ketonization of model short-chain acids.

Although its inception started in the 19th century with the use of metal carboxylate salts via bulk C-C coupling mechanisms, amphoteric metal oxides have shown their superior activity, selectivity and stability via heterogeneously catalysed surface pathways. While there is still an ongoing discussion about the exact elementary steps of the surface mechanism, it is generally acknowledged that the β-keto acid surface mechanism is the most likely one. Additionally, very recent concepts such as the reversibility of (some of) its elementary steps have been presented. Via surface adsorption studies, multiple binding configurations of the carboxylic acid molecules have been shown, which can show distinct interactions and differences in reactivity, as calculated by DFT modelling. Various structure-function correlations have contributed to a better understanding of the necessary requirements for suitable active sites on these catalysts, which generally are described as weak or medium strength Lewis acid-base pairs (M-O). Furthermore, properties such as surface area, porosity, crystallinity and dimensionality have been shown to impact performance. As a result, targeted modifications such as (metal) doping, support addition, reductive pre-treatments and metal impregnation have been established to improve their activity, selectivity and stability depending on the reaction environment. While advancements have been made to improve catalyst stability of the most active materials, more research is needed in this field, including development of suitable regeneration procedures. Alternatively, the use of zeolite catalysts has been shown to possess significant drawbacks compared to metal oxides, as the nature of their Brönsted acid sites promotes competing and undesired side reactions.

Crucial carboxylic acid substrate properties that impact overall ketone yield have been discussed, where it is shown that in general an increase in carbon chain length and degree of branching reduces their reactivity, while unsaturation decreases the ketonization yield due to side reactions and catalyst fouling. Additionally, multiple kinetic and thermodynamic aspects have been reviewed, showing the wide range of kinetic models such as LH, ER, power laws, etc. that have been used by researchers in the field to describe the experimental kinetic data. Product inhibition for carbon dioxide, water and ketone has been observed and described in various degrees of depth, often depending on the exact substrate, catalyst and reaction conditions applied. Specifically, a significant difference exists when performing gas-phase *vs*. (aqueous) condensed phase reactions with regard to the overall energetics of the C-C coupling reaction when considering biomass derived feedstock streams.

En route to the implementation of real biomass substrates, the (negative) impact of some common organic compounds and inorganic impurities present in these complex organic/aqueous mixtures has been shown, suggesting the need for different pre-treatment and purification steps in larger cascade process schemes for future biorefineries, or the development of catalyst that are less sensitive to such deactivation. Depending on the target end-products, additional downstream processing reactions such as hydrogenation, condensation, hydrodeoxygenation, (hydro-)isomerisation, amination, sulfonation etc. can ultimately deliver bio-based fuels, lubricants, waxes, surfactants and other chemicals. The realization of future techno-economic analyses based on realistic process scenarios and with that the assessment of (environmental) sustainability, providing carbon dioxide footprints, will be crucial to determine the true value and industrial potential of biomass carboxylic acid ketonization.

Conflicts of interest

There are no conflicts of interest to declare.

Acknowledgements

B.B. acknowledges the Research Foundation-Flanders (FWO) for a PhD Fellowship (strategic basic research - SB). B.S. acknowledges VLAIO for the Catalisti FISCH-ICON Biowax Project.

References

1. Friedel, C., *Ueber s. g. gemischte Acetone.* Justus Liebigs Annalen der Chemie, 1858. **108**(1): p. 122-125.
2. Squibb, E.R., Improvement in the manufacture of acetone.*1.* Journal of the American Chemical Society, 1895. **17**(3): p. 187-201.
3. Vennestrøm, P.N.R., et al., *Beyond Petrochemicals: The Renewable Chemicals Industry.* Angewandte Chemie International Edition, 2011. **50**(45): p. 10502-10509.
4. Sheldon, R.A., *Green and sustainable manufacture of chemicals from biomass: state of the art.* Green Chemistry, 2014. **16**(3): p. 950-963.
5. Climent, M.J., A. Corma, and S. Iborra, *Conversion of biomass platform molecules into fuel additives and liquid hydrocarbon fuels.* Green Chemistry, 2014. **16**(2): p. 516-547.
6. Klass, D.L., *Chapter 3 - Photosynthesis of Biomass and Its Conversion-Related Properties*, in *Biomass for Renewable Energy, Fuels, and Chemicals*, D.L. Klass, Editor. 1998, Academic Press: San Diego. p. 51-90.
7. Lange, J.-P., *Lignocellulose conversion: an introduction to chemistry, process and economics.* Biofuels, Bioproducts and Biorefining, 2007. **1**(1): p. 39-48.
8. Kan, T., V. Strezov, and T.J. Evans, *Lignocellulosic biomass pyrolysis: A review of product properties and effects of pyrolysis parameters.* Renewable and Sustainable Energy Reviews, 2016. **57**: p. 1126-1140.
9. Isahak, W.N.R.W., et al., *A review on bio-oil production from biomass by using pyrolysis method.* Renewable and Sustainable Energy Reviews, 2012. **16**(8): p. 5910-5923.
10. Wang, H.M., J. Male, and Y. Wang, *Recent Advances in Hydrotreating of Pyrolysis Bio-Oil and Its Oxygen-Containing Model Compounds.* ACS Catal., 2013. **3**(5): p. 1047-1070.
11. Lian, X., et al., *Progress on upgrading methods of bio-oil: A review.* International Journal of Energy Research, 2017. **41**(13): p. 1798-1816.
12. King, A.E., et al., *Understanding Ketone Hydrodeoxygenation for the Production of Fuels and Feedstocks From Biomass.* ACS Catalysis, 2015. **5**(2): p. 1223-1226.
13. Hayes, D., et al., *The Biofine Process – Production of Levulinic Acid, Furfural, and Formic Acid from Lignocellulosic Feedstocks*. 2008. p. 139-164.
14. Becker, J., et al., *Top value platform chemicals: bio-based production of organic acids.* Current Opinion in Biotechnology, 2015. **36**: p. 168-175.
15. Choi, S., et al., *Biorefineries for the production of top building block chemicals and their derivatives.* Metabolic Engineering, 2015. **28**: p. 223-239.
16. Schwartz, T.J., B.H. Shanks, and J.A. Dumesic, *Coupling chemical and biological catalysis: a flexible paradigm for producing biobased chemicals.* Current Opinion in Biotechnology, 2016. **38**: p. 54-62.
17. Steen, E.J., et al., *Microbial production of fatty-acid-derived fuels and chemicals from plant biomass.* Nature, 2010. **463**(7280): p. 559-562.
18. Lennen, R.M. and B.F. Pfleger, *Microbial production of fatty acid-derived fuels and chemicals.* Current Opinion in Biotechnology, 2013. **24**(6): p. 1044-1053.
19. Shahab, R.L., et al., *A heterogeneous microbial consortium producing short-chain fatty acids from lignocellulose.* Science, 2020. **369**(6507): p. eabb1214.
20. Dijkstra, A., *The Lipid Handbook - 3rd edition.* Modification processes and food uses, 2007: p. 263-354.
21. Behr, A., A. Westfechtel, and J. Gomes, *Catalytic Processes for the Technical Use of Natural Fats and Oils.* Chemical Engineering & Technology, 2008. **31**: p. 700-714.

22. Biermann, U., et al., *Oils and Fats as Renewable Raw Materials in Chemistry.* Angewandte Chemie International Edition, 2011. **50**(17): p. 3854-3871.
23. Barnebey, H.L. and A.C. Brown, *Continuous fat splitting plants using the colgate-emery process.* Journal of the American Oil Chemists' Society, 1948. **25**(3): p. 95-99.
24. Malhotra Shadi, L., W. Wong Raymond, and P. Breton Marcel, *Ink Compositions*. 2002, XEROX CORP: US.
25. Tomlinson Alan, D., *Dish Washing Compositions*. 2005, UNILEVER PLC, UNILEVER NV: EP.
26. Seipel, W., N. Boyxen, and H. Hensen, *Use Of Nanoscale Waxes*. 2001, COGNIS DEUTSCHLAND GMBH:WO.
27. Stewart Ray, F. and L. Dunson Debra, *Temperature-switching Materials Having Improved Strength And Thermal Properties*. 2010, BAY MATERIALS LLC: WO.
28. Shanker, K.S., et al., *Isolation and antimicrobial evaluation of isomeric hydroxy ketones in leaf cuticular waxes of Annona squamosa.* Phytochemical Analysis, 2007. **18**(1): p. 7-12.
29. Kettunen, M., et al., *Simultaneous Production Of Base Oil And Fuel Components From Renewable Feedstock*. 2014, NESTE OIL OYJ: EP.
30. Koivusalmi, E., et al., *Process For Producing A Branched Hydrocarbon Base Oil From A Feedstock Containing Aldehyde And/or Ketone*. 2010, NESTE OIL OYJ: US.
31. Myllyoja, J., P. Aalto, and R. Piilola, *A Method For Production Of Hydrocarbons By Increasing Hydrocarbon Chain Length*. 2013, NESTE OIL OYJ: WO.
32. Renz, M., *Ketonization of Carboxylic Acids by Decarboxylation: Mechanism and Scope.* European Journal of Organic Chemistry, 2005. **2005**(6): p. 979-988.
33. Pham, T.N., et al., *Ketonization of Carboxylic Acids: Mechanisms, Catalysts, and Implications for Biomass Conversion.* ACS Catalysis, 2013. **3**(11): p. 2456-2473.
34. Rajadurai, S., *Pathways for Carboxylic Acid Decomposition on Transition Metal Oxides.* Catalysis Reviews, 1994. **36**(3): p. 385-403.
35. Pacchioni, G., *Ketonization of Carboxylic Acids in Biomass Conversion over TiO2 and ZrO2 Surfaces: A DFT Perspective.* ACS Catalysis, 2014. **4**(9): p. 2874-2888.
36. Ignatchenko, A.V., *Multiscale approach for the optimization of ketones production from carboxylic acids by the decarboxylative ketonization reaction.* Catalysis Today, 2019. **338**: p. 3-17.
37. Kumar, R., et al., *Ketonization of oxygenated hydrocarbons on metal oxide based catalysts.* Catalysis Today, 2018. **302**: p. 16-49.
38. Lee, Y., et al., *Ketonization of hexanoic acid to diesel-blendable 6-undecanone on the stable zirconia aerogel catalyst.* Applied Catalysis A: General, 2015. **506**: p. 288-293.
39. Ignatchenko, A.V., et al., *Cross-selectivity in the catalytic ketonization of carboxylic acids.* Applied Catalysis A: General, 2015. **498**: p. 10-24.
40. Karimi, E., et al., *Ketonization and deoxygenation of alkanoic acids and conversion of levulinic acid to hydrocarbons using a Red Mud bauxite mining waste as the catalyst.* Catalysis Today, 2012. **190**(1): p. 73-88.
41. Pham, T.N., D. Shi, and D.E. Resasco, *Kinetics and Mechanism of Ketonization of Acetic Acid on Ru/TiO2 Catalyst.* Topics in Catalysis, 2014. **57**(6): p. 706-714.
42. Sudarsanam, P., et al., *Vapor phase synthesis of cyclopentanone over nanostructured ceria–zirconia solid solution catalysts.* Journal of Industrial and Engineering Chemistry, 2013. **19**(5): p. 1517-1524.
43. Nagashima, O., et al., *Ketonization of carboxylic acids over CeO2-based composite oxides.* Journal of Molecular Catalysis A: Chemical, 2005. **227**(1): p. 231-239.
44. Gooßen, L., P. Mamone, and C. Oppel, *Catalytic Decarboxylative Cross-Ketonisation of Aryl- and Alkylcarboxylic Acids using Magnetite Nanoparticles.* Advanced Synthesis & Catalysis, 2011. **353**: p. 57-63.
45. Baylon, R.A.L., et al., *Beyond ketonization: selective conversion of carboxylic acids to olefins over balanced Lewis acid–base pairs.* Chemical Communications, 2016. **52**(28): p. 4975-4978.
46. Snell, R.W. and B.H. Shanks, *CeMOx-Promoted Ketonization of Biomass-Derived Carboxylic Acids in the Condensed Phase.* ACS Catalysis, 2014. **4**(2): p. 512-518.
47. Gumidyala, A., T. Sooknoi, and S. Crossley, *Selective ketonization of acetic acid over HZSM-5: The importance of acyl species and the influence of water.* Journal of Catalysis, 2016. **340**: p. 76-84.
48. Phung, T.K., et al., *Catalytic pyrolysis of vegetable oils to biofuels: Catalyst functionalities and the role of ketonization on the oxygenate paths.* Fuel Processing Technology, 2015. **140**: p. 119-124.
49. Oliver-Tomas, B., M. Renz, and A. Corma, *Direct conversion of carboxylic acids (Cn) to alkenes (C2n−1) over titanium oxide in absence of noble metals.* Journal of Molecular Catalysis A: Chemical, 2016. **415**.
50. Jackson, M.A., *Ketonization of Model Pyrolysis Bio-oil Solutions in a Plug-Flow Reactor over a Mixed Oxide of Fe, Ce, and Al.* Energy & Fuels, 2013. **27**(7): p. 3936-3943.
51. Mansur, D., et al., *Production of ketones from pyroligneous acid of woody biomass pyrolysis over an iron-oxide catalyst.* Fuel, 2013. **103**: p. 130-134.
52. Wu, K., et al., *Carbon Promoted ZrO2 Catalysts for Aqueous-Phase Ketonization of Acetic Acid.* ACS Sustainable Chemistry & Engineering, 2017. **5**(4): p. 3509-3516.
53. Aranda-Pérez, N., et al., *Enhanced activity and stability of Ru-TiO2 rutile for liquid phase ketonization.* Applied Catalysis A: General, 2017. **531**: p. 106-118.
54. Funai, S., T. Tago, and T. Masuda, *Selective production of ketones from biomass waste containing a large amount of water using an iron oxide catalyst.* Catalysis Today - CATAL TODAY, 2011. **164**: p. 443-446.

55. Orozco, L.M., M. Renz, and A. Corma, *Cerium oxide as a catalyst for the ketonization of aldehydes: mechanistic insights and a convenient way to alkanes without the consumption of external hydrogen.* Green Chemistry, 2017. **19**(6): p. 1555-1569.
56. Davis, R. and H.P. Schultz, *Studies of Thermal Decarboxylation of Iron Carboxylates. I. Preparation of Symmetrical Aliphatic Ketones1,2.* The Journal of Organic Chemistry, 1962. **27**(3): p. 854-857.
57. Yamada, Y., et al., *Catalytic performance of rare earth oxides in ketonization of acetic acid.* Journal of Molecular Catalysis A: Chemical, 2011. **346**(1): p. 79-86.
58. Gliński, M., W. Szymański, and D. Łomot, *Catalytic ketonization over oxide catalysts : X. Transformations of various alkyl heptanoates.* Applied Catalysis A: General, 2005. **281**: p. 107–113.
59. Klimkiewicz, R., H. Grabowska, and L. Syper, *Vapor-Phase Conversion of Esters into Ketones in the Presence of an Sn-, Ce-, and Rh-Containing Oxide Catalyst.* Kinetics and Catalysis, 2003. **44**(2): p. 283-286.
60. Wang, S. and E. Iglesia, *Experimental and theoretical assessment of the mechanism and site requirements for ketonization of carboxylic acids on oxides.* Journal of Catalysis, 2017. **345**: p. 183-206.
61. Davidson, S.D., et al., *Steam Reforming of Acetic Acid over Co-Supported Catalysts: Coupling Ketonization for Greater Stability.* ACS Sustainable Chemistry & Engineering, 2017. **5**(10): p. 9136-9149.
62. Heracleous, E., et al., *Bio-oil upgrading via vapor-phase ketonization over nanostructured FeO x and MnO x : catalytic performance and mechanistic insight.* Biomass Conversion and Biorefinery, 2017. **7**.
63. Lopez-Ruiz, J.A., et al., *Enhanced Hydrothermal Stability and Catalytic Activity of LaxZryOz Mixed Oxides for the Ketonization of Acetic Acid in the Aqueous Condensed Phase.* ACS Catalysis, 2017. **7**(10): p. 6400-6412.
64. Pham, T., et al., *Aqueous-phase ketonization of acetic acid over Ru/TiO2/carbon Catalysts.* Journal of Catalysis, 2012. **295**: p. 169–178.
65. Randery, S.D., J.S. Warren, and K.M. Dooley, *Cerium oxide-based catalysts for production of ketones by acid condensation.* Applied Catalysis A: General, 2002. **226**(1): p. 265-280.
66. Fernández-Arroyo, A., et al., *Upgrading of oxygenated compounds present in aqueous biomass-derived feedstocks over NbOx-based catalysts.* Catalysis Science & Technology, 2017. **7**(23): p. 5495-5499.
67. Wrzyszcz, J., et al., *Catalytic reactions of oxidized n-C10 derivatives over an iron oxide.* Applied Catalysis A: General, 1999. **185**(1): p. 153-156.
68. Murkute, A.D., J.E. Jackson, and D.J. Miller, *Supported mesoporous solid base catalysts for condensation of carboxylic acids.* Journal of Catalysis, 2011. **278**(2): p. 189-199.
69. Yan, T., et al., *Cascade Conversion of Acetic Acid to Isobutene over Yttrium-Modified Siliceous Beta Zeolites.* ACS Catalysis, 2019. **9**(11): p. 9726-9738.
70. Sugiyama, S., et al., *Ketones from carboxylic acids over supported magnesium oxide and related catalysts.* Catalysis Letters, 1992. **14**(1): p. 127-133.
71. Khromova, S., et al., *Magnesium-containing catalysts for the decarboxylation of bio-oil.* Catalysis in Industry, 2013. **5**: p. 260-268.
72. Hites, R.A. and K. Biemann, *Mechanism of ketonic decarboxylation. Pyrolysis of calcium decanoate.* Journal of the American Chemical Society, 1972. **94**(16): p. 5772-5777.
73. Curtis, R.G., A.G. Dobson, and H.H. Hatt, *The ketonization of higher fatty acids with some observations on.* Journal of the Society of Chemical Industry, 1947. **66**(11): p. 402-407.
74. Ling, H., et al., *Composition-structure-function correlation of Ca/Zn/AlOx catalysts for the ketonization of acetic acid.* Catalysis Today, 2019.
75. Mekhemer, G.A.H., et al., *Ketonization of acetic acid vapour over polycrystalline magnesia: in situ Fourier transform infrared spectroscopy and kinetic studies.* Journal of Catalysis, 2005. **230**(1): p. 109-122.
76. Pulido, A., et al., *Ketonic Decarboxylation Reaction Mechanism: A Combined Experimental and DFT Study.* ChemSusChem, 2013. **6**(1): p. 141-151.
77. Hendren, T.S. and K.M. Dooley, *Kinetics of catalyzed acid/acid and acid/aldehyde condensation reactions to non-symmetric ketones.* Catalysis Today, 2003. **85**(2): p. 333-351.
78. Kulyk, K., et al., *Kinetics of Valeric Acid Ketonization and Ketenization in Catalytic Pyrolysis on Nanosized SiO2, γ-Al2O3, CeO2/SiO2, Al2O3/SiO2 and TiO2/SiO2.* ChemPhysChem, 2017. **18**(14): p. 1943-1955.
79. Kim, K.S. and M.A. Barteau, *Structure and composition requirements for deoxygenation, dehydration, and ketonization reactions of carboxylic acids on TiO2(001) single-crystal surfaces.* Journal of Catalysis, 1990. **125**(2): p. 353-375.
80. Woo, Y., et al., *Role of Anhydride in the Ketonization of Carboxylic Acid: Kinetic Study on Dimerization of Hexanoic Acid.* Industrial & Engineering Chemistry Research, 2017. **56**(4): p. 872-880.
81. Martens, J.A., et al., *Acid-catalyzed ketonization of mixtures of low carbon number carboxylic acids on zeolite H-T*, in *Studies in Surface Science and Catalysis*, M. Guisnet, et al., Editors. 1993, Elsevier. p. 527-534.
82. Vervecken, M., et al., *Zeolite-Induced Selectivity in the Conversion of the Lower Aliphatic Carboxylic Acids*, in *Chemical Reactions in Organic and Inorganic Constrained Systems*, R. Setton, Editor. 1986, Springer Netherlands: Dordrecht. p. 95-114.
83. González, F., G. Munuera, and J.A. Prieto, *Mechanism of ketonization of acetic acid on anatase TiO2 surfaces.* Journal of the Chemical Society, Faraday Transactions 1: Physical Chemistry in Condensed Phases, 1978. **74**(0): p. 1517-1529.
84. Pestman, R., et al., *Reactions of Carboxylic Acids on Oxides: 2. Bimolecular Reaction of Aliphatic Acids to Ketones.* Journal of Catalysis, 1997. **168**(2): p. 265-272.
85. Pestman, R., et al., *The formation of ketones and aldehydes from carboxylic acids, structure-activity relationship for two competitive reactions.* Journal of Molecular Catalysis A: Chemical, 1995. **103**(3): p. 175-180.

86. Martinez, R., M.C. Huff, and M.A. Barteau, *Ketonization of acetic acid on titania-functionalized silica monoliths.* Journal of Catalysis, 2004. **222**(2): p. 404-409.
87. Wang, S. and E. Iglesia, *Experimental and Theoretical Evidence for the Reactivity of Bound Intermediates in Ketonization of Carboxylic Acids and Consequences of Acid–Base Properties of Oxide Catalysts.* The Journal of Physical Chemistry C, 2017. **121**(33): p. 18030-18046.
88. Almutairi, S.T., E.F. Kozhevnikova, and I.V. Kozhevnikov, *Ketonisation of acetic acid on metal oxides: Catalyst activity, stability and mechanistic insights.* Applied Catalysis A: General, 2018. **565**: p. 135-145.
89. Ignatchenko, A.V., et al., *Ab initio study of the mechanism of carboxylic acids cross-ketonization on monoclinic zirconia via condensation to beta-keto acids followed by decarboxylation.* Molecular Catalysis, 2017. **441**: p. 35-62.
90. Pham, T.N., D. Shi, and D.E. Resasco, *Reaction kinetics and mechanism of ketonization of aliphatic carboxylic acids with different carbon chain lengths over Ru/TiO2 catalyst.* Journal of Catalysis, 2014. **314**: p. 149-158.
91. Panchenko, V.N., et al., *DRIFTS and UV–vis DRS study of valeric acid ketonization mechanism over ZrO2 in hydrogen atmosphere.* Journal of Molecular Catalysis A: Chemical, 2014. **388-389**: p. 133-140.
92. Tosoni, S., *Acetic acid ketonization on tetragonal zirconia: Role of surface reduction.* Journal of catalysis, 2016. **v. 344**: p. pp. 465-473-2016 v.344.
93. Oliver-Tomas, B., M. Renz, and A. Corma, *Ketone Formation from Carboxylic Acids by Ketonic Decarboxylation: The Exceptional Case of the Tertiary Carboxylic Acids.* Chemistry – A European Journal, 2017. **23**(52): p. 12900-12908.
94. Shylesh, S., et al., *Experimental and Computational Studies of Carbon–Carbon Bond Formation via Ketonization and Aldol Condensation over Site-Isolated Zirconium Catalysts.* ACS Catalysis, 2020. **10**(8): p. 4566-4579.
95. Ignatchenko, A.V. and A.J. Cohen, *Reversibility of the catalytic ketonization of carboxylic acids and of beta-keto acids decarboxylation.* Catalysis Communications, 2018. **111**: p. 104-107.
96. Ignatchenko, A.V., et al., *Equilibrium in the Catalytic Condensation of Carboxylic Acids with Methyl Ketones to 1,3-Diketones and the Origin of the Reketonization Effect.* ACS omega, 2019. **4**(6): p. 11032-11043.
97. Pei, Z.F. and V. Ponec, *On the intermediates of the acetic acid reactions on oxides: an IR study.* Applied Surface Science, 1996. **103**(2): p. 171-182.
98. Ding, S., et al., *Ketonization of Propionic Acid to 3-Pentanone over CexZr1–xO2 Catalysts: The Importance of Acid–Base Balance.* Industrial & Engineering Chemistry Research, 2018. **57**(50): p. 17086-17096.
99. Jahangiri, H., et al., *Zirconia catalysed acetic acid ketonisation for pre-treatment of biomass fast pyrolysis vapours.* Catalysis Science & Technology, 2018. **8**(4): p. 1134-1141.
100. Wu, K., et al., *ZrMn Oxides for Aqueous-Phase Ketonization of Acetic Acid: Effect of Crystal and Porosity.* Chemistry – An Asian Journal, 2018. **13**(9): p. 1180-1186.
101. Bennett, J.A., et al., *Acetic Acid Ketonization over Fe3O4/SiO2 for Pyrolysis Bio-Oil Upgrading.* ChemCatChem, 2017. **9**(9): p. 1648-1654.
102. Foraita, S., et al., *Impact of the Oxygen Defects and the Hydrogen Concentration on the Surface of Tetragonal and Monoclinic ZrO2 on the Reduction Rates of Stearic Acid on Ni/ZrO2.* Chemistry – A European Journal, 2015. **21**(6): p. 2423-2434.
103. Fernández-Arroyo, A., et al., *High {0 0 1} faceted TiO2 nanoparticles for the valorization of oxygenated compounds present in aqueous biomass-derived feedstocks.* Journal of Catalysis, 2018. **358**: p. 266-276.
104. Jewur, S.S. and J.C. Kuriacose, Influence of products and pretreatments on the ketonisation of acetic acid over iron oxide. Journal of the research institute for catalysis Hokkaido University, 1977. **24**(2): p. 73-82.
105. Gliński, M., J. Kijeński, and A. Jakubowski, *Ketones from monocarboxylic acids: Catalytic ketonization over oxide systems.* Applied Catalysis A: General, 1995. **128**(2): p. 209-217.
106. Lu, F., et al., *Promotional effect of Ti doping on the ketonization of acetic acid over a CeO2 catalyst.* RSC Advances, 2017. **7**(36): p. 22017-22026.
107. Lu, F., et al., *Insights into the improvement effect of Fe doping into the CeO2 catalyst for vapor phase ketonization of carboxylic acids.* Molecular Catalysis, 2018. **444**: p. 22-33.
108. Dooley, K.M., et al., *Ketones from acid condensation using supported CeO2 catalysts: Effect of additives.* Applied Catalysis A: General, 2007. **320**: p. 122-133.
109. Bayahia, H., *Catalytic Activity of Cobalt-Molybdenum in Gas-Phase Ketonisation of Pentanoic Acid.* Science Journal of Chemistry, 2018. **6**: p. 11.
110. Jiang, B., et al., *Ce/MgAl mixed oxides derived from hydrotalcite LDH precursors as highly efficient catalysts for ketonization of carboxylic acid.* Catalysis Science & Technology, 2019. **9**(22): p. 6335-6344.
111. Weber, J., et al., *Effect of Metal Oxide Redox State in Red Mud Catalysts on Ketonization of Fast Pyrolysis Oil Derived Oxygenates.* Applied Catalysis B: Environmental, 2018. **241**.
112. Syzgantseva, O.A., M. Calatayud, and C. Minot, *Revealing the Surface Reactivity of Zirconia by Periodic DFT Calculations.* The Journal of Physical Chemistry C, 2012. **116**(11): p. 6636-6644.
113. Tosoni, S., et al., *TiO2 and ZrO2 in biomass conversion: why catalyst reduction helps.* Philosophical Transactions of the Royal Society A: Mathematical, Physical and Engineering Sciences, 2018. **376**(2110): p. 20170056.
114. Lee, K., M.Y. Kim, and M. Choi, *Effects of Fatty Acid Structures on Ketonization Selectivity and Catalyst Deactivation.* ACS Sustainable Chemistry & Engineering, 2018. **6**(10): p. 13035-13044.
115. Gayubo, A.G., et al., *Transformation of Oxygenate Components of Biomass Pyrolysis Oil on a HZSM-5 Zeolite. II. Aldehydes, Ketones, and Acids.* Industrial & Engineering Chemistry Research, 2004. **43**(11): p. 2619-2626.
116. Jahangiri, H., et al., *Ga/HZSM-5 Catalysed Acetic Acid Ketonisation for Upgrading of Biomass Pyrolysis Vapours.* Catalysts, 2019. **9**: p. 841.

117. Cao, J., et al., *Conversion of C2–4 Carboxylic Acids to Hydrocarbons on HZSM-5: Effect of Carbon Chain Length.* Industrial & Engineering Chemistry Research, 2019. **58**(24): p. 10307-10316.
118. Kots, P.A., A.V. Zabilska, and I.I. Ivanova, *Selective Self-Condensation of Butanal over Zr-BEA Zeolites.* ChemCatChem, 2020. **12**(1): p. 248-258.
119. Wang, X., et al., *Conversion of propionic acid and 3-pentanone to hydrocarbons on ZSM-5 catalysts: Reaction pathway and active site.* Applied Catalysis A: General, 2017. **545**.
120. Palizdar, A. and S.M. Sadrameli, *Catalytic upgrading of beech wood pyrolysis oil over iron- and zinc-promoted hierarchical MFI zeolites.* Fuel, 2020. **264**: p. 116813.
121. Gaertner, C.A., et al., *Ketonization Reactions of Carboxylic Acids and Esters over Ceria–Zirconia as Biomass-Upgrading Processes.* Industrial & Engineering Chemistry Research, 2010. **49**(13): p. 6027-6033.
122. Parida, K.M., A. Samal, and N.N. Das, *Catalytic ketonization of monocarboxylic acids over Indian Ocean manganese nodules.* Applied Catalysis A: General, 1998. **166**(1): p. 201-205.
123. Oliver-Tomas, B., et al., *Effect of the Cα substitution on the ketonic decarboxylation of carboxylic acids over m-ZrO2: the role of entropy.* Catalysis Science & Technology, 2016. **6**(14): p. 5561-5566.
124. Diebold, J., *A Review of the Chemical and Physical Mechanisms of the Storage Stability of Fast Pyrolysis Bio-Oils.* Energy, 2000. **2**.
125. Gliński, M. and J. Kijeński, *Catalytic Ketonization of Carboxylic Acids Synthesis of Saturated and Unsaturated Ketones.* Reaction Kinetics and Catalysis Letters, 2000. **69**(1): p. 123-128.
126. Renz, M. and A. Corma, *Ketonic Decarboxylation Catalysed by Weak Bases and Its Application to an Optically Pure Substrate.* European Journal of Organic Chemistry, 2004. **2004**: p. 2036-2039.
127. Liberman, A.L. and T.V. Vasina, *Some improvements in the method for the ketonization of dicarboxylic acids.* Bulletin of the Academy of Sciences of the USSR, Division of chemical science, 1968. **17**(3): p. 609-612.
128. Vasina, T.V., S.A. Chelmakova, and A.L. Liberman, *Cycloketonization and linear polyketonization of α,ω-dicarboxylic acids Communication 6. Synthesis and ketonization of 3,7-dimethylazelaic acid.* Bulletin of the Academy of Sciences of the USSR, Division of chemical science, 1975. **24**(7): p. 1439-1442.
129. Liberman, A. and T. Vasina, O*n cycloketonization and linear polyketonization of alpha, omega-dicarboxylic acids part 5, synthesis of dispiro(5,2,5,3)heptadecan-16-one and some new data on the mechanism of cycloketonization*. Chemischer Informationsdienst, 1975. **6**.
130. Vasina, T., et al., *Cycloketonization and linear polyketonization of α,ω-dicarboxylic acids Communication 7. Preparation and reactions of zinc salts of unbranched dicarboxylic acids.* Russian Chemical Bulletin - RUSS CHEM BULL, 1982. **31**: p. 2046-2048.
131. Liberman, A.L. and T.V. Vasina, *Cycloketonization and linear polyketonization of α,ω-dicarboxylic acids.* Bulletin of the Academy of Sciences of the USSR, Division of chemical science, 1975. **24**(4): p. 771-775.
132. Lilga, M., et al., *Ketonization of Levulinic Acid and γ-Valerolactone to Hydrocarbon Fuel Precursors.* Catalysis Today, 2017. **302**.
133. Al-Naji, M., et al., *Pentanoic acid from γ-valerolactone and formic acid using bifunctional catalysis.* Green Chemistry, 2020. **22**(4): p. 1171-1181.
134. Luo, W., P.C.A. Bruijnincx, and B.M. Weckhuysen, *Selective, one-pot catalytic conversion of levulinic acid to pentanoic acid over Ru/H-ZSM5.* Journal of Catalysis, 2014. **320**: p. 33-41.
135. Serrano-Ruiz, J.C., D. Wang, and J.A. Dumesic, *Catalytic upgrading of levulinic acid to 5-nonanone.* Green Chemistry, 2010. **12**(4): p. 574-577.
136. Mäki-Arvela, P., et al., *Production of Lactic Acid/Lactates from Biomass and Their Catalytic Transformations to Commodities.* Chemical Reviews, 2014. **114**(3): p. 1909-1971.
137. Carlos Serrano-Ruiz, J. and J.A. Dumesic, *Catalytic upgrading of lactic acid to fuels and chemicals by dehydration/hydrogenation and C–C coupling reactions.* Green Chemistry, 2009. **11**(8): p. 1101-1104.
138. Serrano-Ruiz, J.C. and J.A. Dumesic, *Catalytic Processing of Lactic Acid over Pt/Nb2O5.* ChemSusChem, 2009. **2**(6): p. 581-586.
139. Gaertner, C.A., et al., *Catalytic coupling of carboxylic acids by ketonization as a processing step in biomass conversion.* Journal of Catalysis, 2009. **266**(1): p. 71-78.
140. Cai, Q., et al., *Aqueous-Phase Acetic Acid Ketonization over Monoclinic Zirconia.* ACS Catalysis, 2018. **8**(1): p. 488-502.
141. Marie, O., A.V. Ignatchenko, and M. Renz, *Methyl ketones from carboxylic acids as valuable target molecules in the biorefinery.* Catalysis Today, 2020.
142. Deng, L., Y. Fu, and Q.-X. Guo, *Upgraded Acidic Components of Bio-oil through Catalytic Ketonic Condensation.* Energy & Fuels, 2009. **23**(1): p. 564-568.
143. Weber, J., et al., *Coupling Red-Mud Ketonization of a Model Bio-Oil Mixture with Aqueous Phase Hydrogenation Using Activated Carbon Monoliths.* Energy & Fuels, 2017. **31**(9): p. 9529-9541.
144. Deneyer, A., et al., *Direct upstream integration of biogasoline production into current light straight run naphtha petrorefinery processes.* Nature Energy, 2018. **3**(11): p. 969-977.
145. Deneyer, A., et al., *Compositional and structural feedstock requirements of a liquid phase cellulose-to-naphtha process in a carbon- and hydrogen-neutral biorefinery context.* Green Chemistry, 2016. **18**(20): p. 5594-5606.
146. Op de Beeck, B., et al., *Direct catalytic conversion of cellulose to liquid straight-chain alkanes.* Energy & Environmental Science, 2015. **8**(1): p. 230-240.
147. Liu, S., et al., *Catalytic conversion of sorbitol to gasoline-ranged products without external hydrogen over Pt-modified Ir-ReOx/SiO2.* Catalysis Today, 2016. **269**: p. 122-131.

148. Serrano-Ruiz, J.C., et al., *Conversion of cellulose to hydrocarbon fuels by progressive removal of oxygen.* Applied Catalysis B: Environmental, 2010. **100**(1): p. 184-189.
149. Hernando, H., et al., *Cascade Deoxygenation Process Integrating Acid and Base Catalysts for the Efficient Production of Second-Generation Biofuels.* ACS Sustainable Chemistry & Engineering, 2019. **7**(21): p. 18027-18037.
150. Shylesh, S., et al., *Integrated catalytic sequences for catalytic upgrading of bio-derived carboxylic acids to fuels, lubricants and chemical feedstocks.* Sustainable Energy & Fuels, 2017. **1**(8): p. 1805-1809.
151. Huo, X., et al., *Tailoring diesel bioblendstock from integrated catalytic upgrading of carboxylic acids: a "fuel property first" approach.* Green Chemistry, 2019. **21**(21): p. 5813-5827.
152. Davidson, S.D., et al., *Strategies To Valorize the Hydrothermal Liquefaction-Derived Aqueous Phase into Fuels and Chemicals.* ACS Sustainable Chemistry & Engineering, 2019. **7**(24): p. 19889-19901.
153. Vienescu, D.N., et al., *A life cycle assessment of options for producing synthetic fuel via pyrolysis.* Bioresource Technology, 2018. **249**: p. 626-634.
154. Easterfield, T.H. and C.M. Taylor, *CCLIII.—The preparation of the ketones of the higher fatty acids.* Journal of the Chemical Society, Transactions, 1911. **99**(0): p. 2298-2307.
155. Klimkiewicz, R., H. Grabowska, and H. Teterycz, *Application of Zr-Mg-Y-O Catalyst for Ketonization of Ester and Alcohol Type Industrial Wastes.* Pol J Environ Stud, 2003. **12**.
156. Corma, A., M. Renz, and C. Schaverien, *Coupling Fatty Acids by Ketonic Decarboxylation Using Solid Catalysts for the Direct Production of Diesel, Lubricants, and Chemicals.* ChemSusChem, 2008. **1**(8-9): p. 739-741.
157. Kemp, S.J., et al., *Monodisperse magnetite nanoparticles with nearly ideal saturation magnetization.* RSC Advances, 2016. **6**(81): p. 77452-77464.
158. Jackson, M.A. and S.C. Cermak, *Cross ketonization of Cuphea sp. oil with acetic acid over a composite oxide of Fe, Ce, and Al.* Applied Catalysis A: General, 2012. **431-432**: p. 157-163.
159. Murzin, D.Y., et al., *Ketonization kinetics of stearic acid.* Reaction Kinetics, Mechanisms and Catalysis, 2019. **126**(2): p. 601-610.
160. Smith, B., et al., *Ketone Formation via Decarboxylation Reactions of Fatty Acids Using Solid Hydroxide/Oxide Catalysts.* Inorganics, 2018. **6**: p. 121.
161. Klimkiewicz, R. and H. Teterycz, *Transformation of methyl laurate to tricosanone-12 over Sn-Ce-Rh-O catalyst.* Reaction Kinetics and Catalysis Letters, 2002. **75**(1): p. 165-168.
162. Klimkiewicz, R., et al., *Ketonization of long chain esters from transesterification of technical waste fats.* Journal of Chemical Technology and Biotechnology, 2001. **76**: p. 35-38.
163. Oliver-Tomas, B., M. Renz, and A. Corma, *High Quality Biowaxes from Fatty Acids and Fatty Esters: Catalyst and Reaction Mechanism for Accompanying Reactions.* Industrial & Engineering Chemistry Research, 2017. **56**(45): p. 12870-12877.
164. Klimkiewicz, R., et al., *Ketonization of fatty methyl esters over Sn–Ce–Rh–O catalyst.* Journal of the American Oil Chemists' Society, 2001. **78**(5): p. 533-535.
165. Klimkiewicz, R., H. Grabowska, and L. Syper, *Ketonization of Long-Chain Esters.* Pol J Environ Stud, 2000. **9**.
166. Teterycz, H., R. Klimkiewicz, and M. Laniecki, *The Role of Lewis Acidic Centers in Stabilized Zirconium Dioxide.* Applied Catalysis A: General, 2003. **249**: p. 313-326.
167. Myllyoja, J., et al., *Process For Producing A Hydrocarbon Component*. 2007, NESTE OIL OYJ: US.
168. Fahim, M.A., T.A. Alsahhaf, and A. Elkilani, *Chapter 7 - Hydroconversion*, in *Fundamentals of Petroleum Refining*, 2010, Elsevier: Amsterdam. p. 153-198.
169. Hommeltoft Sven, I., *Ketonization Process Using Oxidative Catalyst Regeneration*. 2016, CHEVRON USA INC: US.
170. Jackson Michael, A. and C. Cermak Steven, *Method For Synthesis Of Ketones From Plant Oils*. 2013, US AGRICULTURE: US.
171. Kettunen, M., et al., *Dual Catalyst System For Performing A Ketonisation Reaction And A Hydrotreatment Reaction Simultaneously*. 2017, NESTE OIL OYJ: US.
172. Back, O., R. Leroy, and P. Marion, *Process For The Decarboxylative Ketonization Of Fatty Acids Or Fatty Acid Derivatives*. 2018, RHODIA OPERATIONS: US.
173. Meyer Ronald, E. and P. Otto Ferdinand, *Method Of Preparing High Molecular Weight Aliphatic Ketones*. 1946, SOCONY VACUUM OIL CO INC: US.
174. Kim Yong, W.O.O., et al., *Estolide Compound Containing Ketone Functional Group And Method For Preparing The Same*. 2016, SK INNOVATION CO LTD, SK LUBRICANTS CO LTD: EP.
175. McNeff Clayton, V., et al., *Hydrocarbon Synthesis Methods, Apparatus, And Systems*. 2014, WO.
176. Christensen Carl, W., S. Hammerberg Edgar, and C. Russell, *Aliphatic Ketone Production*. 1957, ARMOUR & CO: US.
177. Hermann, V., *Liquid Phase Decarboxylation Of Fatty Acids To Ketones*. 1968, GOLDSCHMIDT AG TH: US.
178. Graille, J. and D. Pioch, *Process For The Catalytic Condensation Of Carboxylic Acids And/or Their Derivatives And Its Application For The Preparation Of Ketones, Alcohols, Amines And Amides*. 1991, COOPERATION INTERNATIONAL EN R: EP.
179. Otto, S. and H. Karl, *Production Of Unsaturated Ketones*. 1935, IG FARBENINDUSTRIE AG: US.
180. Back, O. and P. Marion, *Process For The Catalytic Decarboxylative Cross-ketonization Of Aryl And Aliphatic Carboxylic Acid*. 2018, RHODIA OPERATIONS: WO.
181. Myllyoja, J., et al., *Tio2 Catalyst In Ketonisation Reactions To Produce Rbo*. 2018, NESTE OYJ: WO.
182. Kanervo, J., S. Toppinen, and P. Nurmi, *Method For Producing Ketones For Fuel And Oil Applications*. 2019, NESTE OYJ: US.
183. Back, O., R. Leroy, and P. Marion, *Processes For The Manufacture Of Secondary Fatty Alcohols, Internal Olefins And Internal Olefin Sulfonates*. 2019, RHODIA OPERATIONS SOLVAY: WO.